



Norwegian University  
of Life Sciences

Master's Thesis 2017 60 ECTS  
Faculty of Chemistry, Biotechnology and Food Science

# **Impact of Steam Explosion on Spruce Lignin Structure and Pyrolyzates**

Hördur Gunnarsson  
Chemistry





## Preface

This project was undertaken at the Norwegian University of Life Sciences (NMBU) within the Faculty of Chemistry, Biotechnology and Food Science (IKBM). The research project provides 60 of the 120 credits (ECTS) required to complete a Masters' degree in chemistry, and work on the project was performed in the period from August 2016 to May 2017.

The practical work was performed within the research group Natural Product Chemistry and Organic Analysis at IKBM. The project was a collaboration between two research teams: Natural Products Chemistry and Organic Analysis. Working on this project has been exciting, enjoyable, and challenging, providing me invaluable experience in current pyrolytic gas chromatographic and NMR spectroscopic techniques. I would like to thank everyone that have contributed to my completion of this research project. Specially, I would like to thank:

My supervisor, Yngve Stenstrøm, for helpful and constructive comments during the writing process, and general guidance during the whole project.

My supervisor, Ida Aarum, for laboratory training during the sample preparation and training using the analytical instruments, also for the support, guidance, and constructive comments during the project work and writing process.

My supervisors, Dag Ekeberg and Hanne Devle, for helpful advices during the sample preparation and interpretation of analytical data.

Finally, I would like to thank my wife, Ólöf Önundardóttir, for endless support during my Masters studies, walking the dog and me when we need fresh air after long hours spent inside with books and the computer, and for always having dinner ready after long days at the lab.

Ås, May 11th, 2017

Hörður Gunnarsson

## Abstract

The impact of steam explosion (SE) on spruce lignin structure and product formation during flash pyrolysis was investigated by HSQC and pyrolysis-GC-MS (py-GC-MS) experiments, with the aim to understand how lignin structure changes during SE treatment. Milled wood lignin (MWL) was isolated from untreated Norway spruce and steam exploded spruce samples treated at eight different severities. The second parallel gave yields comparable to literature for all of the nine samples. In an attempt for further purification, a part of all MWL samples was dissolved in tetrahydrofuran to obtain THF dissolvable MWL in surprisingly inconsistent yields.

Signals from twenty-eight different  $^{13}\text{C}$ - $^1\text{H}$  correlations for thirteen lignin substructures and structural units were identified by HSQC experiments, including  $\beta$ -aryl ether ( $\beta$ -O-4'), phenylcoumarane ( $\beta$ -5'), resinol ( $\beta$ - $\beta'$ ), dibenzodioxocine (5-5'-O-4), diphenyl-ethane ( $\beta$ -1'), and spirodienone ( $\alpha$ -O- $\alpha'$ ) lignin interunit bonds. The high abundant  $\beta$ -O-4' linkages were partially cleaved during the SE treatment, resulting in reduced amount with increased SE temperature, while raised abundance of  $\beta$ -5' linkages with SE temperature indicated condensation reactions. The low abundance of  $\beta$ - $\beta'$  linkages remained similar with more severe SE conditions, indicating balance between formation and degradation, while the lowest abundant linkages (5-5'-O-4,  $\beta$ -1', and  $\alpha$ -O- $\alpha'$ ) were only detected in untreated spruce and therefore completely degraded by the SE treatment.

Considerably fewer pyrolyzates were found in py-GC-MS of MWL from untreated spruce (26) than steam exploded spruce (34). Most pyrolyzates that were only formed from SE samples were derived from carbohydrates that were isolated as MWL due to pseudo-lignin formation in the SE treatment. G-lignin derivatives with shorter and more reduced side-chains were formed in relatively higher amounts with increased SE temperature, confirming partial depolymerization during steam explosion. Hydrolysis of  $\beta$ -O-4' linkages during the pretreatment facilitated the formation of 4-hydroxy-3-methoxybenzaldehyde, while decrease was observed with increased SE temperature due to aldehyde instability.

Similarities between samples treated for five and ten minutes indicated that steam temperature is the dominant factor for lignin structural changes during steam explosion. Differences observed after dissolving MWL in THF confirmed that lignin analysis depends on purification methods. Furthermore, comparison between pyrolyzates from MWL and THF dissolvable MWL indicated less heterogeneity in the lignin polymer after SE treatment.

## Sammendrag

Virkingen av dampeksplasjon (SE) på granligninstruktur og produktdannelse under pyrolyse ble undersøkt med HSQC og pyrolyse-GC-MS (py-GC-MS), med mål om å forstå hvordan ligninstruktur endres under SE behandling. Ballmølllet lignin (MWL) ble isolert fra ubehandlet gran og dampeksploderte granprøver som var behandlet ved åtte forskjellige betingelser. Den andre parallellen gav resultater tilnærmet litteraturen, for alle ni prøvene. I et forsøk på ytterligere rensing ble en del mengde av alle MWL prøvene løst i tetrahydrofuran for å oppnå THF oppløselig MWL, men i overraskende varierende utbytter.

Signaler fra 28 forskjellige  $^{13}\text{C}$ - $^1\text{H}$  korrelasjoner for 13 lignin understrukturer og strukturelle enheter, ble identifisert ved HSQC eksperimenter, inkludert  $\beta$ -aryleter ( $\beta$ -O-4'), fenylicoumaran ( $\beta$ -5'), resinol ( $\beta$ - $\beta'$ ), dibenzodioxocine (5-5'-O-4), difenyletan ( $\beta$ -1') og spirodienone ( $\alpha$ -O- $\alpha'$ ) lignin bindingstyper. De hyppigste fremkommende  $\beta$ -O-4'-bindingene ble delvis spaltet under SE behandlingen, hvilket resulterte i redusert mengde av disse med økt SE temperatur, mens økt mengde av  $\beta$ -5'-bindinger med SE temperatur ga indikasjoner på kondensasjonsreaksjoner. Den lave mengden av  $\beta$ - $\beta'$ -bindinger var uforandret med hardere betingelser under SE behandlingen, noe som indikerte balanse mellom dannelse og nedbrytning, mens de bindingene med laveste mengde (5-5'-O-4,  $\beta$ -1', and  $\alpha$ -O- $\alpha'$ ) kun ble detektert i ubehandlet gran og derfor fullstendig degradert i SE behandlingen.

Betraktelig færre pyrolysater ble funnet i py-GC-MS av MWL fra ubehandlet gran (26) enn dampeksploderte gran (34). De fleste pyrolysater som ble dannet kun i SE prøver, ble avledet fra karbohydrater, som ble isolert som MWL på grunn av pseudo-lignindannelse under SE behandlingen. G-ligninderivater med kortere og mer reduserte sidekjeder ble dannet i relativt høyere mengder med økt SE temperatur, som bekrefter delvis depolymerisering under dampeksplasjonen. Hydrolyse av  $\beta$ -O-4' bindinger under forbehandling øket dannelsen av 4-hydroksy-3-metoksybenzaldehyd, mens reduksjon ble observert med økt SE temperatur på grunn av reaktiviteten til aldehydet.

Likheter mellom prøver behandlet i fem og ti minutter indikerte at dampeksplasjons-temperaturen er den dominerende faktor for ligninstrukturendringer under behandlingen. Observert forskjeller etter oppløsning av MWL i THF bekreftet at ligninanalysen avhenger av opprensingsmetoder. Sammenligning mellom pyrolysater fra MWL og THF oppløselig MWL indikerte mindre heterogenitet in ligninpolymeren etter SE behandling.

## Abbreviations

---

**The following abbreviations are used in the thesis**

---

ADF	Acid detergent fiber
BDE	Bond dissociation energy
CEL	Cellulolytic enzyme lignin
DFRC	Derivatization followed by reductive cleavage
DMSO-d <sub>6</sub>	Deuterated dimethyl sulfoxide
EIC	Extracted ion chromatogram
EMAL	Enzymatic mild acidolysis lignin
FT-IR	Fourier transform infrared
GC	Gas chromatography
HETCOR	<sup>13</sup> C- <sup>1</sup> H Heteronuclear correlation
HMBC	Heteronuclear multiple bond connectivity
HMQC	Heteronuclear multiple quantum coherence
HSQC	Heteronuclear single quantum coherence
ILL	Ionic liquid lignin
LCC	Lignin-carbohydrate complexes
L-Phe	L-Phenylalanine
L-Tyr	L-Tyrosine
MS	Mass spectrometry
MWEL	Milled wood enzyme lignin
MWL	Milled wood lignin
MWLc	Crude milled wood lignin
NaOH	Sodium Hydroxide
Organosolv	Organic or an aqueous organic solvent mixture
PAHs	Polycyclic aromatic hydrocarbons
PAL	Phenylalanine ammonia lyase
Py	Pyrolysis
RT	Retention time
SD	Standard deviation
SE	Steam explosion
TAL	Tyrosine ammonia lyase
THF	Tetrahydrofuran
TIC	Total ion chromatogram
UVR	Ultraviolet resonance Raman
<sup>1</sup> H NMR	Proton nuclear magnetic resonance
<sup>13</sup> C NMR	Carbon nuclear magnetic resonance
2D NMR	Two-dimensional nuclear magnetic resonance

---

## Table of Contents

Preface.....	I
Abstract .....	II
Sammendrag.....	III
Abbreviations .....	IV
Table of Contents .....	V
1. Introduction .....	1
1.1 The Industrial Use of Biomass and Potential Valorization of Lignin .....	1
1.2 Pretreatment of Biomass.....	2
1.3 Lignin Structure and Biosynthesis.....	4
1.4 Lignin Isolation .....	7
1.5 Lignin Analysis .....	8
1.5.1 Wet-Chemistry Methods .....	9
1.5.2 Pyrolysis-Gas Chromatography-Mass Spectrometry (Py-GC-MS).....	9
1.5.3 Ultraviolet and Infrared Spectroscopy Techniques .....	12
1.5.4 Nuclear Magnetic Resonance Spectroscopic Techniques .....	13
1.6 This Study and Its Aim.....	15
2. Materials and Methods .....	17
2.1 Overview of Sample Preparation and Analytical Methods .....	17
2.2 Materials and Equipment.....	18
2.2.1 Laboratory Materials .....	18
2.2.2 Chemicals .....	18
2.2.3 Standards .....	18
2.2.4 Laboratory Equipment.....	19
2.2.5 Steam Explosion Unit.....	19
2.2.6 Setup of the Extraction and Vacuum Distillation Equipment .....	20
2.2.7 Raw Material .....	21
2.3 Synthesis of 2-(4-Hydroxy-3-methoxyphenyl)acetaldehyde.....	21
2.4 Sample Preparation.....	22
2.4.1 Steam Explosion Pretreatment of Norway Spruce .....	22
2.4.2 Sample Preparation of Milled Wood Lignin .....	23
2.4.3 Sample Preparation of THF Dissolvable Lignin .....	26
2.5 Analysis.....	26
2.5.1 HSQC Experiments .....	27
2.5.2 Py-GC-MS Analysis.....	30



## Table of Contents

3. Results and Discussion.....	33
3.1 Lignin Yield .....	33
3.1.1 Yield of MWL isolated from untreated and steam exploded spruce .....	33
3.1.2 Yield of THF dissolvable MWL.....	34
3.2 HSQC Experiments .....	35
3.2.1 Identification of <sup>13</sup> C- <sup>1</sup> H correlations in HSQC spectra.....	35
3.2.2 Quantification of Interunit Linkages in Norway Spruce .....	48
3.3 Py-GC-MS Analysis.....	52
3.3.1 Identification of Volatile Pyrolyzates.....	52
3.3.2 Relative Quantification of Volatile Pyrolyzates.....	58
4. Conclusion.....	71
5. References .....	73
6. Appendix .....	83
6.1 HSQC Spectra of MWL From All Steam Exploded Samples.....	83
6.2 HSQC Spectra of THF Dissolvable MWL From Spruce Samples.....	87
6.3 Pyrograms of MWL and THF Dissolvable MWL from All Samples .....	89
6.4 Relative Amount of Pyrolyzates Formed from All Lignin Samples .....	95

# 1. Introduction

## 1.1 The Industrial Use of Biomass and Potential Valorization of Lignin

Concerns over the environmental effects of fossil fuels and their diminishing supplies have led to growing interest in renewable and sustainable bio-resources. With the steady need for compensating oil-based products, the concept of biorefineries has emerged. Biorefineries convert biomass into various products such as fuels, energy and value-added chemicals<sup>1</sup>. Fractionation of the plant raw material into its core constituents is one of the most important steps in the production. The composition of the main constituents in plant cell wall is variable between species, but softwood stems consists generally of 45-50% cellulose, 25-35% hemicellulose<sup>(1)</sup>, and 25-35% lignin<sup>2</sup>. With the focus on fuel production from cellulose and hemicellulose, biorefineries generate large amounts of lignin as a side product. Today, lignin is mainly burned to generate energy and heat to power the operation. However, with optimization of the cellulosic fuel production, less lignin is needed in this purpose. Therefore, the development of valuable products from lignin is vital for the economy of biorefineries.

Possible valuable products derived from lignin include plastics<sup>3, 4</sup>, adhesives<sup>5, 6</sup>, biofuels<sup>7</sup>, cosmetics<sup>8</sup> and carbon fibers<sup>9, 10</sup>. Studies have shown that incorporation of lignin into plastics, such as polypropylene and polyethylene, can provide polymers with improved strength, elongation at break, and other mechanical properties<sup>3, 4</sup>. The use of lignin in adhesives has been suggested in fiberboard production and technologies trialed, where cross reaction of lignin via laccases were used to provide boards comparable in strength to those produced using urea-formaldehyde adhesives<sup>5, 6</sup>. Kleinert and Barth<sup>7</sup> reported a liquefaction process, converting lignin into a liquid bio-oil that can be combined with conventional fossil fuel. Furthermore, they suggested combining this process with bio-ethanol production from lignocellulosic carbohydrates and thereby converting all wood fractions into liquid fuels. Studies of lignin as an antioxidant<sup>11, 12</sup> have led to investigations of potential use in cosmetics, concluding that lignin has high antioxidant capacity and is safe for eyes and skin<sup>8</sup>. Recent studies<sup>9, 10</sup> have demonstrated great potentials for lignin as precursor for carbon fiber production, reducing both production time and costs.

---

<sup>(1)</sup> Hemicelluloses are heteropolysaccharides formed by various building blocks including pentoses, hexoses, and uronic acids. The units can form unbranched, helical, and branched chains in a rodlike structure which facilitates interaction with cellulose and lignin<sup>29</sup>.

## Introduction

The end products of the discussed applications of lignin depend on the source and purity of the lignin. Generally, less heterogeneous lignin provides more possibilities for valuable end products, emphasizing the importance of understanding lignin structure and how it is degraded in all production stages<sup>13</sup>.

### 1.2 Pretreatment of Biomass

Pretreatment of biomass is essential because of the chemical and physical resistance of plant cell structure, inhibiting their susceptibility to processes such as hydrolysis and fermentation that are important for the industry. Pretreatment methods enhance the conversion of lignocellulosic material, aiming to maximize the recovery of each component. A variety of biological, physical and chemical methods have been evaluated for the effectiveness at pretreating biomass<sup>14-20</sup>.

Biological pretreatments result in partial delignification of biomass using lignin-degrading microorganisms, such as fungi and bacteria, offering advantages like low chemical and energy use, in addition to mild conditions<sup>16</sup>. Of the fungi species, white-rot fungi are the most effective for biological pretreatment of lignocellulosic materials<sup>2</sup>. Reductions up to 65% in the lignin content of cotton straw were reported using white-rot fungi<sup>21</sup> and biodegradation of Bermuda grass stems was improved by 63-77% after six weeks of white-rot fungi treatment<sup>14</sup>. Furthermore, white-rot fungi have been genetically modified to produce more of lignin degrading enzymes such as versatile peroxidases (VPs), creating a VP overproduction system that enhances the degradation<sup>22</sup>. However, lignin biodegradation is a slow process and a rapid, controllable bioprocessing system has not been developed to date<sup>2, 23</sup>.

Chemical pretreatments tend to solubilize hemicellulose and lignin by adding chemicals such as dilute or concentrated acids, alkaline, or organic solvents with acid catalysts in order to retrieve cellulose<sup>24</sup>. Concentrated acids are powerful agents for cellulose hydrolysis, but toxic, corrosive, and hazardous. Additionally, the acid must be recovered after hydrolysis for an economically feasible process<sup>25</sup>. Dilute acid hydrolysis offers less hazardous conditions, but high temperature is favorable and the cost relatively high<sup>2</sup>. Some bases can also be used for cellulose hydrolysis and lignin removal, but the effect of alkaline pretreatment depends on the biomass nature and lignin content. Dilute NaOH treatment of hardwood decreased lignin content from 24-55% to 20%, but no effect was observed for softwood with lignin content higher than 26%<sup>26</sup>. In the organosolv process, an organic or an

## Introduction

aqueous organic solvent mixture with acid catalysts is used to break internal lignin and hemicellulose bonds, obtaining high yield of carbohydrates from the biomass. However, the solvents used in the process must be retrieved and recycled to reduce cost. Also, removal of solvents from the system is necessary because they may inhibit enzymatic hydrolysis and fermentation<sup>2</sup>. Generally, chemical pretreatment methods show high degree of selectivity for the biomass component they degrade, but also involve relatively harsh conditions, which may not be ideal for biorefineries due to possible effects on downstream biological processing<sup>27</sup>.

Physical pretreatments such as mechanical comminution and ultrasound treatment have been used to increase enzymatic activity in the hydrolysis of biomass<sup>17, 28</sup>. Khanal *et al.*<sup>17</sup> used high power ultrasonic energy to treat corn slurry in dry torn milling ethanol plants, and the resulting samples exposed to enzymes to convert cornstarch into glucose. The corn particle size declined nearly 20-fold following the treatment and the glucose release rate increased up to threefold compared to the control group. Biomass can be pulverized by chipping and grinding or milling to reduce cellulose crystallinity, and often used in combination with other pretreatment methods. Planetary ball milling was found to improve enzymatic digestibility of ethanol/water/acetic acid pretreated Eucalyptus wood chips<sup>28</sup>. Enzymatic hydrolysis experiments demonstrated that the conversion of cellulosic components into glucose attained completion under optimal conditions. However, without combination with other pretreatments, physical pretreatment methods exhibit comparatively lower performance and higher cost due to high energy requirements<sup>27</sup>.

Steam explosion, which combines elements of physical and chemical methods, has been claimed one of the most successful option for wood fractionation and enhancing the susceptibility of cellulose to enzymatic attack<sup>15, 19, 20</sup>. Steam pretreatment in a batch reactor involves subjecting wood chips to saturated steam at elevated pressure for a certain time, then releasing the pressure rapidly resulting in explosion or bleeding the steam pressure carefully down without explosion. The high-pressure steam modifies the cell wall structure, partially hydrolyzing hemicelluloses which are easily recovered by water washing, leaving a water-insoluble fraction containing cellulose, residual hemicelluloses and a chemically modified lignin<sup>19, 29</sup>. The temperature and residence time inside the reactor have been recognized as the most important factors that affect the treatment and by combining them in a single severity parameter, a variety of process parameters can be predicted such as the recovery yield of steam-treated fractions, yield of enzymatic hydrolysis, and extent of lignin and hemicellulose removal after pretreatment<sup>30</sup>. Severity of the steam treatment (temperature, residence time in

## Introduction

the steam reactor) is vital for the optimization of bioprocesses. Vivekanand *et al.*<sup>31</sup> observed that with increased severity, enzymatic hydrolysis yields higher amounts of carbohydrates until a maximum is reached at a certain severity. However, the amounts decreased with higher severities, indicating decreased susceptibility of cellulose to enzymatic attack. The selection of steam explosion severity depends on the specific biomass used, for example softwood requires more severe conditions than hardwood due to difference in hemicellulose content<sup>29</sup>. Hardwood hemicelluloses are mostly composed of highly acetylated glucuronoxylans with acidic characteristics that facilitate acid hydrolysis under relatively mild conditions. In contrast, softwood contain only a small fraction of xylans, but high proportion partly acetylated glucomannans and galactoglucomannans, resulting in more resistance to acid hydrolysis.<sup>32</sup> Due to this variability between lignocellulosic materials, research is needed for all types of raw materials used in the industry, especially effects on the lignin fraction of the biomass. Furthermore, effects on the lignin fraction of the biomass during steam explosion of different severities need research. Knowledge of lignin structure and its changes during steam explosion of different severities can play an important role for both the overall delignification and further use of the lignin fraction<sup>33</sup>.

### 1.3 Lignin Structure and Biosynthesis

Lignin is an aromatic plant polymer and serves as a strengthening material for plant cell wall. The ability to synthesize lignin was essential in the evolutionary adaption of plants from an aquatic environment to land. Lignin is vital for stiffness and strength of the stem along with the structural integrity of the cell wall<sup>34, 35</sup>. Additionally, lignin waterproofs the cell wall allowing water transport through the vascular system, and plays an important role in providing protection against pathogens due to the insolubility and complexity of the lignin polymer<sup>36</sup>.

Lignin is mainly formed by the coupling of three monomers; 4-hydroxycinnamyl alcohol, coniferyl alcohol, and sinapyl alcohol, giving rise to p-hydroxyphenyl (H), guaiacyl (G), and syringyl (S) phenylpropanoid units when incorporated into the lignin polymer. Structures are found in Figure 1.1, which demonstrates how the phenylpropanoid lignin monomers are biosynthesized from their amino acid precursors. All plants can deaminate L-phenylalanine (L-Phe) via the enzyme phenylalanine ammonia lyase (PAL), but the deamination of L-

## Introduction

tyrosine (L-Tyr) is limited to members of the grass family.<sup>37</sup> Text and reviews on the biosynthesis of lignin have been written several authors<sup>36, 38, 39</sup>.

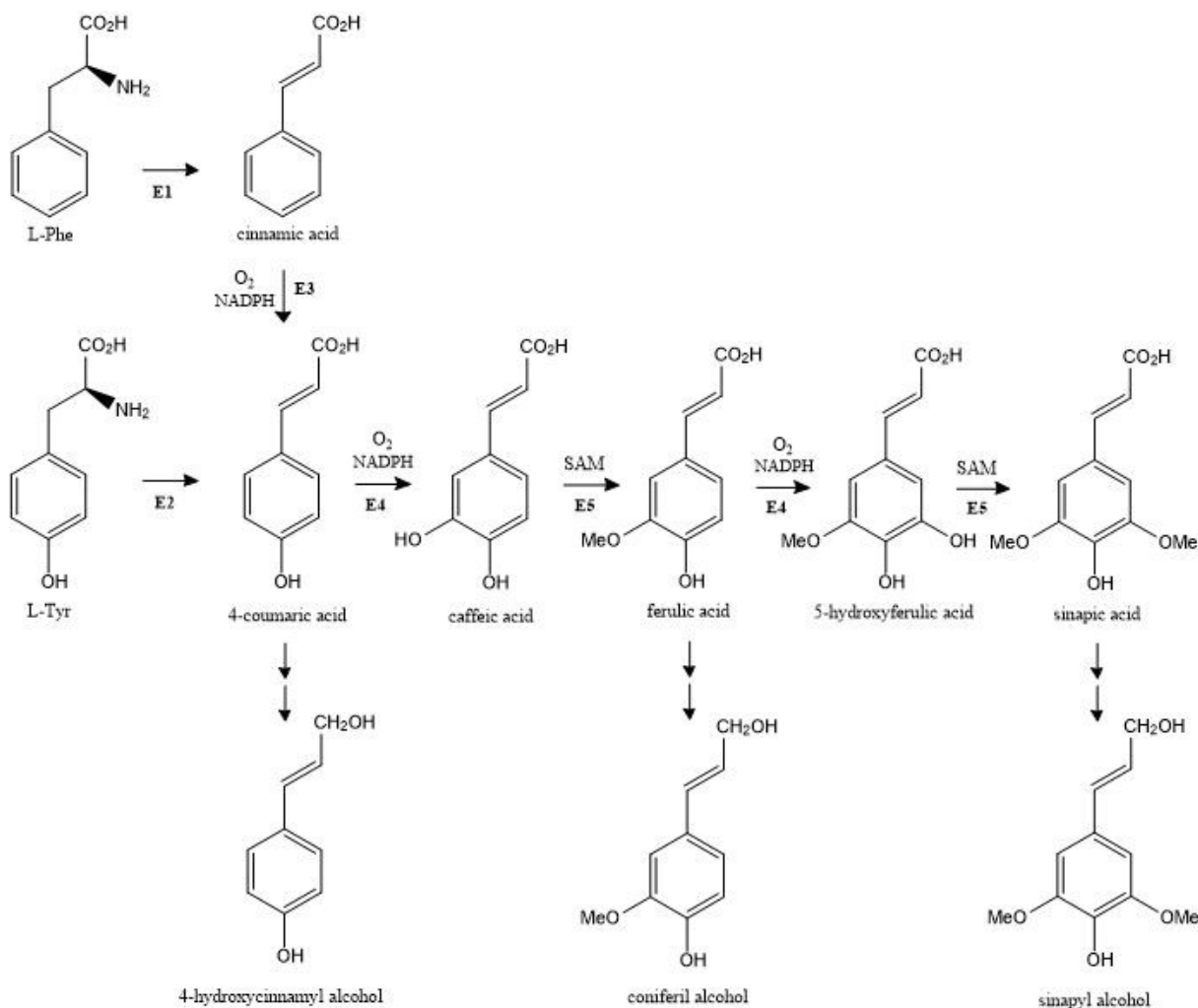


Figure 1.1: Biosynthesis of the lignin monomers. E1: phenylalanine ammonia lyase (PAL), E2: tyrosine ammonia lyase (TAL) or PAL (still debated), E3: cinnamate 4-hydroxylase, E4: *p*-coumarate 3-hydroxylase, E5: caffeic acid *O*-methyltransferase. Adapted from Dewick<sup>37</sup>.

Lignin is formed by phenolic oxidative coupling of the phenylpropanoid units in a process called lignification. Peroxidases, laccases, or oxidases generate the monolignol radicals by dehydrogenation and one-electron oxidation of the phenol group. The radicals are relatively stable due to electron delocalization, giving resonance forms with the electron residing on the side chain, and positions *ortho* and *para* to the oxygen (Figure 1.2). Radical pairing provides various dimers, called lignans. The favored radical has the free electron at the side chain  $\beta$  position, giving rise to  $\beta$ -aryl ether ( $\beta$ -O-4'), phenylcoumaran ( $\beta$ -5'), pinoresinol ( $\beta$ - $\beta'$ ), spirodienone ( $\alpha$ -O- $\alpha'$ ), and diphenylethane ( $\beta$ -1') dimers. Coupling of the radicals with the electron residing on the aromatic positions is theoretically possible yielding diphenyl (5-5') and diaryl ether (4-O-5') dimers. However, these two dimers do not arise in any significant

## Introduction

way from monomer dimerization reactions, but from coupling between preformed lignin oligomers. The diphenyl subunits can give rise to further complication in lignin by undergoing  $\alpha$ - $\beta$ -O-4-4' coupling to form dibenzodioxocine (5-5'-O-4). Figure 1.2 shows a general structure of lignin and the main interunit linkages. The general structure demonstrates how dibenzodioxocine and diaryl ether linkages act as branching point in lignin.

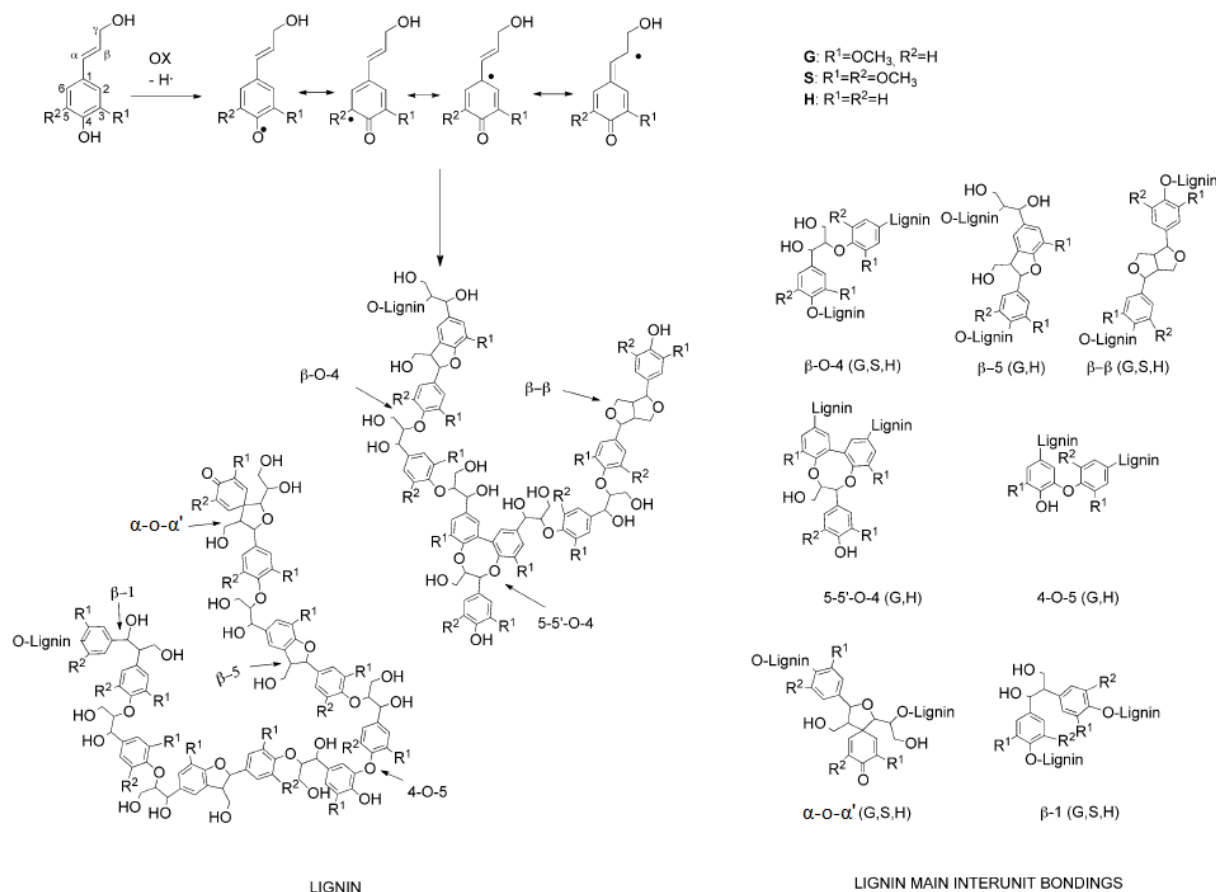


Figure 1.2: Lignin biosynthesis, general structure, and main interunit linkages. Adapted from Sette *et al.*<sup>40</sup>

Besides the linkages within lignin itself, lignin is known to be covalently linked to cellulose and hemicellulose, forming lignin-carbohydrate complexes (LCC)<sup>41</sup>. Among confirmed LCC linkages are phenyl glycoside,  $\gamma$ -ester, and benzyl ether bonds<sup>42</sup> (Figure 1.3). Despite relatively low abundance in wood, they play an important role since almost all wood lignin is linked to polysaccharides, mainly hemicelluloses<sup>43</sup>. However, the complex structure of the lignin-hemicellulose network creates significant problems in separating the wood components in biorefining processes, and is the main reason for the difficulty in isolating lignin without altering its structure<sup>44, 45</sup>.

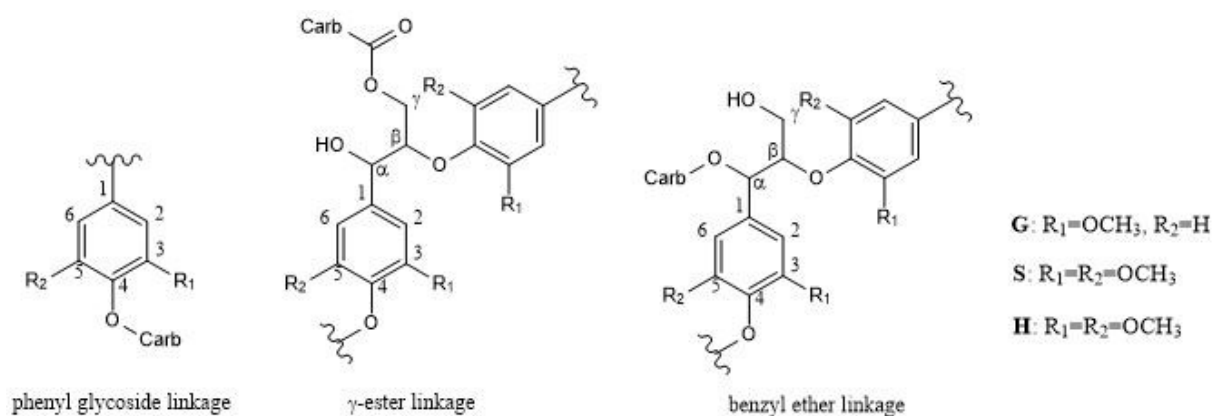


Figure 1.3: Main lignin-carbohydrate linkages. Adapted from Balakshin et al.<sup>42</sup>

## 1.4 Lignin Isolation

Isolation of lignin for analytical purpose has provided challenges for chemists for over a century, resulting in various isolation methods such as the preparation of Klason lignin, Björkman milled wood lignin, milled wood enzyme lignin, cellulolytic enzyme lignin and enzymatic mild acidolysis lignin<sup>46, 47</sup>.

Klason lignin is obtained by treating wood with sulfuric acid, thus hydrolyzing the polysaccharides to water-soluble sugars while the lignin is recovered as an insoluble residue in over 90% yield of the total lignin. The analytical use of this method is limited to determining lignin content due to the highly condensed and altered structure. For chemical characterization or studies of biological modification and degradation, an isolated lignin is needed that is representative of the lignocellulosic lignin called protolignin.

The lignin preparation that has been considered most representative of protolignin is Björkman milled wood lignin (MWL). After extractives removal with organic solvents, finely milled wood is extracted with aqueous dioxane and then purified to yield MWL, which is considered to be appropriate for most chemical and biological studies. Milled wood lignin can be obtained in 20-30% yields, based on the total amount of lignin in the wood.

Finely milled wood, prepared in the way as used for MWL extractions, may be treated with polysaccharidase enzymes to solubilize the carbohydrates, yielding milled wood enzyme lignin (MWEL). This lignin residue contains nearly all lignin in the wood and is the most representative isolated lignin. However, the high carbohydrate content due to LCC linkages and high molecular weight, it is not completely soluble in common lignin solvents, resulting in experimental difficulties in handling, purifying and analyzing MWELs.



## Introduction

Cellulolytic enzyme lignin (CEL) is prepared by the aqueous dioxane extraction of MWEL and purified in the same manner as MWL. It is considered to be more representative of protolignin than MWL, but additional steps in the CEL preparation are usually not justifiable since MWL is adequate for most studies.

More recently, Wu and Argyropoulos<sup>48</sup> proposed a lignin isolation procedure composed of a mild cellulolytic hydrolysis of milled wood, followed by a mild acid hydrolysis. In this procedure, the initial hydrolysis removes most of the carbohydrates and the acid hydrolysis cleaves the remaining lignin-carbohydrate bonds, resulting in enzymatic mild acidolysis lignin (EMAL). The yield is significantly greater than of the corresponding MWL and structural analysis performed by Wu and Argyropoulos offered no evidence of marked differences. Therefore, both MWL and EMAL can be used to analyze the native lignin from plant cell wall. Furthermore, using one of those isolation methods offers the possibility of analytically compare lignin from different sources or differently pretreated biomass.

### 1.5 Lignin Analysis

When analyzing the lignin polymer, its complexity must be taken into consideration. Therefore, most analytical methods are based on degradation of the polymer to lignin monomers or dimers. A considerable number of wet-chemistry methods were developed during the last century including permanganate oxidation, thioacidolysis, and derivatization followed by reductive cleavage (DFRC). Pyrolysis-gas chromatography-mass spectrometry (Py-GC-MS) is another degradative method that has been popular in lignin analysis for decades. However, these methods liberate only a fraction of the polymer for analysis and are based on cleavage of the lignin backbone, analyzing the fragments obtained<sup>40</sup>.

Non-degradative methods have historically been more difficult to apply on the lignin polymer. With technological advances in the last decades, these methods have grown in popularity for lignin analysis. Various spectroscopic methods have been used for the structural analysis of lignin such as ultraviolet resonance Raman (UVR), Fourier transform infrared (FT-IR), and nuclear magnetic resonance NMR spectroscopy. Modern NMR techniques are undoubtedly superior in structural characterization of lignin, but the best analysis is generally obtained by combination of non-degradative and degradative methods.

### 1.5.1 Wet-Chemistry Methods

Permanganate oxidation is a four-step reaction sequence leading to methylated aromatic carboxylic acid methyl esters of the lignin-containing sample<sup>49</sup>. Information of lignin substructures are obtained, but mostly qualitative since the low yields of degradation acids make it difficult to evaluate relative amount of structural units<sup>50</sup>.

Thioacidolysis is a solvolysis in dioxane-ethanethiol with boron trifluoride etherate, resulting in a selective cleavage of  $\beta$ -aryl ether bonds. Monomeric and dimeric products substituted with thioethyl groups are formed and analyzed by GC-MS, the monomers with the thioethyl groups and the dimers after desulphuration<sup>51</sup>. However, detection is limited to structural units bound by arylglycero- $\beta$ -ether bonds<sup>40</sup>.

The DFRC method is another  $\beta$ -aryl ether cleavage method. The lignin sample is brominated at the benzylic positions and free hydroxyl groups are acetylated in the same reaction using acetyl bromide. Reductive cleavage of the brominated  $\beta$ -aryl ether is performed by using zinc, followed by acetylation<sup>52</sup>. The monomeric products are quantified by gas chromatography. However, the presence of bromine and  $\beta$ -O-4 linkages in the DFRC-treated lignin revealed that lignin polymer is not completely degraded<sup>53</sup>.

Therefore, no wet-chemistry method is available that identifies and quantifies all the interunit linkages in lignin. Furthermore, these degradative methods require workup that is time consuming and often use of expensive reagents.

### 1.5.2 Pyrolysis-Gas Chromatography-Mass Spectrometry (Py-GC-MS)

Of all degradation methods available for lignin characterization, pyrolysis is particularly interesting, because it can be easily coupled to GC-MS allowing analysis of lignin fragments. Galletti and Bocchini<sup>54</sup> wrote a review on analytical pyrolysis on lignocellulosic material. When pyrolyzed, the sample is decomposed by heat in the absence of oxygen, into molecules of lower mass. These volatile compounds are separated by gas chromatography and analyzed by mass spectrometry. In analytical pyrolysis, it is desirable that the lignin sample is decomposed to the greatest possible extent while maintaining the size of the fragments as large as possible, allowing detection of all the volatile compounds that are characteristic for the sample. However, the conditions of the pyrolysis are a vital factor for a representative analysis.

## Introduction

Important condition factor for a representative and reproducible pyrolytic analysis are temperature control in the pyrolysis, position of the pyrolysis unit, removal of the pyrolysis fragments out of the pyrolysis zone, and the sample size. Figure 1.4 illustrates a typical pyrolysis temperature profile of a sample. The sample is heated rapidly, usually by

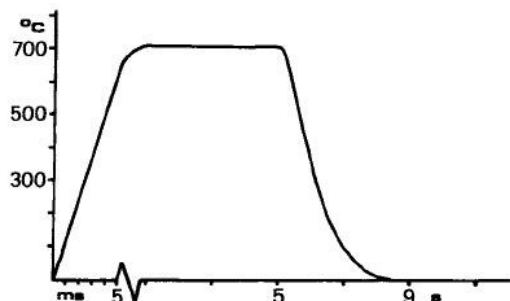


Figure 1.4: A typical pyrolysis temperature vs. time profile. Reprinted from Galletti and Bocchini<sup>54</sup>.

electronically controlled resistance element made from platinum coil or ribbon. It is important that the heating happens in only few milliseconds to a precisely controlled equilibrium temperature in the range 400-1000°C. In the most common mode, isothermal pyrolysis, the temperature is held constant for a few seconds and cooled

rapidly to avoid non-isothermal pyrolysis. The pyrolysis fragments must be rapidly removed from the pyrolysis zone into the GC-MS instrument without further intense heating to avoid secondary reactions, *i.e.* the recombination of the pyrolysis fragments into larger fragments, that would destroy part of volatile products to be analyzed, resulting in a less representative analysis. This is accomplished by positioning the pyrolysis unit close to the chromatographic column, and by blowing the fragments out of the pyrolysis zone by using an inert gas, which is also used as a carrier gas. Small sample size is necessary for isothermal pyrolysis to avoid temperature gradients within the sample during the heating.

The selected equilibrium temperature used in an isothermal pyrolysis effects the product formation according to previous studies.<sup>55-58</sup> This is due the different amount of energy needed to break the different linkages in lignin. Relatively low temperatures (around 400°C) will therefore give fewer products than higher temperatures. Typically, temperatures between 600-800°C are used for analyzing lignin containing samples, resulting in formation of diverse gaseous products degraded from the lignin polymer. However, formation of undesirable condensation products such as polycyclic aromatic hydrocarbons (PAHs) elevates at temperatures above 700°C.<sup>59, 60</sup> Bond dissociation energies have been estimated for the main interunit linkages in lignin by BDE calculations of various lignin model dimers (Figure 1.5)<sup>61-</sup>

## Introduction

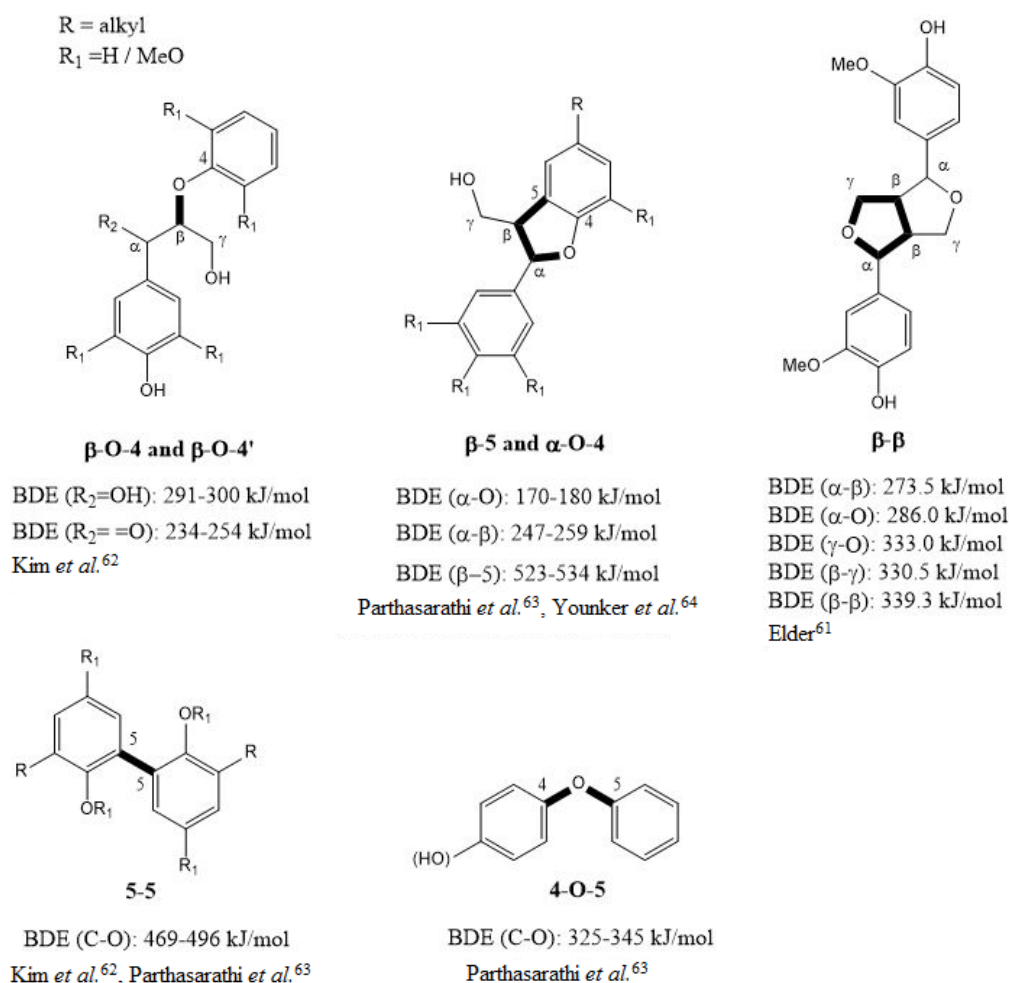


Figure 1.5: Calculated bond dissociation energy (BDE) in lignin model compounds. The selected bonds are marked bold.

By identifying the monomeric pyrolysis products, valuable information about the structure of the lignin polymer can be obtained by understanding reaction pathways in pyrolysis. Pyrolysis reactions are generally divided into two stages, primary and secondary reactions<sup>65</sup>. Primary reaction pathways that compete against each other are depolymerization, fragmentation, and char formation. Analysis of the pyrolysis products of model lignin dimers along with NMR analysis of pyrolyzed lignin samples revealed that  $\alpha$ - and  $\beta$ -ether bonds are cleaved during the primary pyrolysis stage, but condensed (C-C) type linkages are stable during depolymerization<sup>66-68</sup>. However, phenyl  $\beta$ -aryl type dimers display fragmentation to stilbenes but these reactions do not lead to depolymerization of lignin<sup>67, 68</sup>. Undesirable char formation increases slightly with increased temperature at the primary reaction stage, but formation of desirable gaseous lignin monomers due to depolymerization and fragmentation increases at a much faster rate. Secondary pyrolysis reactions include rearrangements starting with the homolytic cleavage of the O-CH<sub>3</sub> bonds attached to the lignin aromatic rings, occurring via rearrangement mechanism starting from the phenoxy radical of guaiacols<sup>69</sup>.

## Introduction

Rearrangement of the aromatic substituents results in the formation of volatile products such as catechols, phenols, and *o*-cresols<sup>70-72</sup>.

Analytical pyrolysis is a useful tool to compare the degradation of lignin samples that have been isolated from differently pretreated biomass and to compare different isolation methods. It can provide information of efficiency and kinetic of chemical and biological delignification treatments. Chiavari *et al.*<sup>73</sup> studied changes in organic material during fungal fermentation processing of wheat straw, resulting in significant changes in six of fifteen quantified pyrolyzates. In another study<sup>74</sup>, chemical delignification of wheat straw was examined. Wheat straw, its acid detergent fiber (ADF) and residues from lignin assay procedures were analyzed, resulting in decreased carbohydrate products and reduced aromatics in the ADF fraction, indicating cleavage of some side chains or condensation reactions. The permanganate lignin residue showed no aromatic fragments, indicating complete lignin removal. Evans *et al.*<sup>75</sup> studied biomass and their differently extracted lignins; MWL, steam explosion, Kraft, and organosolv. MWL and native lignin showed nearly identical product spectra, dominated by monolignols. Spectra of other lignin isolations differed from native lignin, showing less amount of monolignols and increased yield of lighter phenols. Kraft lignin showed the most deviation from native lignin pyrolyzates with the lowest amount of monolignols, followed by organosolv lignin and then steam explosion lignin.

Analytical pyrolysis is an attractive option for lignin characterization because the sample size is small (less than a milligram), sample preparation negligible, and short analysis time. It can provide valuable information of the structure of lignin. However, with the nature of degradation methods it is necessary to work by retrospective approach to deduce the structure and interunit linkages of lignin. Furthermore, such approaches have limited use when quantitative determinations are needed. Therefore, information from spectroscopic structural elucidation techniques such as nuclear magnetic resonance (NMR) and infrared spectroscopy (IR) are often combined with information from degradation techniques<sup>45, 76-78</sup>.

### 1.5.3 Ultraviolet and Infrared Spectroscopy Techniques

Various spectroscopic methods on the ultraviolet and infrared region have been used for the structural analysis of lignin. Ultraviolet resonance Raman (UVRR) spectroscopy and Fourier transform infrared (FT-IR) spectroscopy are among those methods and are often used to give supporting information to other analytical methods. Both UVRR and FT-IR have been

useful for identifying functional groups and structural moieties in lignin isolated with different methods from various sources<sup>45, 77, 79</sup>. Saariaho *et al.*<sup>79</sup> determined characteristic vibration of H, G, and S lignin structures in compression wood, softwood, and hardwood of model compounds by using UVRR. Also, they found those characteristic bands in compression wood, softwood, and hardwood, and suggesting that UVRR can be applied in lignin structural determination. Wen *et al.*<sup>45</sup> studied birch lignin isolated with two different methods, resulting in cellulolytic enzyme lignin (CEL) and ionic liquid lignin (ILL). FT-IR spectra showed more pronounced stretching of conjugated C=O groups in CEL than in ILL, suggesting that CEL contained more conjugated C=O groups. Both UVRR and FT-IR are limited in structural elucidation of lignin and are therefore generally used in combination with other techniques. However, NMR spectroscopy allows a larger amount of information to be obtained due to much higher resolution<sup>80</sup>.

### 1.5.4 Nuclear Magnetic Resonance Spectroscopic Techniques

NMR spectroscopy has been shown to be reliable and effective method in the structural characterization of the lignin polymer. Despite the complexity and low resolution of lignin one-dimensional NMR spectra, chemists in the late 19<sup>th</sup> century were able to obtain valuable structural information from both <sup>1</sup>H NMR and <sup>13</sup>C NMR experiments. With high-resolution instruments and the development of two-dimensional NMR techniques, the spectra obtained from various NMR experiments can contribute more to lignin characterization than any other analytical method.

#### 1.5.4.1 One-Dimensional NMR Techniques

In the past, lignin characterization by NMR spectroscopy was limited to identifying and estimating the amount of the most common interunit linkages by using proton NMR (<sup>1</sup>H NMR). Studies by Lundquist *et al.*<sup>81, 82</sup> showed the dominance of  $\beta$ -O-4 linkages and a few percent of  $\beta$ - $\beta$  linkages in spruce. In addition, the presence of  $\beta$ -5 linkages was confirmed and <sup>1</sup>H NMR signals were assigned to some protons from lignin units such as cinnamyl alcohol, cinnamaldehyde, and benzaldehyde units. However, the signals in the <sup>1</sup>H NMR spectrum are broad, irregular and tend to overlap due to the complex structure and polymeric nature of lignin, thus limiting its application.

## Introduction

With the progress of NMR techniques,  $^{13}\text{C}$  NMR became useful in lignin structural analysis, mainly providing qualitative and semi-quantitative information of specific lignin moieties. In early  $^{13}\text{C}$  NMR studies, the amount of hydroxy groups, double bonds, condensed and uncondensed aliphatic carbons, and methoxyl groups, were estimated for comparing different wood types or treatments<sup>83-85</sup>. More recent studies have allowed identification and quantification of various substructures, interunit linkages and functional groups of lignin, making  $^{13}\text{C}$  NMR a powerful analytical tool in lignin structural elucidation<sup>80, 86</sup>. However, the low natural abundance of the  $^{13}\text{C}$  isotope makes  $^{13}\text{C}$  NMR less sensitive, requiring long acquisition times and high sample concentrations for enhancing the signals that make quantification possible. In addition,  $^{13}\text{C}$  NMR spectra of lignin do not allow detailed assignment and quantification of individual signals due to broad and overlapping signals, resulting in low-resolution spectra. By combining proton and carbon NMR techniques in a 2D NMR approach, possibilities have multiplied for the use of NMR spectroscopy in lignin structure determination.

### *1.5.4.2 Two-Dimensional NMR Techniques*

With the development of modern NMR techniques, the  $^{13}\text{C}$ - $^1\text{H}$  heteronuclear correlation (HETCOR) experiments became popular for lignin characterization. In these experiments, the proton spectrum is correlated with the carbon spectrum, combining the sensitivity of  $^1\text{H}$  NMR with the higher resolution of  $^{13}\text{C}$  NMR, resulting in easier signal assignments for both<sup>87</sup>. Of the three HETCOR experiments; Heteronuclear Multiple Quantum Coherence (HMQC), Heteronuclear Single Quantum Coherence (HSQC), and Heteronuclear Multiple Bond Connectivity (HMBC), HSQC is the most useful for interpreting complex spectra where peaks often overlap. In contrast to HMQC, HSQC shows none of the proton-proton coupling that stretches the peaks out in the horizontal direction, resulting in smaller and more nearly circular cross-peaks<sup>87</sup>.

HSQC experiments allow identification of lignin substructures because of relentless work of many researchers and groups, synthesizing and analyzing lignin model compounds, which has resulted in an NMR database of lignin and cell wall model compounds<sup>88</sup>. These include the major structural features such as  $\beta$ -aryl ether, phenylcoumaran, and resinol interunit linkages, and more importantly, features that other structural analytical techniques failed to identify, such as dibenzodioxocine and spirodienone interunit linkages<sup>89-91</sup>. Additionally, LCC linkages in wood, such as phenyl glycoside, benzyl ether, and ester bonds have been detected

and quantified in HSQC experiments<sup>44, 92</sup>. Quantification of all these different linkages by HSQC can be difficult, since the volume of correlation peaks depends on factors such as  $T_1$  and  $T_2$  relaxation rates, carbon pulse offset effects, multiplicity and magnitude of coupling constants<sup>40</sup>. A semi-quantitative method has been the most used strategy without an internal standard, where the relative abundance of the signals from the  $\alpha$ -protons of the different substructures is calculated<sup>93, 94</sup>. Since normalization is used in this method, the absolute differences between the substructures are not compared. Quantitative strategy based on HSQC spectra with selected aromatic units as internal standards has been applied for lignin from various types of biomaterial<sup>40, 95</sup>. As an internal standard, this method uses a cluster of signals that are representative of all  $C_9$  lignin units in the sample and therefore depends of the type of biomass analyzed; softwood, hardwood, and grass. Sette *et al.*<sup>40</sup> developed this method for softwood, using the lignin-guaiacyl C2-H cross peak signal as an internal standard to calculate the amount of  $C_9$  units, producing direct, reliable and reproducible quantification of lignin interunit bonding. Comparison of lignin from different types of softwood and lignin isolated with different methods was achieved, with the occurrence of interunit linkages found to agree with previous literature reports. In addition, amount of interunit linkages in MWL from one type of hardwood was evaluated in this study, using the sum of half the syringyl signal plus the  $G_2$  signal as an internal standard. Wen *et al.*<sup>95</sup> used this method in the quantification of grass lignin interunit linkages by adding signals from the hydroxycinnamyl units to the internal standard equation, obtaining structural comparison between differently pretreated bamboo.

### 1.6 This Study and Its Aim

In this study, milled wood lignin (MWL) was isolated from Norway spruce that had been treated with steam explosion. Samples with eight different severities of steam explosion were studied by HSQC and Py-GC-MS. For comparison, MWL from untreated Norwegian spruce was isolated and studied identically. In addition, a part of all purified lignin samples (MWL) were dissolved in tetrahydrofuran (THF) in an attempt for further purification. The THF dissolvable MWL was studied by the same analytical methods.

The aim was to understand how steam explosion pretreatment changes the structure of lignin by analyzing the samples with HSQC and how it effects the product formation during pyrolysis.





## 2. Materials and Methods

### 2.1 Overview of Sample Preparation and Analytical Methods

Graphical overview of the sample preparation and analytical methods is shown in Figure 2.1.

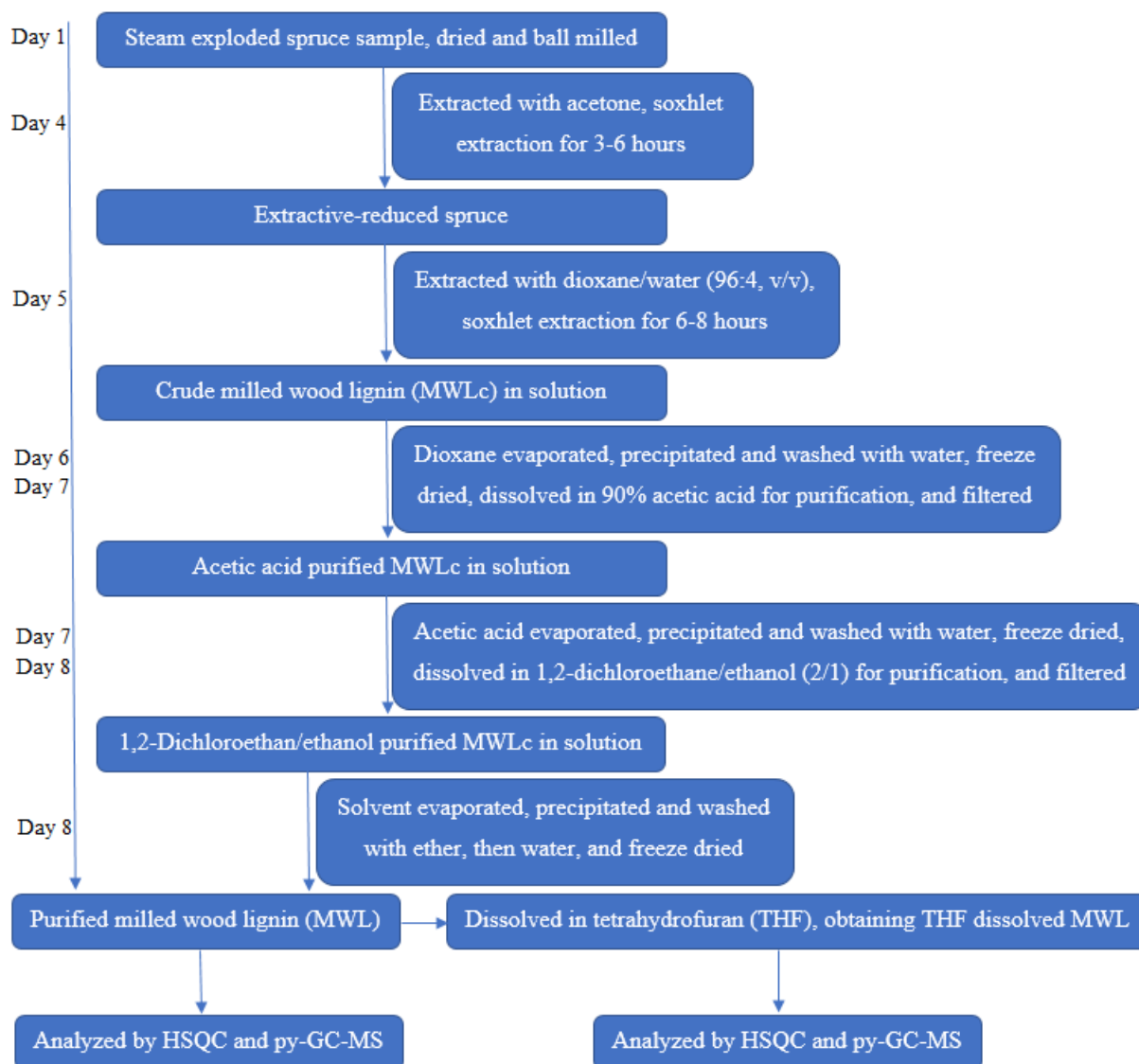


Figure 2.1: Flowchart with an overview of the sample preparation and analytical methods used in the study.

## Materials and Methods

### 2.2 Materials and Equipment

#### 2.2.1 Laboratory Materials

A list of laboratory materials used in the project is presented in Table 2.1.

Table 2.1: Laboratory materials.

Laboratory Material	Producer
NMR tubes 5 mm diam.	Sigma-Aldrich
Weighing sheets, 3 x 3 in.	Schleicher & Schuell
Extraction thimbles, 22 x 80 mm	Schleicher & Schuell
Filter paper, 5-13 µm particle retention	VWR
Pasteur pipettes	VWR
Glass vials with plastic snap caps	VWR
Syringe needles	Becton Dickinson S.A.
Plastic syringes 50 mL	Becton Dickinson S.A.
Conical tubes 50 mL	Greiner Bio One

#### 2.2.2 Chemicals

A list of chemicals used in the project is presented in Table 2.2.

Table 2.2: List of chemicals. The chemicals used in the project with information of purity, quality, producer and CAS no.

Chemical	Purity [%]	Quality	Producer	CAS no.
Acetic acid	≥99.8	p.a.	Honeywell	64-19-7
Acetone	≥99.5	p.a.	Sigma-Aldrich	67-64-1
Carbon dioxide	100	Pure	AGA	124-38-9
1,2-Dichloroethane	≥99.0	ACS Reagent	Sigma-Aldrich	107-06-2
Diethyl ether	≥99.9	For HPLC	Honeywell	60-29-7
Dimethyl sulfoxide-d <sub>6</sub>	100	99.96 atom % D	Sigma-Aldrich	2206-27-1
1,4-Dioxane	≥99	Reagentplus	Honeywell	123-91-1
Ethanol	≥90	GPR Rectapur	VWR	64-17-5
Helium	99.9999	6.0	Yara	7440-59-7
Milli-Q water		Type 2	Millipore	
Nitrogen	99.999	Pure	AGA	7727-37-9
Phosphorous pentoxide	≥98.0	p.a.	Sigma-Aldrich	1314-56-3
Tetrahydrofuran	≥99.9	Anhydrous	Sigma-Aldrich	109-99-9

#### 2.2.3 Standards

Table 2.3 shows compounds that were used as standards for the py-GC-MS analysis. The standards were acquired from Sigma-Aldrich, Steinheim, Germany and VWR. The standard 2-(4-hydroxy-3-methoxyphenyl)acetaldehyde was synthesized.

Table 2.3: Standards used in the py-GC-MS analysis, with vendor information.

Standard	Producer	CAS no.
1,2-Dihydroxybenzene	Sigma-Aldrich	120-80-9
4-Hydroxy-3-methoxybenzaldehyde	Sigma-Aldrich	121-33-5
1-(4-Hydroxy-3-methoxyphenyl)ethanone	Sigma-Aldrich	498-02-2
2-Methoxyphenol	Sigma-Aldrich	90-05-1
2-Methoxy-4-propenylphenol	VWR	97-54-1
2-Methoxy-4-prop-2-enylphenol	VWR	97-53-0
2-(4-Hydroxy-3-methoxyphenyl)acetaldehyde	Synthesized	5703-24-2
2-Methylphenol	Sigma-Aldrich	95-48-7
4-Methylphenol	Sigma-Aldrich	106-44-5

## 2.2.4 Laboratory Equipment

A list of laboratory equipment used in the project is presented in Table 2.4.

Table 2.4: Laboratory equipment.

Laboratory equipment	Specification	Producer
Büchner funnel	Porcelain	Made in England
Centrifuge	Model 5430R	Eppendorf Research
Condenser		Normschliff Gerätebau Wertheim
Extraction tube	Quickfit, England	SciLabware
Filter flask	Duran 250 mL	Schott, Germany
Freeze dryer	Alpha 2-4 LDplus	Christ GmbH
Grinding bowl	500 mL zirconium oxide bowl	Retsch GmbH
Hot plate magnetic stirrer	Model VMS-A	VWR
Measuring cylinders	10 mL and 250 mL	VWR
Milling balls	0,5 cm diameter ZrO <sub>2</sub> balls	Retsch GmbH
Planetary ball mill	Planetary Ball Mill PM100	Retsch GmbH
Round flasks	Pyrex quickfit UK	SciLabware
Thermometer	Assistant	Glaswarenfabrik Karl Hecht
Three-way adaptor	Quickfit, England, SH 4/23	SciLabware
Vacuum adapter	Quickfit, England, RA 3/23	SciLabware
Vacuum desiccator		Glaswerk Wertheim
Weighing scale	Model CP2245	Sartorius
Weighing scale	Model CP2P	Sartorius

## 2.2.5 Steam Explosion Unit

Figure 2.2 is a schematic representation of the steam explosion unit (Cambi, Asker, Norway) used in the spruce pretreatment. It consists of a 20 L pressure vessel and a flash tank with a removable bucket to collect the pretreated material. Function of the steam explosion unit is described thoroughly by Horn *et al.*<sup>96</sup>

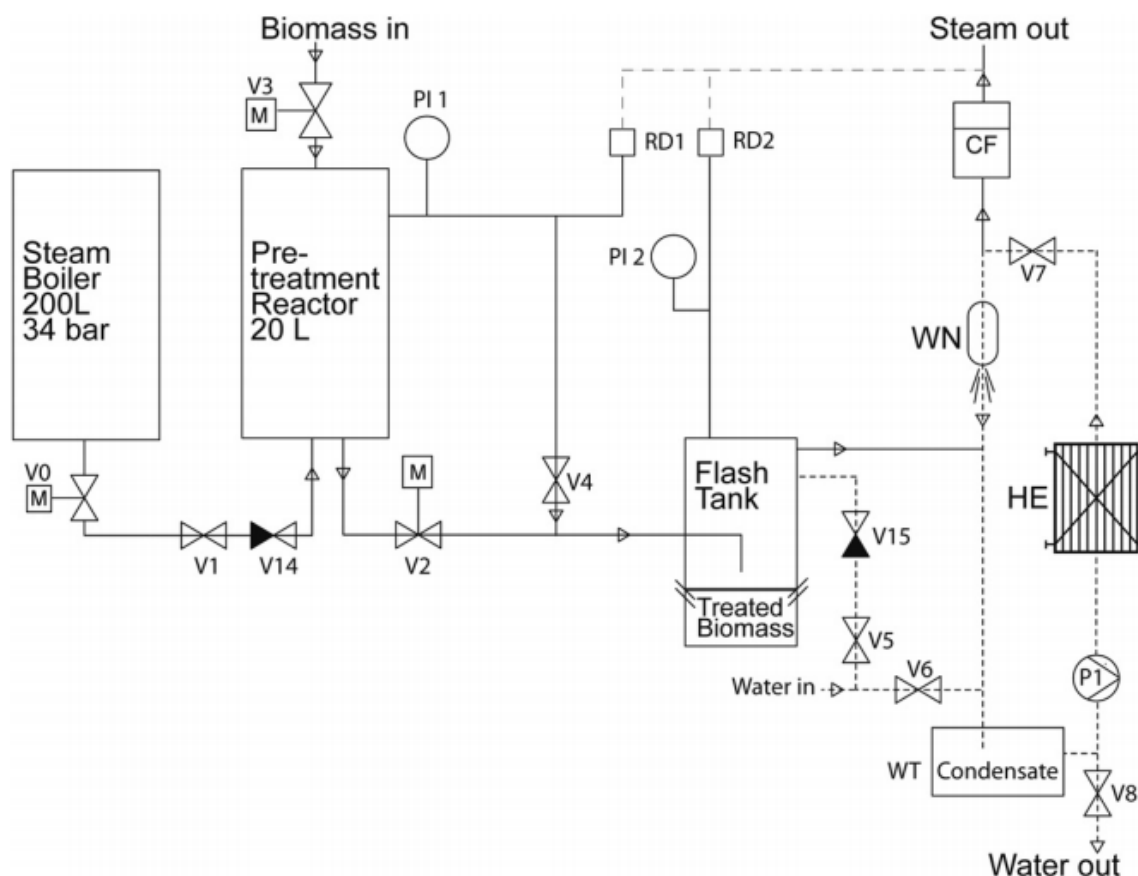


Figure 2.2: The steam explosion unit. “V” refers to valves, and “M” to motorized valves. “PI 1” and “PI 2” are manometers used to measure pressure. “RD1” and “RD2” are safety valves that open if the pressure reaches certain thresholds. “CF”, carbon filter; “WN”, water nozzle; “HE”, heat exchanger; “WT”, water tank; “P1”, pump. Valves with solid triangles (V14 and V15) indicate one way valves. Dotted lines in the bottom right corner indicate water flow. Valves V6 and V8 are used to regulate the amount of water in WT. Valve V7 may be used to close the water circuit. See section 2.2 in the study by Horn et al.<sup>96</sup>. Reprinted from Horn et al.<sup>96</sup>

### 2.2.6 Setup of the Extraction and Vacuum Distillation Equipment

Figure 2.3 shows the setup of the extraction and vacuum distillation equipment used in the study. For the extraction, the sample is placed in the extraction thimble and the extraction solvent boiled, its vapor reaching the extraction tube and condensing due to the flow of cold water through the condenser. When the extraction tube has been filled with warm solvent, it flows down the siphon arm to the boiling flask. The circulation continues as long as the solvent is boiling. The extraction is performed under nitrogen flow. For the vacuum distillation, the solution is evaporated from the distilling flask to the receiving flask via the condenser. The solution is boiled by warming under low air pressure by suction of air through the vacuum inlet. The condensation systems are connected by a water hose, allowing

distillation and extraction of two different samples at the same time, using only one water source.

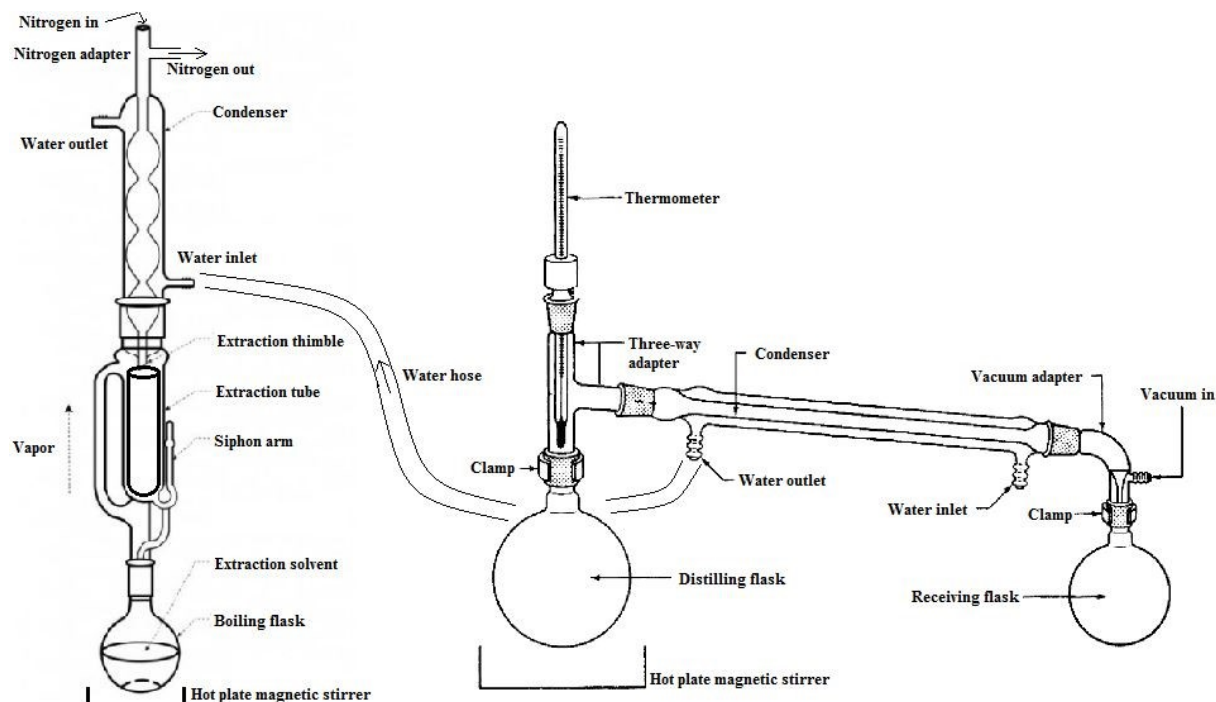


Figure 2.3: Setup of the extraction and vacuum distillation equipment. See section 2.2.6 for description of the setup and its function.

### 2.2.7 Raw Material

Stem wood from Norway spruce (*Picea abies*) without bark was shredded (20-30 mm chips), packed and shipped to the Norwegian University of Life Sciences, Ås, Norway. The wood was dried at room temperature, using a drum dryer, then milled to pass a sieve of 6 mm (SM2000, Retsch GmbH, Haan, Germany), and stored at room temperature. The dry matter content (DM) of the milled material was 85-90%.

## 2.3 Synthesis of 2-(4-Hydroxy-3-methoxyphenyl)acetaldehyde

The following synthesis was performed by Ida Aarum at the Norwegian University of Life Sciences, Ås.

The standard, 2-(4-hydroxy-3-methoxyphenyl)acetaldehyde was synthesized from 2-methoxy-4-(prop-2-en-1-yl)phenol (500 mg, 3.045 mol) in 14 mL 1,4-dioxane:water (3:1) by adding 2,6-dimethylpyridine (653 mg, 6.09 mmol), osmium tetroxide solution in 2.5 wt.% *t*-butanol (630  $\mu$ L) and sodium periodate (2.6 g, 12 mmol) to the solution. The reaction was

## Materials and Methods

stirred at ambient temperature for 1.5 h and monitored by thin-layer chromatography, until completed. The reaction was quenched by adding dichloromethane:water (2:1, 30 mL), and the organic layer was separated. The water phase was extracted three times and the organic layers were combined, washed with saturated aqueous sodium chloride solution and dried with sodium sulfate. The organic layer was filtered through a Hirsch funnel with a layer of deactivated silica gel (10% v/v of triethylamine), before evaporation.

### 2.4 Sample Preparation

#### 2.4.1 Steam Explosion Pretreatment of Norway Spruce

The following steam explosion procedure was performed by Dayanand Kalyani at the Norwegian University of Life Sciences, Ås.

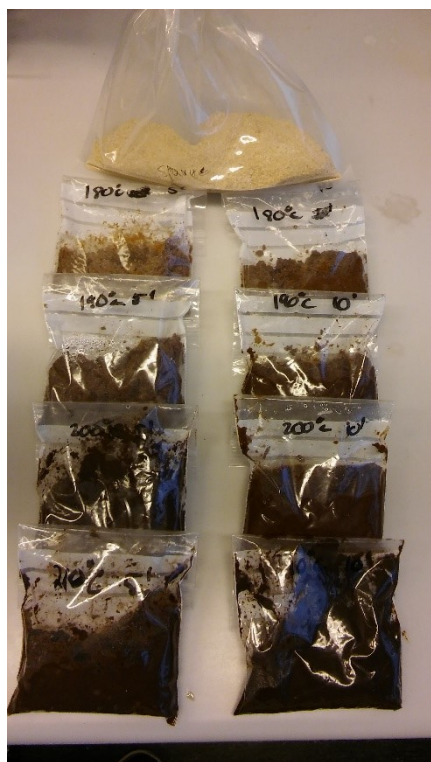


*Figure 2.4: The spruce samples used in the study. The untreated spruce is at the top of the figure. To the left are the SE treated samples using 5 min residence time and to the right, samples treated for 10 min.*

Before the steam explosion (SE) pretreatment, the milled spruce was pretreated by acid catalysis under mild conditions. The spruce sample was presoaked in a dilute sulfuric acid solution, 0.5 % solids (w/w) at room temperature overnight. The steam explosion pretreatment was performed as described previously<sup>96</sup> using the facility designed by Cambi AS, Asker, Norway. Three hundred grams dry matter (DM) of dilute sulfuric acid treated spruce were added to the pressure vessel for different pretreatment conditions. The spruce was pretreated at temperatures from 180 °C to 210 °C using intervals of 10 °C. The residence time was 5 and 10 min, resulting in eight different samples. Prior to each pretreatment, the pressure vessel was preheated for 10 min at same temperature as the pretreatment temperature. The pretreated fractions were stored at 4 °C. The dry matter (DM) content of the steam exploded samples was in the range of 20-31%. Figure 2.4 shows the untreated spruce and all the eight steam exploded spruce samples used in the study. The color of the samples becomes darker with increased severity of the steam explosion.

## 2.4.2 Sample Preparation of Milled Wood Lignin

The preparation of the milled wood lignin samples was performed with the Björkman method<sup>47,97</sup>. MWL was prepared from all the eight steam exploded spruce samples, two parallels for each sample. For comparison, MWL was prepared from untreated spruce, two parallels. All eighteen MWL samples were prepared according to the sample preparation described in the chapters below, except the untreated spruce did not need drying before the ball milling.

### 2.4.2.1 Drying and Milling of the Spruce Samples

Approximately 10 g of wet, steam exploded spruce sample was dried in a vacuum desiccator with silica gel as drying agent (Figure 2.5). Phosphorous pentoxide ( $P_4O_{10}(s)$ )



Figure 2.5: SE spruce sample drying in a vacuum desiccator. The sample is to the left and the phosphorous pentoxide drying agent is to the right. The silica gel is in the chamber below.

drying agent was placed in a small glass bowl and put in the desiccator for more effective drying. After 24 to 48 hours of drying, the glass bowl was removed from the desiccator and another portion of phosphorous pentoxide added to ensure the dryness of the sample. After 24 hours, the sample was transferred into a 500 mL grinding bowl of zirconium oxide ( $ZrO_2$ ) and milling balls (0,5 cm diameter)

added. The bowl was placed in a milling instrument (Planetary Ball Mill PM 100, Retsch GmbH, Haan, Germany), and the program set on 350 rpm for 16 h, with 15 min on/off increments.

### 2.4.2.2 Extraction

Soxhlet extraction was performed on the ball milled spruce, first by using acetone as a solvent to remove extractives from the wood powder, and then to extract lignin from the wood by using 1,4-dioxane/water (96:4, v/v) as a solvent. An overview of both the extractions for each sample is given in Table 2.5.



Table 2.5: An overview of the extractions; color of the solution in the extraction tube and duration of each extraction.

Sample	Acetone extraction		Dioxane/water extraction	
	Color	Duration	Color	Duration
No pretreatment	Very light brown	3h	Yellow	6h
180°C for 5min	Light yellow	3h	Yellow/brown	6h
190°C for 5min	Light brown/yellow	3h	Brown/yellow	6h
200°C for 5min	Brown/yellow	4h	Dark brown	6h
210°C for 5min	Brown	4h	Dark brown	6h
180°C for 10min	Light brown	3h	Brown	6h
190°C for 10min	Brown	4h	Brown	6h
200°C for 10min	Brown	4h	Dark brown	6h
210°C for 10min	Dark brown	6h	Dark Brown	8h

The ball milled wood was removed from the grinding bowl and weighed into an extraction thimble. Soxhlet extraction was performed with 60-70 mL of acetone as a solvent to remove extractives from the wood. For the untreated spruce and the spruce that had been treated at lower temperatures the solution became yellow or light brown, but for the samples treated with increased severity of the steam explosion, the solution became darker. The extraction

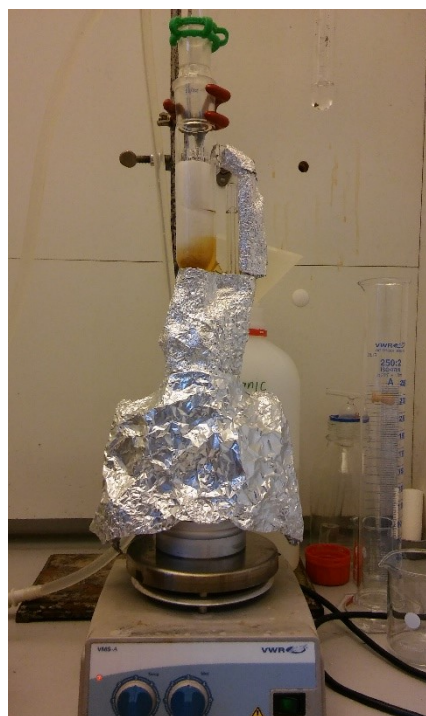


Figure 2.6: Extraction of lignin from untreated spruce sample using 1,4-dioxane/water (96:4, v/v) as a solvent.

was continued until the color of the solution in the extraction tube became clear or almost clear. Duration of the extraction was 3-4 h, depending on the pretreatment severity, except for the sample that was treated under the most severe conditions, which needed 6 h extraction. The samples were then dried at room temperature for minimum 16 h.

Soxhlet extraction was performed with 70-80 mL of 1,4-dioxane/water (96:4, v/v) as a solvent to extract lignin from the wood sample. For the untreated spruce, the solution became yellow (Figure 2.6). For the least severely treated steam exploded spruce, the solution became brown/yellow, but dark brown for the steam exploded spruce that was most severely treated. The extraction was continued until the color of the solution in the extraction

tube became clear or almost clear. Duration of the extraction was 6 h, except for the sample that was treated under the most severe conditions, which needed 8 h extraction. The lignin containing solution cooled down overnight.

### 2.4.2.3 Purification

The purification of the lignin containing solution was performed in three steps, that all included precipitation of lignin, evaporation of a solvent, and exchanging solvent with water before freeze drying.

In the first step, the solution that contained lignin, water, and 1,4-dioxane was transferred into a round flask and the lignin precipitated by adding water. Vacuum distillation was performed to evaporate the solution to 20 mL. Another portion of water (50-100 mL) was added to wash the solution and it evaporated to 20 mL. This was repeated 1-3 times, or until 1,4-dioxane was exchanged with water. After that, 50-100 mL portion of water was added and the flask swirled in a dry ice/ethanol bath until the water was frozen. Finally, the round flask was placed in a freeze dryer, where the solid material dried in 16-48 h.

The round flask containing crude milled wood lignin (MWLc) was removed from the freeze dryer and the MWLc dissolved in 90% acetic acid. The solution was filtered (Qualitative filter paper 303, 5-13  $\mu\text{m}$ , VWR) by suction filtration using Büchner funnel and

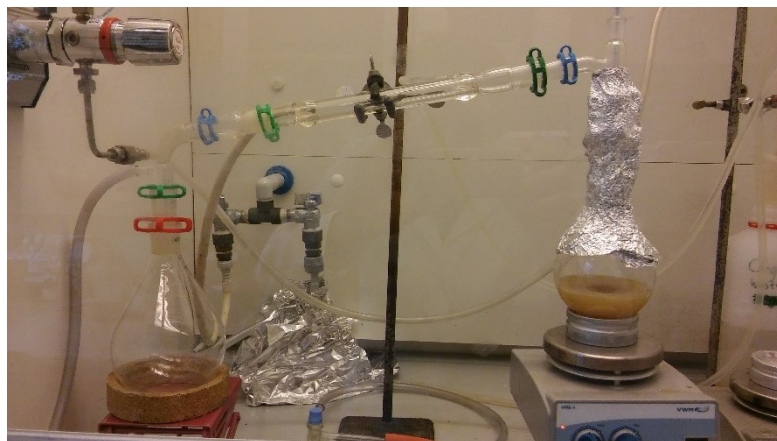


Figure 2.7: Vacuum distillation of acetic acid/water solution in the purification process of MWL.

transferred into a round flask. Water was added to precipitate the lignin and vacuum distillation was performed (Figure 2.7) until 15 mL remained in the flask. Another portion (50-100 mL) of water was added to wash the solution and it evaporated to 15 mL.

This was repeated 1-3 times, or until acetic acid was exchanged with water, before freezing it in dry ice/ethanol bath and placing the flask in a freeze dryer.

In the final step, the lignin was dissolved in 1,2-dichloroethane/ethanol (2:1, v/v), filtered by suction filtration and transferred into a round flask. Diethyl ether was added to precipitate

## Materials and Methods

the lignin and vacuum distillation was performed until 15 mL remained in the flask. Another portion of diethyl ether (50-100 mL) was added for washing and the solution evaporated to 15 mL. This was repeated 1-3 times to remove 1,2-dichloroethane. Then, a portion of water (50-100 mL) of water was added and the solution evaporated until containing only water and lignin. After freezing the contents in a dry ice/ethanol bath, the flask was placed in a freeze dryer. When dry, the purified milled wood lignin (MWL) was weighed into a snap cap vial. The vial was stored in a vacuum desiccator at room temperature.

### 2.4.3 Sample Preparation of THF Dissolvable Lignin

An attempt was made to purify the MWL samples further by dissolving a part of all the samples in THF. This attempt was inspired by an article by Shuai *et al.*<sup>98</sup>, in which the dried residue from a dioxane extracted lignin from beach wood was dissolved in THF to extract lignin, leaving carbohydrates as precipitates.

A portion (50-100 mg) of the MWL was removed from the snap cap vial and weighed in a 50 mL conical tube. Then, 20 mL of THF was added and the contents mixed thoroughly. The tube was placed in a centrifuge (Centrifuge 5430R, Eppendorf) and the program set on 5 min at 6500 rpm. The solution was transferred into a round flask and evaporated to 5 mL by vacuum distillation. A portion of water (20 mL) was added and the solution evaporated until THF was removed. The flask was placed in a freezer until the water was frozen, before placing it in a freeze dryer.

## 2.5 Analysis

In this work, two methods were used for the analysis of both the purified milled wood lignin samples and the THF dissolvable MWL samples. One of the methods was degradative, py-GC-MS, and the other was non-degradative, HSQC. The volatile pyrolyzates of dry lignin powder were analyzed by py-GC-MS while the structural analysis of lignin dissolved in dimethylsulfoxide- $d_6$  (DMSO- $d_6$ ) was performed with HSQC experiments.

### 2.5.1 HSQC Experiments

HSQC experiments were performed on all the samples for the structural analysis of lignin. For the first parallel of the MWL isolated from the steam exploded spruce samples and both parallels of the MWL from untreated spruce, 15 mg of MWL sample were dissolved in 0,5 mL of DMSO-d<sub>6</sub> for the HSQC experiments. In the attempt to obtain more detailed signals, HSQC experiments were performed using 20 mg of sample in 0,5 mL DMSO-d<sub>6</sub> for the MWL from the second parallel of the steam exploded spruce samples. The same amount of sample was used for the analysis of the THF dissolved MWL in the attempt to obtain more details on the aromatic region. One experiment was performed for each sample and the duration of each experiment was over sixteen hours. For the quantitative HSQC experiments of the MWL second parallels, 60 mg of sample in 0,5 mL DMSO-d<sub>6</sub> were used and each experiment performed three times on the same sample. Table 2.6 and Table 2.7 show an overview of the HSQC experiments performed for each lignin sample.

Table 2.6: Overview of the HSQC experiments performed in the study. MWL.

MWL	Parallel I		Parallel II	
	C <sub>sample</sub> (g/L)	n <sub>experiments</sub>	C <sub>sample</sub> (g/L)	n <sub>experiments</sub>
No pretreatment	30	1	30,120	1,3
180°C for 5min	30	1	40,120	1,3
190°C for 5min	30	1	40,120	1,3
200°C for 5min	30	1	40,120	1,3
210°C for 5min	14	1	40,120	1,3
180°C for 10min	30	2	40,120	1,3
190°C for 10min	30	1	40,120	1,3
200°C for 10min	30	1	40,120	1,3
210°C for 10min	30	1	40,120	1,3

Table 2.7: Overview of the HSQC experiments performed in the study. THF dissolvable MWL.

THF dissolvable MWL	Parallel I		Parallel II	
	C <sub>sample</sub> (g/L)	n <sub>experiments</sub>	C <sub>sample</sub> (g/L)	n <sub>experiments</sub>
No pretreatment	-	-	40	1
180°C for 5min	-	-	40	1
190°C for 5min	-	-	-	-
200°C for 5min	-	-	-	-
210°C for 5min	-	-	-	-
180°C for 10min	40	1	40	1
190°C for 10min	40	1	40	1
200°C for 10min	30	1	40	1
210°C for 10min	40	1	40	1

## Materials and Methods

### *2.5.1.1 Quantitative HSQC Experiments*

The NMR spectra were acquired at 300K using a Bruker ASCEND 400 spectrometer equipped with a 5 mm PABBO probe. For the quantitative HSQC experiments, 60 mg of sample was dissolved in 0.5 mL DMSO-d<sub>6</sub>. The Bruker pulse program hsqcedetgpsisp2.3 was used. The NMR spectra were recorded with a spectral width of 0-10 ppm and 0-165 ppm for <sup>1</sup>H and <sup>13</sup>C respectively. The number of scans for both were 128. For the <sup>1</sup>H-<sup>13</sup>C parameters, the relaxation delay was 1.5 s and the free induction decay dimensions were 2048 and 256, while the number of scans were 120. Data from the experiments was processed using Topspin 3.5p16 (Bruker) after Fourier transformation. The frequency axis was calibrated manually according to the ppm values of the reference peak, DMSO-d<sub>6</sub>, at 2.50 and 39.51 for x and y axis respectively. Phase correction, including baseline correction, was applied in both dimensions. The final matrix consisted of 2048 x 2048 points and cross-peaks were integrated with the same software that allows the typical shape of peaks present in the spectrum to be taken into account. Error analysis was performed by acquiring the same experiment three times on the same sample.

### *2.5.1.2 HSQC Spectra Demonstrating the Change by Increasing Sample Concentration*

The HSQC experiments were performed for all the lignin samples as described in section 2.5.1.1, except for the amount of sample dissolved in 0.5 mL DMSO-d<sub>6</sub>. Figure 2.8 and Figure 2.9 demonstrate the difference between the spectra obtained by using 60 mg sample and 15 mg sample.

Figure 2.8 shows the sidechain region ( $\delta_C/\delta_H$  50-90/2.7-5.7) for MWL from the untreated spruce sample. Signals representing the most common C-H correlations in lignin are clear and easily detected in both spectra. However, some of the signals representing important C-H correlations in lignin substructures are weak and irregular in shape for the 40 mg/mL sample, for example at  $\delta_C/\delta_H$  53.4/3.06 (C <sub>$\beta$</sub> -H <sub>$\beta$</sub>  in resinol substructures), but the same signals for the 120 mg/mL sample are clear and regularly shaped. In addition, signals for C-H correlations in very low abundant substructures (not shown in the figures) could only be detected in the 120 mg/mL sample.

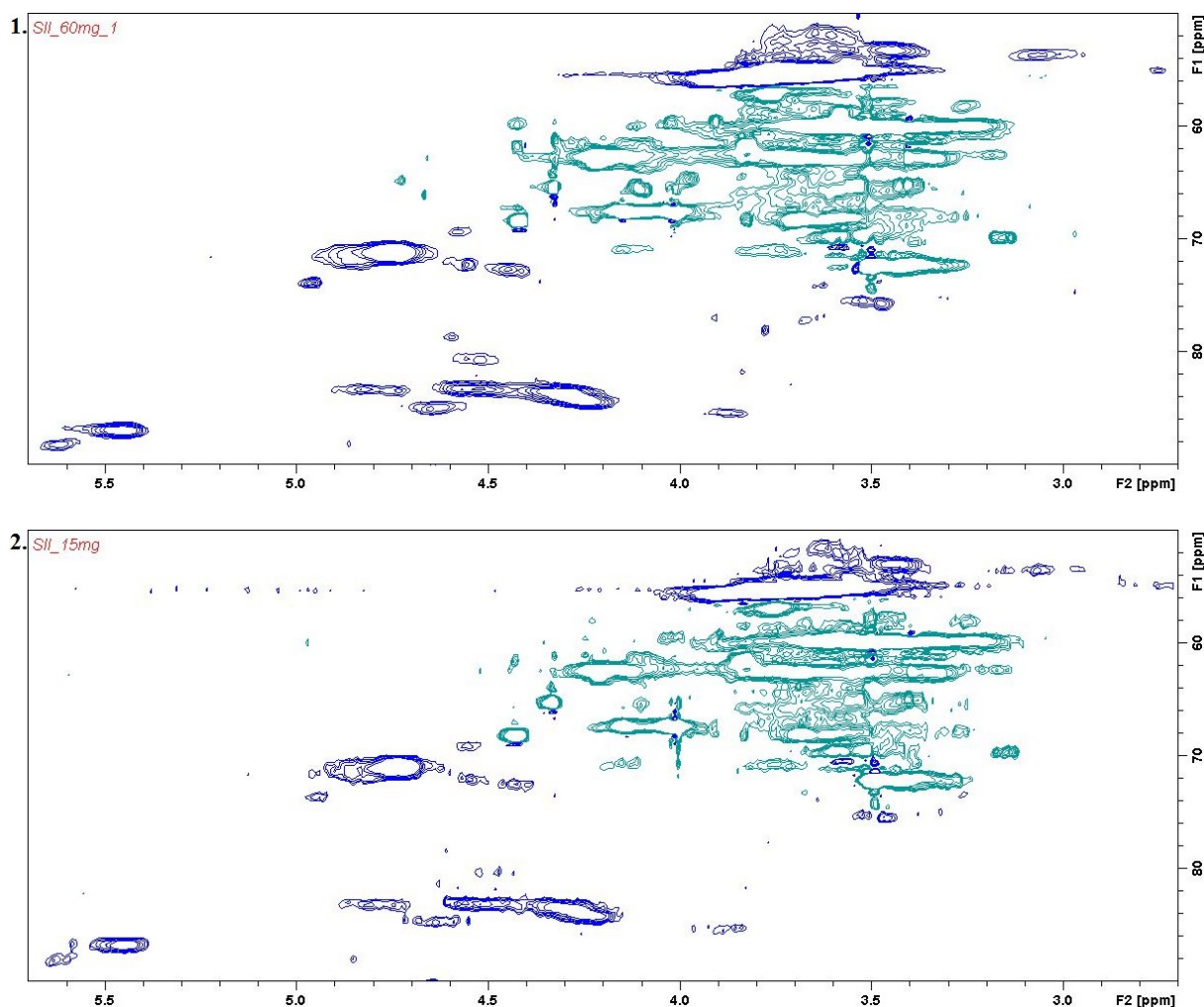


Figure 2.8: HSQC spectra of MWL from untreated spruce dissolved in DMSO- $d_6$ , 120 mg/mL (1) and 30 mg/mL (2). The spectra display the side chain region ( $\delta_C/\delta_H$  50-90/2.7-5.7).

Figure 2.9 shows the aromatic region ( $\delta_C/\delta_H$  105-135/6.2-7.9) for MWL from the untreated spruce sample. As seen in the sidechain region, both spectra show the most common C-H correlations in lignin. However, the identification of C-H correlations from low abundant lignin substructures is difficult for the 40 mg/mL sample. Some of the signals representing C-H correlations in lignin substructures are barely detected and could easily be identified as noise, for example at  $\delta_C/\delta_H$  128.5/6.44 ( $C_\alpha$ - $H_\alpha$  in *p*-hydroxycinnamyl alcohol end groups), but the same signals for the 120 mg/mL sample are clear and regularly shaped. Additionally, signals from some of the low abundant C-H correlations, such as the signal at  $\delta_C/\delta_H$  131/7.7 ( $C_{2,6}$ - $H_{2,6}$  in *p*-hydroxybenzoate substructures), are only detected in the 120 mg/mL sample.

## Materials and Methods

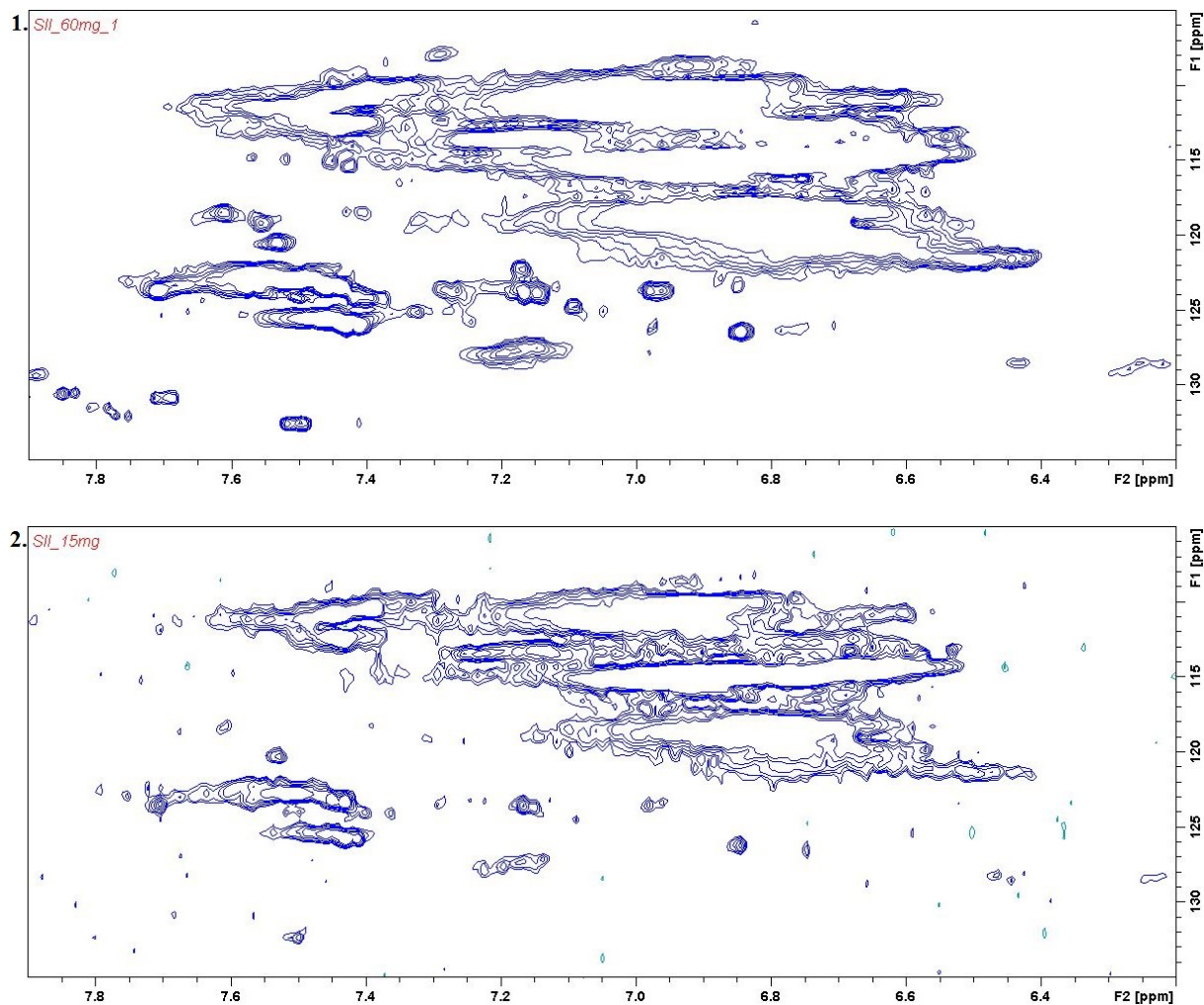


Figure 2.9: HSQC spectra of MWL from untreated spruce dissolved in DMSO- $d_6$ , 120 mg/mL (1) and 30 mg/mL (2). The spectra display the aromatic region ( $\delta_C/\delta_H$  105-135/6.2-7.9).

### 2.5.2 Py-GC-MS Analysis

The flash filament Pyrola 2000 pyrolyzer (Pyrol AB, Lund, Sweden) was coupled to a GC-MS instrument (7000C Triple Quadruple GC/MS System from Agilent Technologies) to identify the volatile pyrolyzates generated from fast pyrolysis of lignin at isothermal temperature. Approximately 0.2  $\mu\text{g}$  of dry lignin powder was placed on the platinum filament. Flash pyrolysis was performed with the isothermal temperature set on 600  $^\circ\text{C}$  and heating rate of 175 000  $^\circ\text{C}/\text{s}$ . The temperature rise time was 8 ms and the total pyrolysis time was 2 s. The volatile pyrolyzates were separated in a capillary column (TraceGOLD TG1701MS, Thermo Fisher Scientific), with 60m length, inner diameter of 0.25 mm, and 0.25  $\mu\text{m}$  film thickness. The carrier gas was helium and its flow set on 1.0 mL with the split ratio 10:1.

## Materials and Methods

The GC temperature program used was 76.35 minutes in duration. The injector temperature was 250 °C. The GC oven temperature was initially set on 50 °C and held for 15 min. The temperature was programmed to rise from 50 °C to 130 °C at the rate 10 °C/min, then to 216 °C at the rate of 2 °C/min, and held at 216 °C for 2 min. Then it was programmed to rise to 270 °C at the rate of 40 °C/min and held at 270 °C for 7 min. A graphical representation of the temperature program is shown in Figure 2.10.

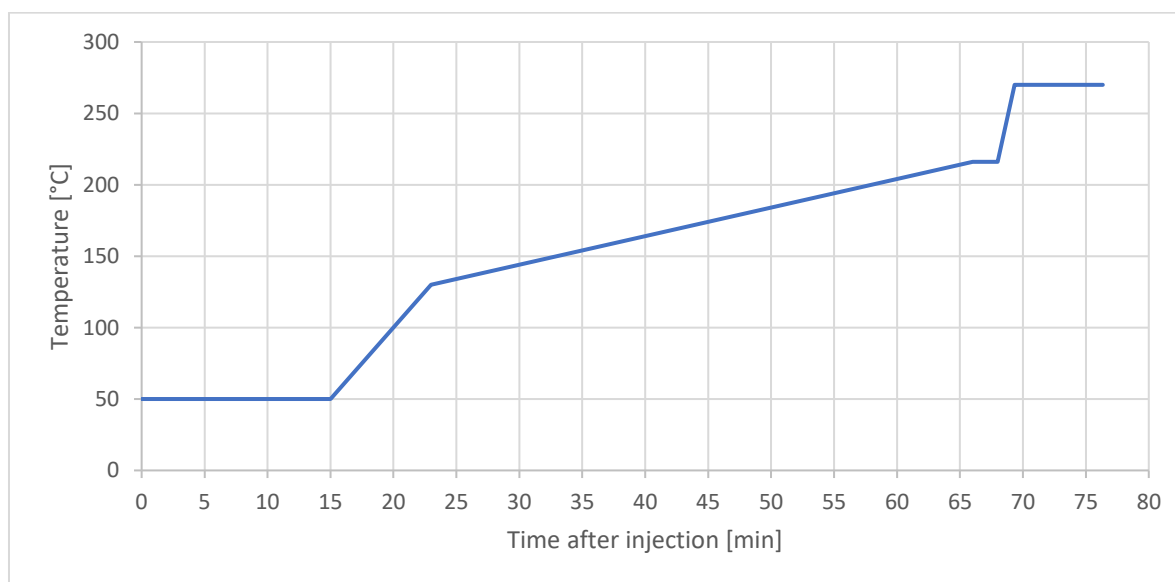


Figure 2.10: The temperature program for the GC/MS method used in the separation of the pyrolyzates from the lignin samples.

The mass spectra were obtained using an electron ionization source in positive mode, producing 70 eV electrons. The source temperature was 230 °C and the quadrupole was scanned from  $m/z$  40 to 700. The compound identification was performed by using NIST 11 mass spectral database and by comparing the retention times with the standards. For the semi-quantitative analysis, the identified peaks were integrated and the total sum of the areas used to calculate the relative amount for each compound.



## Materials and Methods

## 3. Results and Discussion

### 3.1 Lignin Yield

#### 3.1.1 Yield of MWL isolated from untreated and steam exploded spruce

The milled wood lignin yield from the untreated spruce was 6.1% for parallel 1 and 6.8% for parallel 2 as shown in Table 3.1. A yield of this magnitude was expected considering the theoretical amount of lignin in spruce and the reported yields for the isolation method used. The amount of lignin in spruce has been determined 25-30%<sup>99</sup> using the Klason method and the MWL isolation method yields up to 32% of the total lignin content for various wood species<sup>48</sup>. The expected yield would then be up to 8% for wood sample containing 25% lignin, and up to 10% for wood sample containing 30% lignin. However, after pretreatment of wood, the structural changes allow more lignin to be obtained with isolation methods.

Table 3.1: Yield of MWL isolated from the untreated and steam exploded spruce samples.

MWL	Parallel I			Parallel II		
	$m_{\text{sample}}$ [g]	$m_{\text{lignin}}$ [g]	yield [%]	$m_{\text{sample}}$ [g]	$m_{\text{lignin}}$ [g]	yield [%]
<b>No pretreatment</b>	3.137	0.191	6.1	3.175	0.215	6.8
<b>180°C for 5min</b>	2.437	0.284	11.7	1.461	0.218	14.9
<b>190°C for 5min</b>	0.661	0.125	18.9	2.937	0.387	13.2
<b>200°C for 5min</b>	1.693	0.156	9.2	2.909	0.608	20.9
<b>210°C for 5min</b>	0.783	0.012	1.5	3.226	0.477	14.8
<b>180°C for 10min</b>	1.605	0.315	19.6	2.170	0.230	10.6
<b>190°C for 10min</b>	2.155	0.209	9.7	2.175	0.403	18.5
<b>200°C for 10min</b>	2.710	0.082	3.0	2.706	0.352	13.0
<b>210°C for 10min</b>	1.755	0.128	7.3	3.090	0.403	13.0

The milled wood lignin yield from the steam exploded wood was up to 20%, but down to 1.5% for the first parallel of the sample that was treated at 200 °C for 5 minutes. The first parallels provided generally lower yields than the second parallels. Probable reasons for low yields for most of the first parallels were encountered problems during the sample preparation of MWL, including difficulties during vacuum distillation and filtration. Additionally, the MWL amount obtained was barely enough for analysis and dissolving in THF for some of the samples. With more repetitions, the sample preparation became more stable and the yield for each of the second parallels was over 10%. The 10-20% yield was somewhat expected. Li *et al.*<sup>33</sup> isolated MWL from steam exploded aspen wood, pretreated at five different severities from 185 °C (5 min residence time) to 220 °C (10 min residence time), resulting in 10.5-

## Results and Discussion

19.5% yield. However, a trend of increased yield with increasing severity was observed, but the severity of the SE treatment in the present study did not affect the yield. In addition, the MWL amount obtained was over 0.2 g for each sample, providing enough sample for analysis and dissolving in THF.

Due to the increased stability in the sample preparation of the second parallels compared to the first parallels, the purified milled wood lignin (MWL) obtained from the second parallels was more representative for the samples. Therefore, the results from both the py-GC-MS and the HSQC experiments for MWL were interpreted only from the second parallels.

### 3.1.2 Yield of THF dissolvable MWL

The yield of THF dissolvable MWL was surprisingly inconsistent as shown in Table 3.2, ranging from 36% for the second parallel of the MWL isolated from the 210 °C for 10 min sample to 82% for the second parallel of the MWL isolated from the 180 °C for 10 min sample. Despite relatively simple and short sample preparation, the yield was inconsistent for parallels of the MWL isolated from the same sample, for example 43% and 81% for the 190 °C for 5 min sample. For those samples that in theory should give the similar yield, large differences in THF dissolvability may indicate some differences between the parallels or inconsistency in the sample preparation.

Table 3.2: Yield of THF dissolvable MWL.

THF dissolvable MWL	Parallel I			Parallel II		
	m <sub>sample</sub> [g]	m <sub>lignin</sub> [g]	yield [%]	m <sub>sample</sub> [g]	m <sub>lignin</sub> [g]	yield [%]
No pretreatment	0.100	0.071	71	0.095	0.058	61
180°C for 5min	-	-	-	0.101	0.074	73
190°C for 5min	0.098	0.042	43	0.113	0.092	81
200°C for 5min	-	-	-	0.107	0.051	48
210°C for 5min	0.093	0.048	52	0.098	0.065	66
180°C for 10min	0.087	0.048	55	0.113	0.093	82
190°C for 10min	0.045	0.017	38	0.095	0.071	75
200°C for 10min	0.062	0.048	77	0.110	0.057	52
210°C for 10min	0.093	0.046	49	0.092	0.033	36

Despite this inconsistency, the amount of the THF dissolvable MWL obtained from the second parallels of MWL was enough for analysis, with the lowest 33 mg for the 210 °C for

10 min sample. Also, the THF dissolvable MWL yield was generally higher for the second parallels compared to the first parallels and the amount obtained from the first parallels was enough for HSQC analysis for only six of nine samples. Therefore, the results from both the py-GC-MS and the HSQC experiments were interpreted only for THF dissolvable MWL from the second parallels.

### 3.2 HSQC Experiments

#### 3.2.1 Identification of $^{13}\text{C}$ - $^1\text{H}$ correlations in HSQC spectra

$^{13}\text{C}$ - $^1\text{H}$  correlations in HSQC spectra of both the MWL and THF dissolvable MWL samples were identified and assigned to known substructures and structural units of lignin. Assignment of the signals was according to recent literature<sup>45, 78, 92, 100, 101</sup> and the NMR database of lignin and cell wall model compounds. Figure 3.1 shows examples of typical HSQC spectra ( $\delta_{\text{C}}/\delta_{\text{H}}$  35-135/2.4-8.0) of MWL from untreated spruce (1) and MWL from steam exploded spruce (2). As expected, the SE spectrum shows more blue signals (C-H and C-H<sub>3</sub> correlations), probably due to increased amount of methyl groups after bond breaking in the SE treatment. Fewer green signals (C-H<sub>2</sub> correlations) supports this claim. For the signal identification, a closer look at spectra is needed, dividing it into side chain region ( $\delta_{\text{C}}/\delta_{\text{H}}$  50-90/2.7-5.7) and aromatic region ( $\delta_{\text{C}}/\delta_{\text{H}}$  105-135/6.2-7.9). Figure 3.2 shows all the lignin substructures and structural units identified in the HSQC experiments performed in the study.

## Results and Discussion

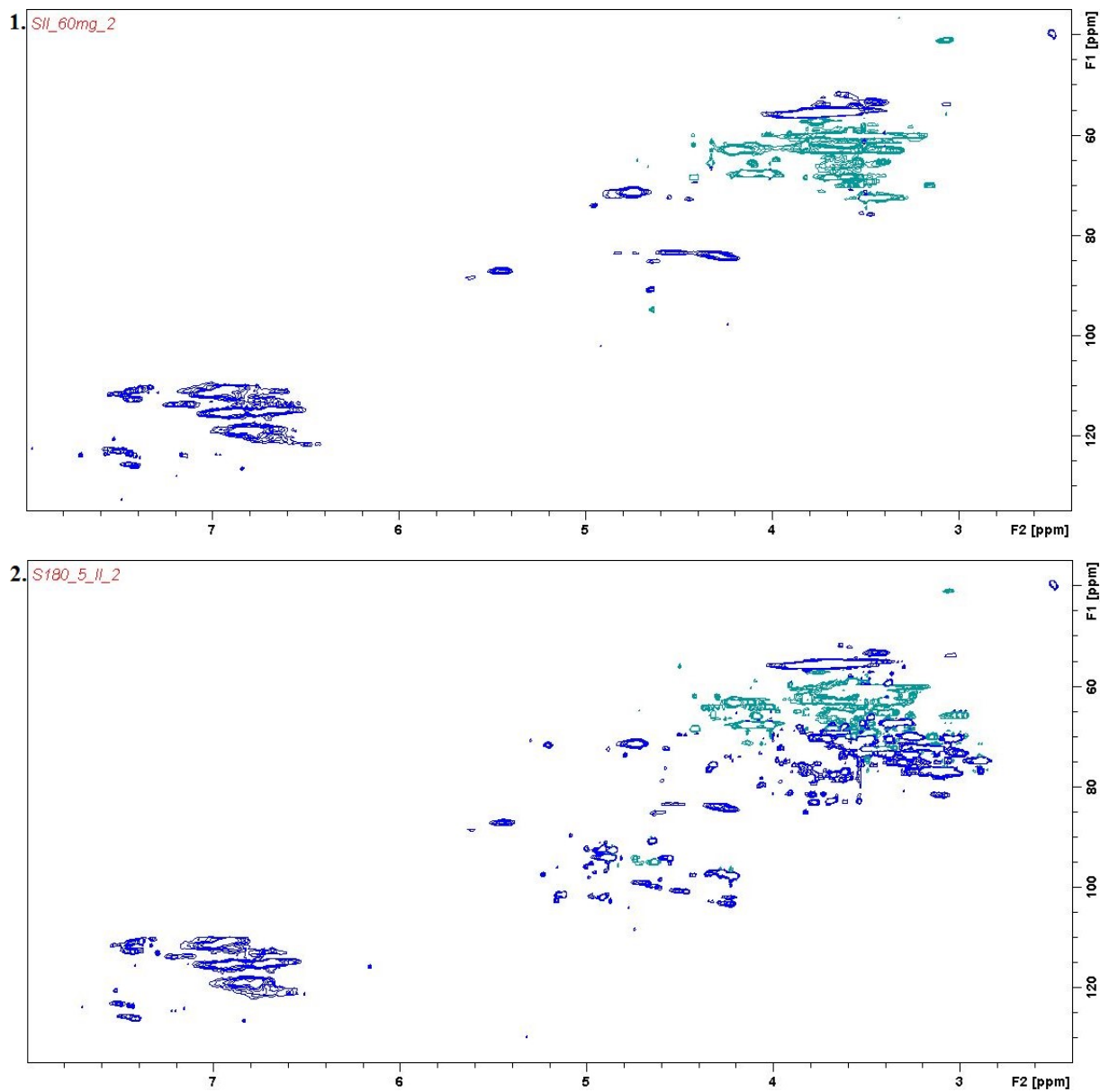


Figure 3.1: HSQC spectra of MWL from untreated spruce (1) and SE (180 °C for 5 min) spruce (2). Green signals represent C-H<sub>2</sub> correlations and blue signals represent C-H and C-H<sub>3</sub> correlations.

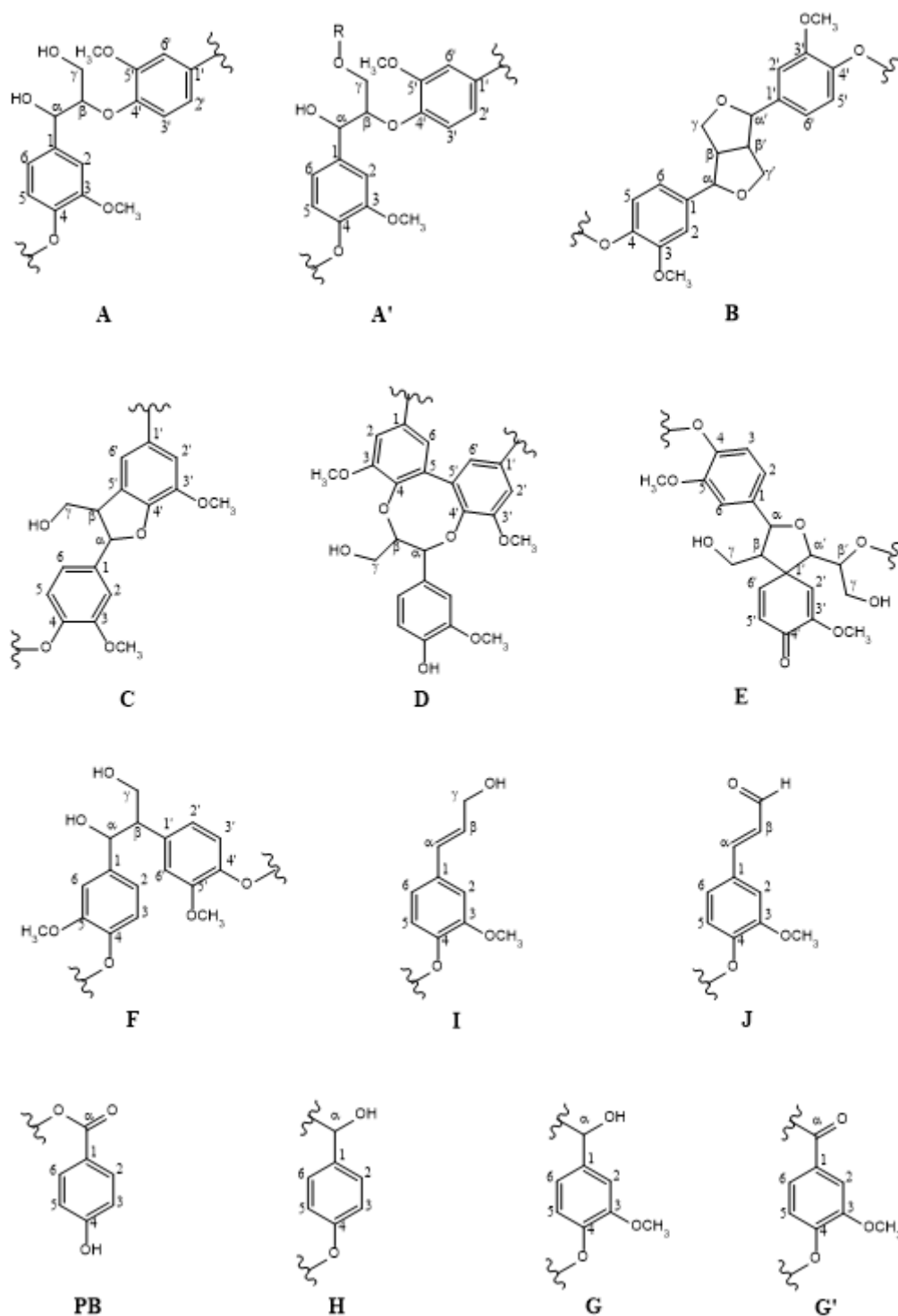


Figure 3.2: Lignin substructures and structural units identified by HSQC experiments in the study: (A)  $\beta$ -O-4' aryl ether linkages with free -OH at the  $\gamma$ -carbon; (A')  $\beta$ -O-4' aryl ether linkages with acylated -OH at the  $\gamma$ -carbon; (B) resinol substructures formed by  $\beta$ - $\beta'$ ,  $\alpha$ -O- $\gamma'$  and  $\gamma$ -O- $\alpha'$  linkages; (C) phenylcoumarane substructures formed by  $\beta$ -5' and  $\alpha$ -O-4' linkages; (D) dibenzodioxocine substructures formed by 5-5',  $\beta$ -O-4 and  $\alpha$ -O-4' linkages; (E) spirodienone substructures formed by  $\beta$ -1' and  $\alpha$ -O- $\alpha'$  linkages; (F) diphenylethane substructures formed by  $\beta$ -1' linkages; (I) *p*-hydroxycinnamyl alcohol end groups; (J) cinnamaldehyde end groups; (PB) *p*-hydroxybenzoate substructures; (H) *p*-hydroxyphenyl units; (G) guaiacyl units; (G') oxidized guaiacyl units with  $\alpha$ -ketone.

## Results and Discussion

### 3.2.1.1 Assignment of $^{13}\text{C}$ - $^1\text{H}$ correlations in HSQC spectra: Untreated spruce MWL

Table 3.3 shows the assignment of  $^{13}\text{C}$ - $^1\text{H}$  correlations in HSQC spectra of MWL from untreated spruce. The assignment was according to the HSQC experiments performed on the sample that was 60 mg MWL dissolved in 0.5 mL of DMSO- $d_6$ .

Table 3.3: Assignment of  $^{13}\text{C}$ - $^1\text{H}$  correlations in HSQC spectra of untreated spruce MWL.

Label	$\delta_C/\delta_H$ [ppm]	Assignment
$C_\beta$	53.1/3.44	$C_\beta - H_\beta$ in phenylcoumarane substructures (C)
$B_\beta$	53.4/3.06	$C_\beta - H_\beta$ in resinol substructures (B)
$F_\beta$	55.0/2.75	$C_\beta - H_\beta$ in diphenylethane substructures (F)
$-\text{OCH}_3$	55.3/3.74	C - H in methoxyls
$E_\beta$	59.4/2.77	$C_\beta - H_\beta$ in spirodienone substructures (E)
$A_\gamma$	59.8/3.3-3.7	$C_\gamma - H_\gamma$ in $\beta$ -O-4' substructures (A)
$I_\gamma$	61.4/4.1	$C_\gamma - H_\gamma$ in <i>p</i> -hydroxycinnamyl alcohol end groups (I)
$C_\gamma$	62.5/3.7	$C_\gamma - H_\gamma$ in phenylcoumarane substructures (C)
$A'_\gamma$	62.8/4.2	$C_\gamma - H_\gamma$ in $\gamma$ -acylated $\beta$ -O-4' substructures (A')
$B_\gamma$	71/3.7 and 4.1	$C_\gamma - H_\gamma$ in resinol substructures (B)
$(A, A')_\alpha$	71.1/4.7	$C_\alpha - H_\alpha$ in $\beta$ -O-4' substructures (A) and $\gamma$ -acylated $\beta$ -O-4' substructures (A')
$E_{\beta'}$	79.5/4.08	$C_{\beta'} - H_{\beta'}$ in spirodienone substructures (E)
$E_\alpha$	81.7/5.03	$C_\alpha - H_\alpha$ in spirodienone substructures (E)
$D_\alpha$	83.3/4.8	$C_\alpha - H_\alpha$ in dibenzodioxocine substructures (D)
$A_\beta$	83.8/4.27	$C_\beta - H_\beta$ in $\beta$ -O-4' substructures (A)
$B_\alpha$	84.7/4.6	$C_\alpha - H_\alpha$ in resinol substructures (B)
$D_\beta$	85.3/3.87	$C_\beta - H_\beta$ in dibenzodioxocine substructures (D)
$C_\alpha$	86.9/5.46	$C_\alpha - H_\alpha$ in phenylcoumarane substructures (C)
$G_2$	110.9/6.98	$C_2 - H_2$ in guaiacyl units (G)
$G'_2$	111.5/7.55	$C_2 - H_2$ in oxidized( $C_\alpha=O$ ) guaiacyl units (G')
$G_5$	115/6.8	$C_5 - H_5$ in guaiacyl units (G)
$G_6$	119/6.8	$C_6 - H_6$ in guaiacyl units (G)
$G'_6$	123.6/7.71	$C_6 - H_6$ in oxidized( $C_\alpha=O$ ) guaiacyl units (G')
$J_\beta$	126.2/6.76	$C_\beta - H_\beta$ in cinnamaldehyde end groups (J)
$H_{2,6}$	127.8/7.19	$C_{2,6} - H_{2,6}$ in <i>p</i> -hydroxyphenyl units (H)
$I_\beta$	128.5/6.25	$C_\beta - H_\beta$ in <i>p</i> -hydroxycinnamyl alcohol end groups (I)
$I_\alpha$	128.5/6.44	$C_\alpha - H_\alpha$ in <i>p</i> -hydroxycinnamyl alcohol end groups (I)
$\text{PB}_{2,6}$	131/7.7	$C_{2,6} - H_{2,6}$ in <i>p</i> -hydroxybenzoate substructures (PB)

Each lignin interunit bonding spin system shows three different signals due to CH and  $\text{CH}_2$  groups in the positions  $\alpha$ ,  $\beta$ , and  $\gamma$  of the side chain (Figure 3.2). The signal strength is according to the abundance of the substructures and since it can vary extremely between each substructure, the contour level of the spectra must be adjusted to identify all the substructures. Figure 3.3 shows the side chain region ( $\delta_C/\delta_H$  50-90/3.1-5.6) of a HSQC spectrum of MWL from untreated spruce, demonstrating the most abundant lignin moieties. The strongest signal is observed at  $\delta_C/\delta_H$  55.3/3.74, attributed to methoxy groups in lignin. The  $\beta$ -O-4' substructure is responsible for four strong signals. The  $C_\alpha$ - $H_\alpha$  correlations were observed at  $\delta_C/\delta_H$  71.1/4.7

(A and A' substructures), whereas the C<sub>β</sub>-H<sub>β</sub> and the C<sub>γ</sub>-H<sub>γ</sub> correlations in structures A were detected at  $\delta_C/\delta_H$  83.8/4.27 and 59.8/3.3-3.7, respectively. Also, the C<sub>γ</sub>-H<sub>γ</sub> correlations in  $\gamma$ -acylated  $\beta$ -O-4' substructures (A') were observed at  $\delta_C/\delta_H$  62.8/4.2. These signals indicated that lignin in Norway spruce is partially acylated at the  $\gamma$ -carbon in  $\beta$ -O-4' aryl ether linkages at the side chain<sup>102, 103</sup>. Finally, the considerably weaker cross-signals at  $\delta_C/\delta_H$  86.7/5.5, 53.1/3.44 and 62.5/3.7 ppm were assigned to phenylcoumarane (C substructures), C <sub>$\alpha$</sub> -H <sub>$\alpha$</sub> , C<sub>β</sub>-H<sub>β</sub>, and C<sub>γ</sub>-H<sub>γ</sub> correlations, respectively.

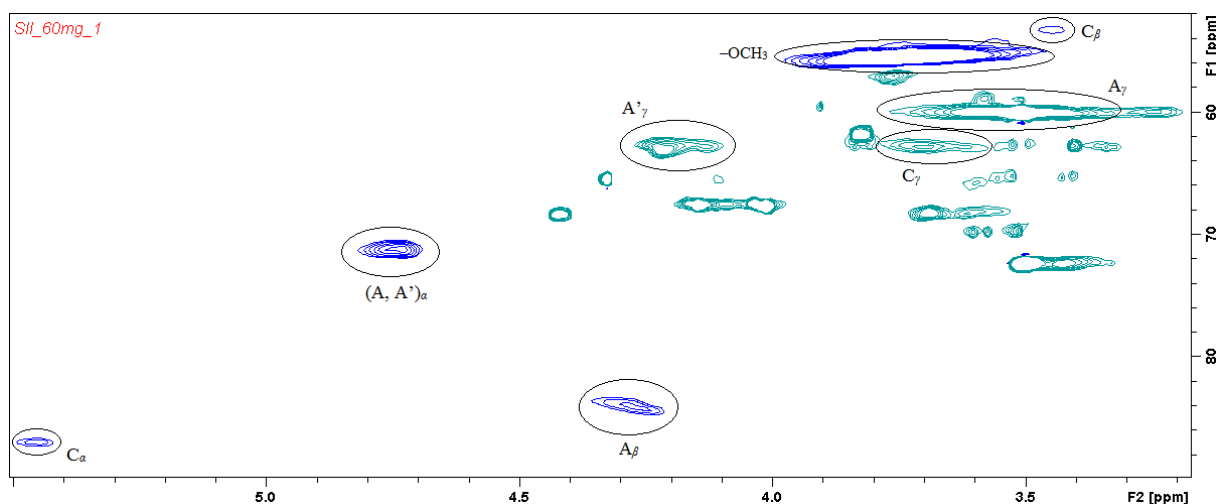


Figure 3.3: HSQC spectrum of untreated spruce MWL. The spectrum displays the side chain region ( $\delta_C/\delta_H$  50-90/3.1-5.6).

By showing more contour lines of the spectrum, less abundant signals from lignin substructures are revealed. Figure 3.4 shows the same spectrum as Figure 3.3, the signals are only more zoomed in. The resinol substructure (B) showed prominent signals for the C <sub>$\alpha$</sub> -H <sub>$\alpha$</sub> , C<sub>β</sub>-H<sub>β</sub>, and the double C<sub>γ</sub>-H<sub>γ</sub> correlation at  $\delta_C/\delta_H$  84.7/4.6, 53.4/3.06 and 71.3/3.7 and 4.1 ppm, respectively. Signals corresponding to C <sub>$\alpha$</sub> -H <sub>$\alpha$</sub>  ( $\delta_C/\delta_H$  83.3/4.8) and C<sub>β</sub>-H<sub>β</sub> ( $\delta_C/\delta_H$  85.5/3.87) correlations in dibenzodioxocine substructures (D) were observed. However, the dibenzodioxocine C<sub>γ</sub>-H<sub>γ</sub> correlations that should be at  $\delta_C/\delta_H$  60.1/3.41 ppm<sup>100</sup> is not observed due to overlapping of the much stronger C<sub>γ</sub>-H<sub>γ</sub> signal from  $\beta$ -O-4' substructures. C<sub>γ</sub>-H<sub>γ</sub> cross signals in *p*-hydroxycinnamyl alcohol end groups (substructure I) are partly overlapped, but nevertheless assigned at  $\delta_C/\delta_H$  61.4/4.1 ppm. Finally, diphenylethane (F) substructures showed a weak C<sub>β</sub>-H<sub>β</sub> correlation at  $\delta_C/\delta_H$  55.0/2.75 ppm.



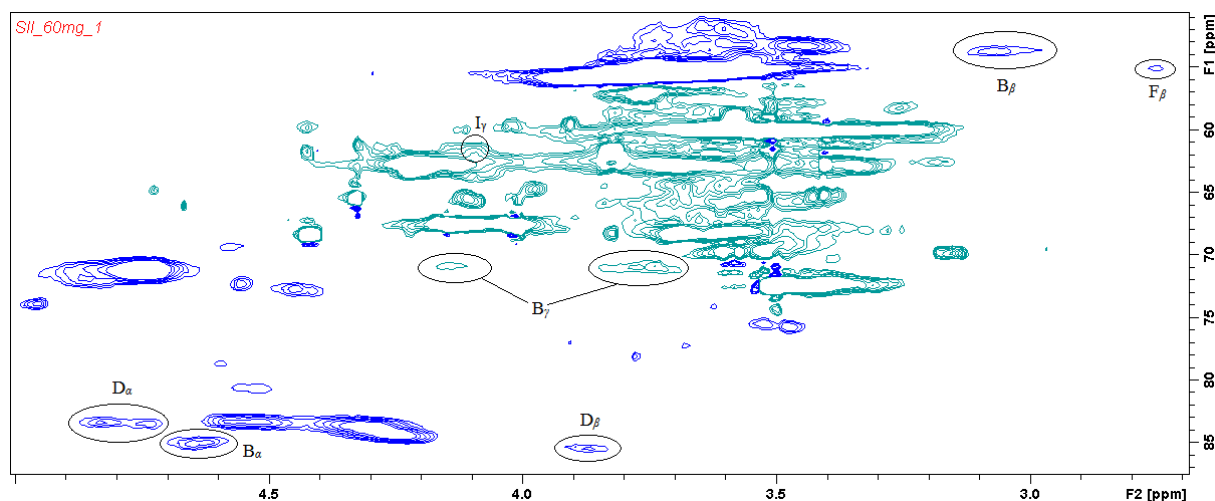


Figure 3.4: HSQC spectrum of untreated spruce MWL. The spectrum displays the side chain region ( $\delta_C/\delta_H$  50-87/2.7-5.0).

To reveal signals corresponding to  $^{13}\text{C}$ - $^1\text{H}$  correlations in the least abundant substructure of lignin, spirodienone (E), even more contour lines of the same HSQC spectrum of untreated spruce MWL were required. Figure 3.5 shows the  $\text{C}_{\alpha}$ - $\text{H}_{\alpha}$ ,  $\text{C}_{\beta}$ - $\text{H}_{\beta}$ , and  $\text{C}_{\beta'}$ - $\text{H}_{\beta'}$  correlations in spirodienone substructures at  $\delta_C/\delta_H$  81.7/5.03, 59.4/2.77 and 79.5/4.08 ppm, respectively.

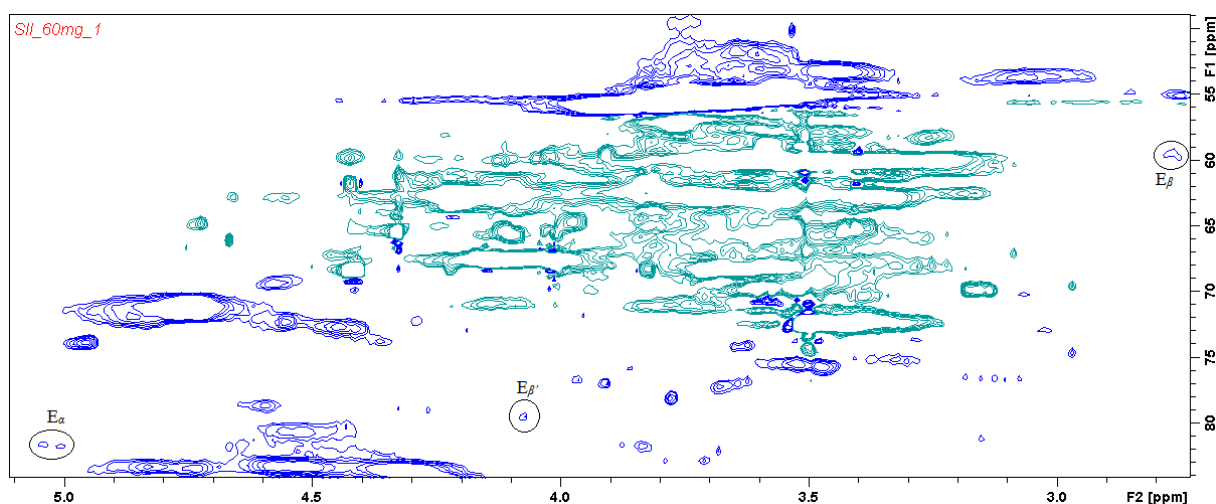


Figure 3.5: HSQC spectrum of untreated spruce MWL. The spectrum displays the side chain region ( $\delta_C/\delta_H$  50-84/2.7-5.1).

The C-H correlations for the aromatic lignin units give signals in the HSQC experiments at the region  $\delta_C/\delta_H$  110-132/6.2-7.8. Figure 3.6 shows the aromatic region of the same HSQC spectrum of MWL from untreated spruce as discussed above, demonstrating the most abundant aromatic lignin units. The main cross-signals corresponded to the aromatic rings of guaiacyl (G) lignin units. The G units showed different correlations for  $\text{C}_2$ - $\text{H}_2$ ,  $\text{C}_5$ - $\text{H}_5$ , and  $\text{C}_6$ - $\text{H}_6$  at  $\delta_C/\delta_H$  110.9/6.98, 115/6.8, and 119/6.8, respectively. The correlations for the  $\text{C}_2$ - $\text{H}_2$  and

C<sub>6</sub>-H<sub>6</sub> in oxidized  $\alpha$ -ketone structures G' were observed at  $\delta_C/\delta_H$  111.5/7.55 and 123.6/7.71. A minor C<sub>2,6</sub>-H<sub>2,6</sub> aromatic correlation from *p*-hydroxyphenyl units (H) was clearly observed at  $\delta_C/\delta_H$  127.8/7.19, but the C<sub>3,5</sub>-H<sub>3,5</sub> position correlations were overlapped with those from G<sub>5</sub>-positions.

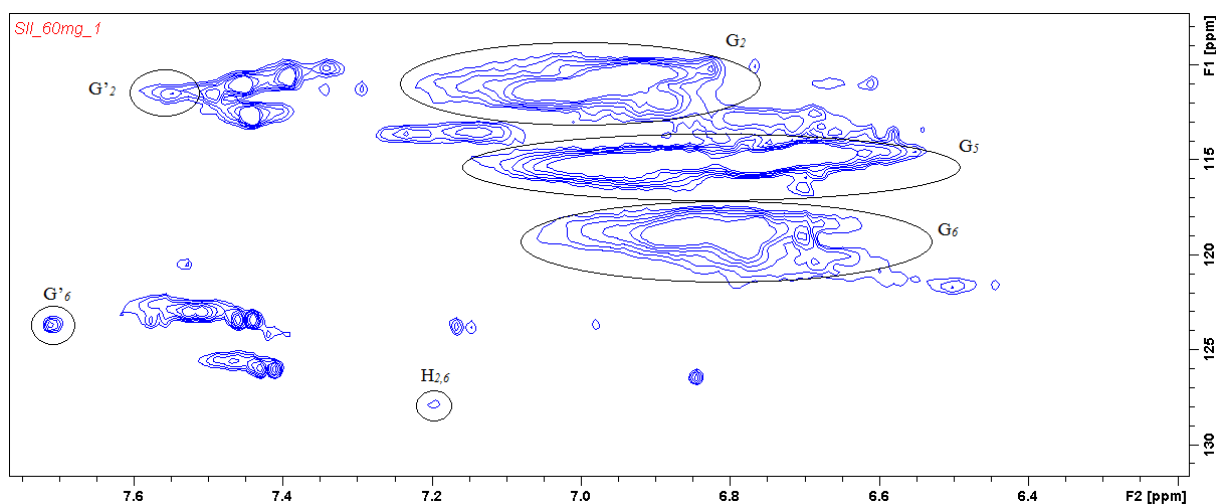


Figure 3.6: HSQC spectrum of untreated spruce MWL. The spectrum displays the aromatic region ( $\delta_C/\delta_H$  108-132/6.2-7.8).

By showing more contour lines of the spectrum, less abundant signals from lignin aromatic units are revealed. Figure 3.7 shows the same spectrum as Figure 3.6, the signals are only more zoomed in. The cross-signals were assigned to *p*-hydroxybenzoate substructures (PB), *p*-hydroxycinnamyl alcohol end groups (I), and cinnamaldehyde end groups (J). Compared to the correlations from the guaiacyl units, these signals are very weak. The C<sub>2,6</sub>-H<sub>2,6</sub> correlations of PB was clearly observed at  $\delta_C/\delta_H$  131/7.7. Very weak signals corresponding to C <sub>$\alpha$</sub> -H <sub>$\alpha$</sub>  and C <sub>$\beta$</sub> -H <sub>$\beta$</sub>  correlations of substructures I were observed at  $\delta_C/\delta_H$  128.5/6.25 and 128.5/6.44, respectively. The signals found at  $\delta_C/\delta_H$  126.2/6.76 assigned to the C <sub>$\beta$</sub> -H <sub>$\beta$</sub>  correlations of substructures J were equally strong as the signals from the *p*-hydroxycinnamyl alcohol end groups (I), indicating equal abundance of these two substructures in MWL isolated from untreated Norway spruce. However, the signal for C <sub>$\beta$</sub> -H <sub>$\beta$</sub>  correlation of substructures I could not be observed because the low field limit of the F1 spectrum axis was 152.2545 ppm. The signal should be around  $\delta_C/\delta_H$  153.5/7.6 according to the references used in the signal identification, and was therefore out of range.

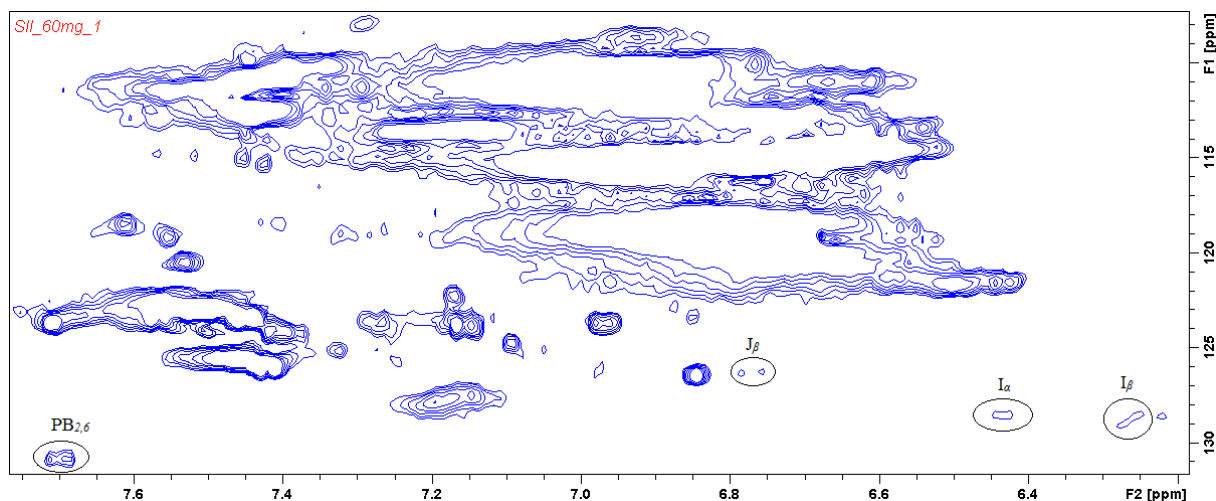


Figure 3.7: HSQC spectrum of untreated spruce MWL. The spectrum displays the aromatic region ( $\delta_C/\delta_H$  108-132/6.2-7.8).

### 3.2.1.2 Assignment of $^{13}\text{C}$ - $^1\text{H}$ correlations in HSQC spectra: Steam exploded spruce MWL

Table 3.4 shows an overview of the assignment of  $^{13}\text{C}$ - $^1\text{H}$  correlations in HSQC spectra of MWL from the steam exploded spruce samples, the second parallels (Figures showing all the spectra are found in the appendix). The assignment was according to the HSQC experiments performed on the samples that were 60 mg MWL dissolved in 0.5 mL of DMSO- $d_6$ . The  $\delta_C/\delta_H$  values of the  $^{13}\text{C}$ - $^1\text{H}$  correlations and their assignments are given in Table 3.3. Only their labels and evaluation of the signals strength for each sample are given in Table 3.4.

Some of the signals corresponding to  $^{13}\text{C}$ - $^1\text{H}$  correlations in lignin substructures and units that are identified in MWL from untreated spruce (Table 3.3) were not detected in MWL from steam exploded spruce (Table 3.4). Diphenylethane (F), spirodienone (E), and dibenzodioxocine (D) substructures, that were identified as minor lignin substructures in MWL from untreated spruce, were not detected in MWL from steam exploded spruce. Also, no  $^{13}\text{C}$ - $^1\text{H}$  correlations were found for p-hydroxycinnamyl alcohol end groups (I), which were barely detected in untreated spruce MWL. Considering the low abundance, structure and model compounds BDE of those substructures, their absence in MWL from steam exploded spruce is not surprising. The Dibenzodioxocine substructures are associated with branching in the lignin polymer and contain an eight ring with two oxygen atoms with relatively weak bonds, lowest BDE calculated 176.6 kJ/mol for the  $\alpha$ -O bond of a model compound<sup>61</sup>. The D substructures are therefore degraded in the steam explosion and no associated signals detected. The cross-signals assigned to the spirodienone substructures were barely detectable

in MWL from untreated spruce and disappeared after the structure changes in the steam explosion treatment. The C<sub>β</sub>-H<sub>β</sub> correlations of substructures F gave a very weak signal in untreated spruce MWL spectra (Figure 3.5) which was not found in SE spruce MWL spectra. The lowest BDE of a model compound was calculated 270.7 kJ/mol for the C<sub>α</sub>-C<sub>β</sub> bond <sup>63</sup>.

Table 3.4: Assignment of <sup>13</sup>C-<sup>1</sup>H correlations in HSQC spectra of MWL from the eight steam exploded spruce samples. The letters indicate the evaluated strength of each signal; N.D.: not detected, O: signal overlaps with another signal, vs: very strong signal, s: strong signal, m: medium strong signal, w: weak signal, vw: very weak signal.

Label	180 °C 5 min	190 °C 5 min	200 °C 5 min	210 °C 5 min	180 °C 10 min	190 °C 10 min	200 °C 10 min	210 °C 10 min
C <sub>β</sub>	m	m	m	m	m	m	m	m
B <sub>β</sub>	w	w	w	w	w	w	w	w
F <sub>β</sub>	N.D.	N.D.	N.D.	N.D.	N.D.	N.D.	N.D.	N.D.
-OCH <sub>3</sub>	vs	vs	vs	vs	vs	vs	vs	vs
E <sub>β</sub>	N.D.	N.D.	N.D.	N.D.	N.D.	N.D.	N.D.	N.D.
A <sub>γ</sub>	vs, O	vs, O	vs, O	vs, O	vs, O	vs, O	vs, O	vs, O
I <sub>γ</sub>	N.D.	N.D.	N.D.	N.D.	N.D.	N.D.	N.D.	N.D.
C <sub>γ</sub>	s, O	s, O	s, O	s, O	s, O	s, O	s, O	s, O
A' <sub>γ</sub>	s	s	m	m	s	s	m	m
B <sub>γ</sub>	w	w	w	w	w	w	w	w
(A, A') <sub>α</sub>	s	s	m	m	s	s	s	s
E <sub>β</sub> '	N.D.	N.D.	N.D.	N.D.	N.D.	N.D.	N.D.	N.D.
E <sub>α</sub>	N.D.	N.D.	N.D.	N.D.	N.D.	N.D.	N.D.	N.D.
D <sub>α</sub>	N.D.	N.D.	N.D.	N.D.	N.D.	N.D.	N.D.	N.D.
A <sub>β</sub>	s	m	m	m	s	m	m	m
B <sub>α</sub>	w	w	w	w	w	w	w	w
D <sub>β</sub>	N.D.	N.D.	N.D.	N.D.	N.D.	N.D.	N.D.	N.D.
C <sub>α</sub>	m	m	m	m	m	m	m	m
G <sub>2</sub>	vs	vs	vs	vs	vs	vs	vs	vs
G' <sub>2</sub>	vw	vw	vw	vw	vw	vw	vw	vw
G <sub>5</sub>	vs	vs	vs	vs	vs	vs	vs	vs
G <sub>6</sub>	vs	vs	vs	vs	vs	vs	vs	vs
G' <sub>6</sub>	vw	vw	vw	vw	vw	vw	vw	vw
J <sub>β</sub>	vw	w	vw	vw	vw	vw	vw	vw
H <sub>2,6</sub>	vw	vw	vw	N.D.	vw	vw	vw	N.D.
I <sub>β</sub>	N.D.	N.D.	N.D.	N.D.	N.D.	N.D.	N.D.	N.D.
I <sub>α</sub>	N.D.	N.D.	N.D.	N.D.	N.D.	N.D.	N.D.	N.D.
PB <sub>2,6</sub>	vw	vw	N.D.	N.D.	vw	vw	N.D.	N.D.

Cross-signals corresponding to C-H correlations in most lignin substructures and units that were identified in untreated spruce MWL spectra were also detected in steam exploded spruce MWL spectra. However, with increased temperature in the steam treatment, fewer signals were identified and some became weaker, confirming increasingly changed lignin structure with SE temperature. Figure 3.8 shows the side chain region ( $\delta_C/\delta_H$  50-90/2.7-5.7) of

## Results and Discussion

HSQC spectra of MWL from steam exploded spruce, 180 °C for 5 min (1) and 210 °C for 5 min (2), demonstrating the differences in lignin substructures with increased SE temperature. The cross-signals for all the substructures seem to have similar strength at both spectra except for the signals corresponding to the C-H correlations of the  $\beta$ -O-4' substructures (A and A'), which are considerably weaker in the 210 °C for 5 min spectrum. The cleavage of  $\beta$ -O-4' linkages are known to be important depolymerization reaction in lignin and the  $\beta$ -O-4' substructures therefore expected to become less abundant with more severe pretreatment conditions. A decrease in the content  $\beta$ -O-4' structures with increasingly severe steam explosion has been previously observed by HSQC of MWL from aspen.<sup>33</sup>

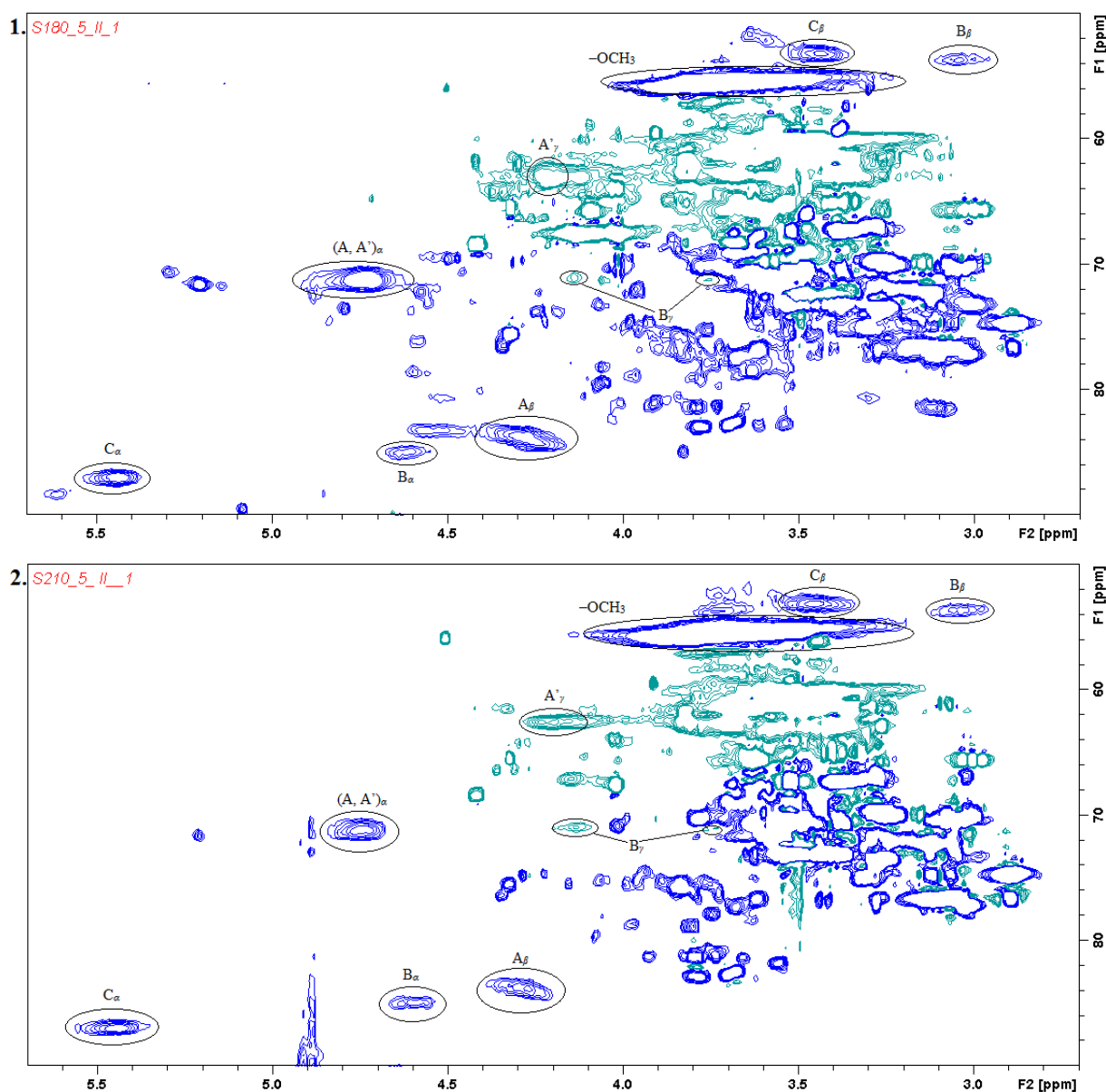


Figure 3.8: HSQC spectra of steam exploded spruce MWL; 180 °C for 5 min (1) and 210 °C for 5 min (2). The spectrum displays the side chain region ( $\delta_C/\delta_H$  50-90/2.7-5.7).

## Results and Discussion

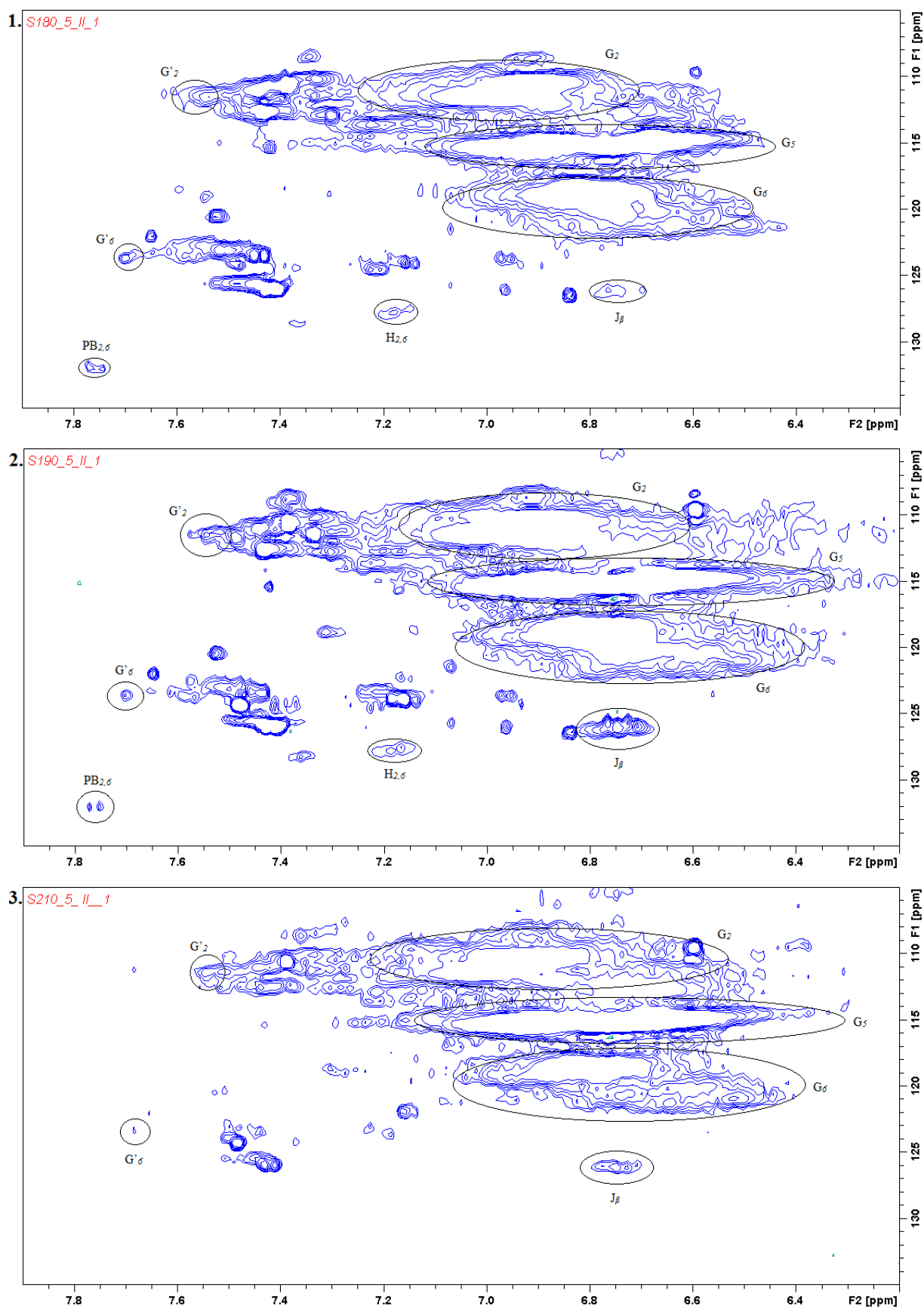


Figure 3.9: HSQC spectra of steam exploded spruce MWL; 180 °C for 5 min (1), 190 °C for 5 min (2) and 210 °C for 5 min (3). The spectrum displays the aromatic region ( $\delta_C/\delta_H$  105-135/6.2-7.9).

Figure 3.9 shows the aromatic region ( $\delta_C/\delta_H$  105-135/6.2-7.9) of HSQC spectra of MWL from steam exploded spruce, 180 °C for 5 min (1), 190 °C for 5 min (2) and 210 °C for 5 min (3), demonstrating the differences in lignin aromatic units and substructures with increased SE temperature. When comparing the two lower severities, the signals seem similar for the aromatic units and substructures, except for the cross-signal assigned to cinnamaldehyde end groups (J) which becomes stronger. Structure J has been suggested one of possible degradation products in the cleavage of  $\beta$ -O-4' linkage<sup>29</sup> and could therefore show higher abundance in lignin with decreased amount of  $\beta$ -O-4' substructure. However, the signal is not as strong for the 210 °C for 5 min spectrum, indicating some balance between the formation and destruction of cinnamaldehyde end groups (J) in samples treated with steam explosion. The highest severities seem also to affect the destruction of some other lignin aromatic substructures. No signal is detected for *p*-hydroxybenzoate substructures (PB) in HSQC spectra of the 200 and 210 °C samples, both 5 and 10 min, and no C<sub>2,6</sub>-H<sub>2,6</sub> correlations for H units are detected in HSQC spectra of the 210 °C samples, both 5 and 10 min (Table 3.4). Since the PB substructures are oxidized H units with  $\alpha$ -ketone and their signals were similarly weak, their behavior was expected to be similar. However, no bond in their structure was expected to be affected in the steam explosion treatment and therefore surprisingly not detected in HSQC spectra of MWL from the most severely treated spruce.

### 3.2.1.3 Assignment of <sup>13</sup>C-<sup>1</sup>H correlations in HSQC spectra: THF dissolvable MWL

Table 3.5 shows an overview of the assignment of <sup>13</sup>C-<sup>1</sup>H correlations in HSQC spectra of THF dissolvable MWL from the untreated and the steam exploded spruce samples, the second parallels. The assignment was according to the HSQC experiments performed on the samples that were 20 mg of THF dissolvable MWL dissolved in 0.5 mL of DMSO-d<sub>6</sub>. The  $\delta_C/\delta_H$  values of the <sup>13</sup>C-<sup>1</sup>H correlations and their assignments are given in Table 3.3. Only their labels and evaluation of the signals strength for each sample are given in Table 3.5. Figures showing spectra of THF dissolvable MWL from all samples are found in the appendix.

Cross-signals corresponding to C-H correlations in most lignin substructures and units that were identified in the MWL spectra were also detected in the THF dissolvable MWL spectra. However, the <sup>13</sup>C-<sup>1</sup>H correlations that were responsible for the weakest cross-signals in the MWL spectra were not detected in the THF dissolvable MWL spectra. For HSQC spectra of the untreated spruce MWL, cross-signals from the spirodienone substructures (E) and the *p*-hydroxycinnamyl alcohol end groups (I) were not detected. The C<sub>2,6</sub>-H<sub>2,6</sub>

correlations for substructures PB that were identified in the spectra of 180 and 190 °C steam exploded MWL were not detected in any of the steam exploded THF dissolvable MWL. In addition, the signal for H units was not found in the 190 °C for 10 min THF dissolvable MWL, but was detected as a very weak signal in the corresponding MWL sample. This lower limit of detection in the MWL HSQC experiments was expected because of the higher sample concentration. Additionally, the weak signals were clearer and more regularly shaped, giving higher quality spectra. When comparing the strength of each signal for MWL and THF dissolvable MWL, small differences are detected (Table 3.4 and Table 3.5), indicating that THF dissolvable MWL is not fully representative for native lignin, but useful for identification.

Table 3.5: Assignment of  $^{13}\text{C}$ - $^1\text{H}$  correlations in HSQC spectra of THF dissolvable MWL from untreated steam exploded spruce samples. The letters indicate the evaluated strength of each signal; N.D: not detected, O: signal overlaps with another signal, vs: very strong signal, s: strong signal, m: medium strong signal, w: weak signal, vw: very weak signal.

Label	Untreated Spruce	180 °C 10 min	190 °C 10 min	200 °C 10 min	210 °C 10 min
$\text{C}_\beta$	m	m	m	m	m
$\text{B}_\beta$	w	w	w	w	w
$\text{F}_\beta$	vw	N.D.	N.D.	N.D.	N.D.
$-\text{OCH}_3$	vs	vs	vs	vs	vs
$\text{E}_\beta$	N.D.	N.D.	N.D.	N.D.	N.D.
$\text{A}_\gamma$	vs	vs, O	vs, O	vs, O	vs, O
$\text{I}_\gamma$	N.D.	N.D.	N.D.	N.D.	N.D.
$\text{C}_\gamma$	m	s, O	s, O	s, O	s, O
$\text{A}'_\gamma$	s	s	s	m	m
$\text{B}_\gamma$	w	w	w	w	w
$(\text{A}, \text{A}')_\alpha$	s	s	s	s	s
$\text{E}_{\beta'}$	N.D.	N.D.	N.D.	N.D.	N.D.
$\text{E}_\alpha$	N.D.	N.D.	N.D.	N.D.	N.D.
$\text{D}_\alpha$	w	N.D.	N.D.	N.D.	N.D.
$\text{A}_\beta$	s	m	m	m	m
$\text{B}_\alpha$	w	w	w	w	w
$\text{D}_\beta$	w	N.D.	N.D.	N.D.	N.D.
$\text{C}_\alpha$	m	m	M	m	m
$\text{G}_2$	vs	vs	vs	vs	vs
$\text{G}'_2$	w	vw	vw	vw	vw
$\text{G}_5$	vs	vs	vs	vs	vs
$\text{G}_6$	vs	vs	vs	vs	vs
$\text{G}'_6$	vw	vw	vw	vw	vw
$\text{J}_\beta$	vw	vw	vw	vw	N.D.
$\text{H}_{2,6}$	w	vw	N.D.	vw	N.D.
$\text{I}_\beta$	N.D.	N.D.	N.D.	N.D.	N.D.
$\text{I}_\alpha$	N.D.	N.D.	N.D.	N.D.	N.D.
$\text{PB}_{2,6}$	vw	N.D.	N.D.	N.D.	N.D.



### 3.2.2 Quantification of Interunit Linkages in Norway Spruce

Quantification of interunit linkages in was performed by integrating selected  $^{13}\text{C}$ - $^1\text{H}$  correlations in HSQC spectra of the MWL samples, second parallels, according to recently published method<sup>40</sup>. The  $\text{C}_2$ - $\text{H}_2$  correlations ( $G_2$ ) in guaiacyl units were used as internal standard. Since the  $\text{C}_2$  position of the guaiacyl unit is never substituted, the amount of  $G_2$  reflects the number of aromatic  $\text{C}_9$  units in lignin. The integral of the  $G_2$  signal was therefore set to 100 to represent 100 lignin  $\text{C}_9$  units and all the interunit linkages in lignin were expressed as number per 100 lignin  $\text{C}_9$  units. The selection of signals was decided by considering the best resolved CH signals that did not overlap with signals from other wood components: The  $\alpha$  signals for the  $\beta$ -aryl ether ( $\beta$ -O-4') and phenylcoumarane ( $\beta$ -5'), and  $\beta$  signals for the resinol ( $\beta$ - $\beta'$ ), dibenzodioxocine (5-5'-O-4), diphenylethane ( $\beta$ -1'), and spirodienone ( $\alpha$ -O- $\alpha'$ ) lignin interunit bonds.

The amounts of the different interunit linkages per 100  $\text{C}_9$  units for MWL from untreated spruce are listed in Table 3.6 along with reference values for comparison. The data result from the average of three different spectra acquired on the same sample and the different integrations gave quite reproducible data. The experimental relative error, calculated by using standard deviation, does not exceed 1% for determination of  $\beta$ -O-4' units, 2% for phenylcoumarane units, 5% for resinol units, 55% for diphenylethane units, 23% for dibenzodioxocine units, and 31% for spirodienone units. The increased error with lower abundance of the units shows that HSQC experiments are more reliable for measuring the higher abundant linkages. However, the error of the number of linkages per 100 does not exceed 0.63 units, which confirms the reproducibility of the HSQC experiments.

Table 3.6: Amount of interunit linkages in untreated spruce MWL, as evaluated by HSQC experiments ( $n = 3$ ) and from previous literature data.

Linkage	No. per 100 $\text{C}_9$ units	NMR methods <sup>[a]</sup>			Wet-chemistry methods <sup>[a]</sup>	
		Sette <i>et al.</i> <sup>40</sup>	Zhang <i>et al.</i> <sup>104</sup>	Capanema <i>et al.</i> <sup>80</sup>	Robert <sup>105</sup>	Adler <sup>38</sup>
$\beta$ -O-4'	43.4 $\pm$ 0.3	44.7 $\pm$ 0.9	40-43	36-45	34	48
$\beta$ -5'	10.5 $\pm$ 0.1	10.6 $\pm$ 2.0	10-12	9	10	9-12
$\beta$ - $\beta'$	3.60 $\pm$ 0.16	3.19 $\pm$ 0.01	3.5	3	4	2
$\beta$ -1	1.15 $\pm$ 0.63	1.25 $\pm$ 0.34	2	1	9	2
5-5'-O-4	2.56 $\pm$ 0.57	3.07 $\pm$ 0.05	5	7	-	-
$\alpha$ -O- $\alpha'$	0.45 $\pm$ 0.14	0.24 $\pm$ 0.05	1.2-2	2	-	-

[a] The ranges here reported are not experimental errors, but result from different literature reports that are presented without evaluation of the pertinent experimental errors.

Comparison with the reference values in Table 3.6 showed significant agreement, especially for the values that Sette *et al.*<sup>40</sup> obtained by the same HSQC quantitative method using MWL from acetylated Norway spruce. The amount for each linkage is almost identical and in fact the same for three of six linkages when the error is considered. Comparison with the <sup>13</sup>C NMR methods<sup>80, 104</sup> showed agreement, except for higher values evaluated for spirodienone and dibenzodioxocine by <sup>13</sup>C NMR, probably resulting difficulties in evaluation due to signal overlap in <sup>13</sup>C NMR spectra. The amount of those two linkages could not be evaluated by wet-chemistry methods<sup>38, 105</sup>, but adequate agreement was found for the other four linkages, except for the surprisingly high  $\beta$ -1' value obtained by Robert<sup>105</sup>.

The amounts of the different interunit linkages per 100 C<sub>9</sub> units for MWL from untreated and steam exploded spruce samples are listed in Table 3.7, demonstrating changes in the amount of three interunit linkages with increased severity of steam explosion. The three most abundant interunit linkages ( $\beta$ -O-4',  $\beta$ -5', and  $\beta$ - $\beta$ ') were the only interunit linkages that were identified in steam exploded spruce MWL, and therefore the three least abundant not included in Table 3.7. To demonstrate the trends visually, the steam exploded samples that were treated for ten minutes and five minutes were plotted against the amount of interunit linkages in separate graphs (Figure 3.10). Untreated spruce MWL was included in both graphs to demonstrate the difference between MWL from steam exploded and untreated spruce.

Table 3.7: Amount of interunit linkages (% of C<sub>9</sub> units) in MWL from untreated and steam exploded spruce samples, as evaluated by HSQC experiments (n = 3).

MWL	$\beta$ -O-4'	$\beta$ -5'	$\beta$ - $\beta$ '
Untreated	43.4 ± 0.3	10.5 ± 0.1	3.60 ± 0.16
180°C for 5 min	34.4 ± 0.3	12.5 ± 0.1	3.20 ± 0.14
180°C for 10 min	31.8 ± 0.8	12.9 ± 0.2	2.70 ± 0.36
190°C for 5 min	26.7 ± 1.7	14.3 ± 0.3	3.73 ± 0.26
190°C for 10 min	23.7 ± 0.7	14.6 ± 0.3	3.43 ± 0.12
200°C for 5 min	19.4 ± 0.4	16.2 ± 0.1	4.07 ± 0.05
200°C for 10 min	19.3 ± 0.7	15.5 ± 0.4	3.57 ± 0.14
210°C for 5 min	15.2 ± 1.4	17.2 ± 0.4	3.45 ± 0.38
210°C for 10 min	14.8 ± 1.9	17.0 ± 0.7	4.36 ± 0.29

## Results and Discussion

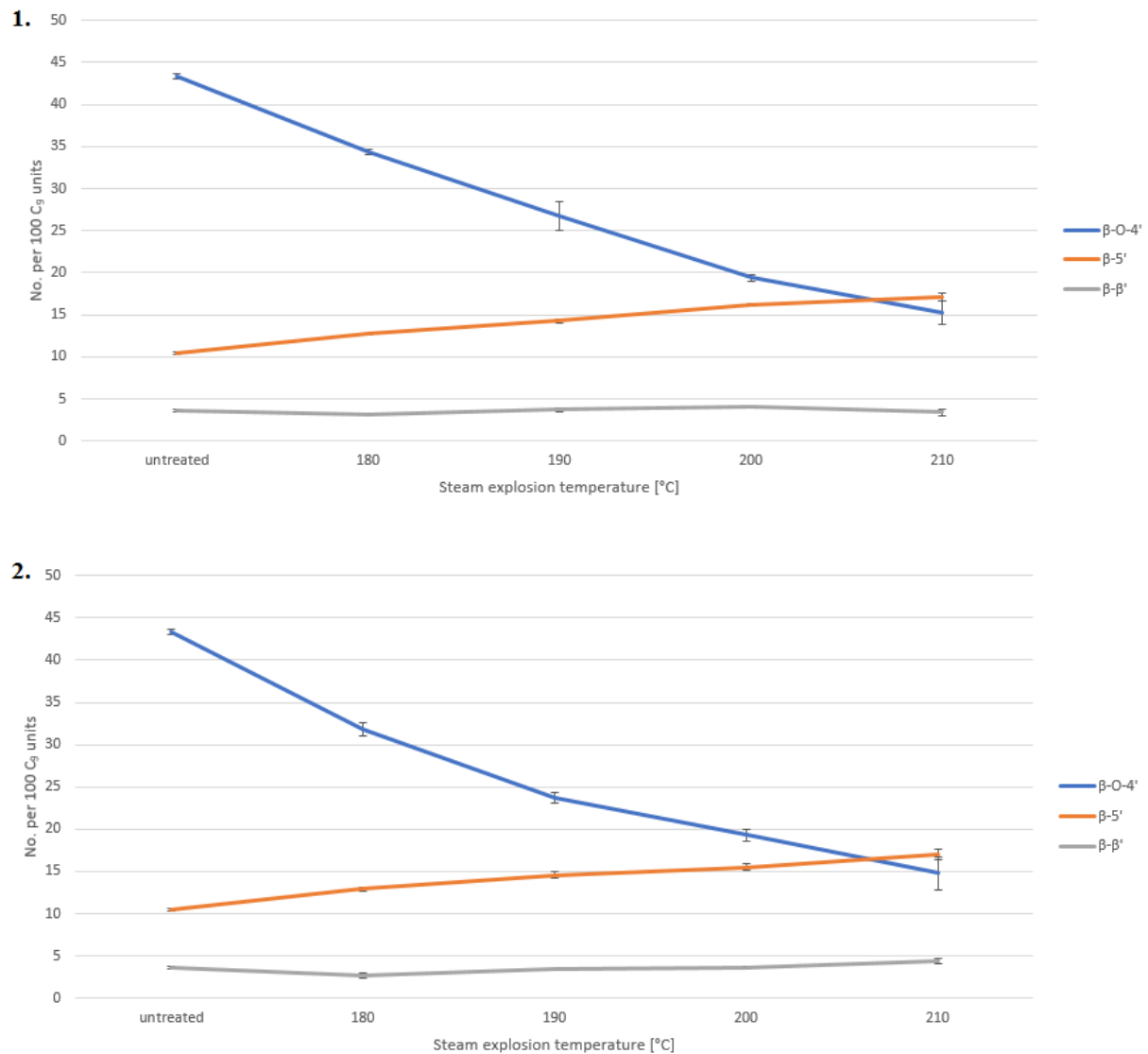


Figure 3.10: Number of interunit linkages per 100  $C_9$  units ( $n = 3$ ) as a function of steam explosion temperature, 5 min residence time (1) and 10 min residence time (2). Untreated spruce MWL is included in both graphs.

The amount of  $\beta$ -O-4' linkages decreases considerably after the spruce has been treated with steam explosion and continues to decrease with more severe conditions. The samples treated for five minutes show close to linear decrease with increased temperature, while the corresponding decrease for the ten-minute samples is exponential. The decrease in  $\beta$ -O-4' linkages is minimal for the same temperatures with different residence times, and for the two highest temperatures, the decrease is within the uncertainty values. Therefore, the SE temperature is the dominant parameter for the decrease of  $\beta$ -O-4' linkages. Similar pattern is observed for the  $\beta$ -5' linkages, but increased instead of decreased amount of linkages with increased temperature. The residence time did not affect the amount of  $\beta$ -5' linkages. The amount of  $\beta$ - $\beta'$  linkages were measured between 3 and 4 per 100  $C_9$  units for most of the

MWL samples. Despite some variations between different SE samples, neither the SE temperature nor the residence time seemed to affect the amount of  $\beta$ - $\beta'$  linkages.

Several studies<sup>33, 101, 106</sup> regarding the impact of SE on the lignin structure agree with the observation of decrease in the level of  $\beta$ -O-4' and increase in  $\beta$ -5' linkages in this study. Rearrangement from alkyl aryl ether ( $\beta$ -O-4') to phenylcoumarane ( $\beta$ -5') was reported<sup>107</sup> after heating the lignin model compound in 100 °C water for seven days, yielding 32% phenylcoumarane. It was proposed that this rearrangement is initiated by the homolytic cleavage of  $\beta$ -O-4', followed by the formation of the new linkage. Heikkinen *et al.*<sup>101</sup> studied structural changes in EMAL lignin from wheat straw after SE treatment at 200 °C for 10 minutes. HSQC quantification showed decrease in  $\beta$ -O-4' linkages from 66 to 51 per 100 C<sub>9</sub> units and increase in  $\beta$ -5' linkages from 10 to 16 per 100 C<sub>9</sub> units, compared to 43 to 19 and 10.5 to 15.5 per 100 C<sub>9</sub> units in this study. The  $\beta$ -5' linkage increase was therefore similar, but the  $\beta$ -O-4' linkage decrease was considerably lower, indicating that same SE conditions do not have the same impact on lignin structure from different type of biomass. Better agreement for the  $\beta$ -O-4' linkage decrease was found for steam exploded spruce EMAL lignin studied by Rahikainen *et al.*<sup>108</sup>. SE treatment at 200 °C for 10 minutes resulted in decrease of 23 per 100 C<sub>9</sub> units when compared to the untreated MWL, while corresponding decrease was 24 per 100 C<sub>9</sub> units in this study.

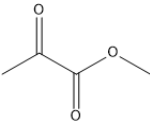
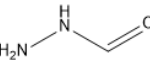
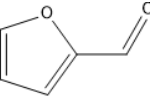
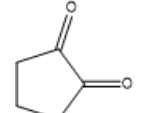
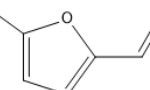
Li *et al.*<sup>33</sup> studied the decrease in  $\beta$ -O-4' linkages with increasingly severe steam explosion by HSQC of MWL from aspen at five different severities, concluding that a linear relationship was between the amount of  $\beta$ -O-4' linkages and a severity factor ( $S_0$ ) calculated according to Overend and Chornet<sup>30</sup>:  $S_0 = \log [\exp((T-100)/14.75)t]$  where T is the steam temperature (°C) and t is the residence time (min). When applying this equation to the data from this study, no linear relationship is found because the residence time effect in this study is minimal, and higher  $S_0$  values even show increased amount  $\beta$ -O-4' linkages. The  $S_0$  factor was therefore not useful in describing changes in lignin structure in this study. Also, the main use of this factor is to predict process parameters such as the recovery yield of steam-treated fractions, yield of enzymatic hydrolysis, and extent of lignin/hemicellulose removal<sup>29</sup>.

### 3.3 Py-GC-MS Analysis

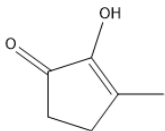
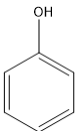
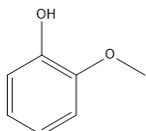
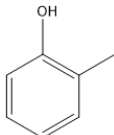
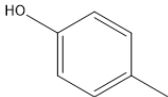
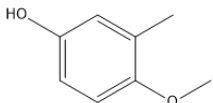
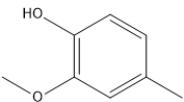
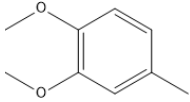
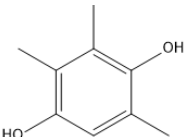
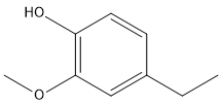
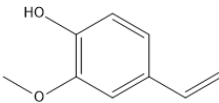
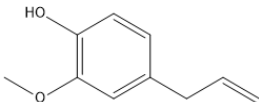
#### 3.3.1 Identification of Volatile Pyrolyzates

Table 3.8 lists all the integrated compounds from the pyrograms acquired after py-GC-MS experiments at 600 °C (isothermal temperature) of the MWL and the THF dissolvable MWL samples. The volatile pyrolyzates are listed by increasing retention times with information of compound number, structure, name, and molecular weight. The compounds eluting at the first 19 minutes of analysis were not considered important for the analysis and therefore not integrated. At the first 5 minutes, only carbon dioxide was eluted for both MWL from untreated and steam exploded spruce. For untreated spruce MWL, no compounds were eluted the next 20 minutes, but few low molecular weight pyrolyzates for MWL from steam exploded spruce. These include compounds such as acetic acid and 1-hydroxy-2-propanone, but identification of other peaks was difficult because of poor chromatographic separation and broad, asymmetric peaks. Figure 3.11 shows a typical full pyrogram of MWL from untreated and steam exploded spruce (190 °C for 10 min) to demonstrate the different complexities. Pyrograms of MWL and THF dissolvable MWL from all samples are found in the appendix.

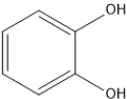
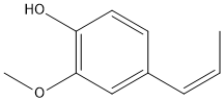
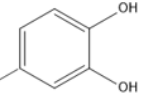
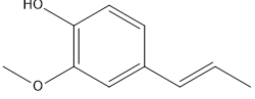
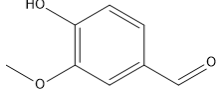
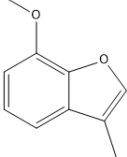
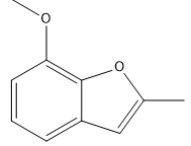
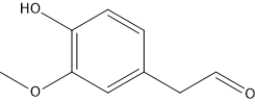
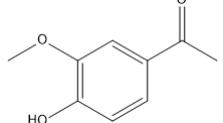
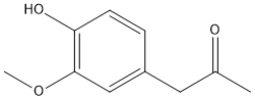
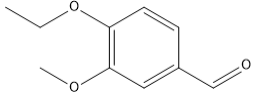
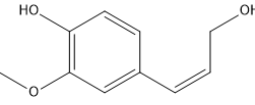
*Table 3.8: All integrated compounds from the pyrograms acquired after py-GC-MS experiments at 600 °C (isothermal temperature) of the MWL and THF dissolvable MWL samples. Compounds marked with \* were not undisputedly identified (discussed in the text).*

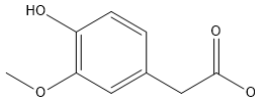
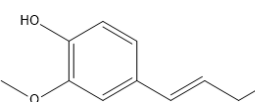
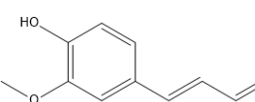
Comp. no.	Structure	IUPAC name	RT [min]	M <sup>+</sup> [m/z]
1		Methyl 2-oxopropanoate*	19.1	102
2		Formic hydrazide*	19.2	60
3		2-Furaldehyde	19.8	96
4		1,2-Cyclopentanedione	23.5	98
5		5-Methyl-2-furaldehyde*	24.2	110
6	Unknown	Unknown	25.8	102

## Results and Discussion

7		2-Hydroxy-3-methyl-2-cyclopenten-1-one*	26.2	112
8		Phenol	26.6	94
9		2-Methoxyphenol	27.5	124
10		2-Methylphenol	28.0	108
11		4-Methylphenol	28.9	108
12		4-Methoxy-3-methylphenol	29.6	138
13		2-Methoxy-4-methylphenol	30.5	138
14		1,2-Dimethoxy-4-methylbenzene	31.2	152
15		2,3,5-Trimethyl-1,4-benzenediol	32.8	152
16		4-Ethyl-2-methoxyphenol	33.4	152
17		4-Ethenyl-2-methoxyphenol	35.5	150
18		2-Methoxy-4-(prop-2-en-1-yl)phenol	36.5	164

## Results and Discussion

19		1,2-Benzenediol	36.7	110
20		2-Methoxy-4-[(1Z)-1-propen-1-yl]phenol	38.9	164
21		4-Methyl-1,2-benzenediol*	40.2	124
22		2-Methoxy-4-[(1E)-1-propen-1-yl]phenol	41.2	164
23		4-Hydroxy-3-methoxybenzaldehyde	41.9	152
24		7-Methoxy-3-methyl-1-benzofuran*	42.9	162
25		7-Methoxy-2-methyl-1-benzofuran*	43.4	162
26		2-(4-hydroxy-3-methoxyphenyl)acetaldehyde	44.5	166
27		1-(4-Hydroxy-3-methoxyphenyl)ethanone	45.7	166
28		1-(4-Hydroxy-3-methoxyphenyl)acetone	48.0	180
29		4-Ethoxy-3-methoxybenzaldehyde*	49.7	180
30		4-[(1Z)-3-Hydroxy-1-propen-1-yl]-2-methoxyphenol*	50.2	180
31	Unknown	Not identified	50.4	178

32		(4-Hydroxy-3-methoxyphenyl)acetic acid*	54.1	182
33		4-[(1E)-3-Hydroxy-1-propen-1-yl]-2-methoxyphenol	59.5	180
34		(2E)-3-(4-hydroxy-3-methoxyphenyl)prop-2-enal	60.2	178

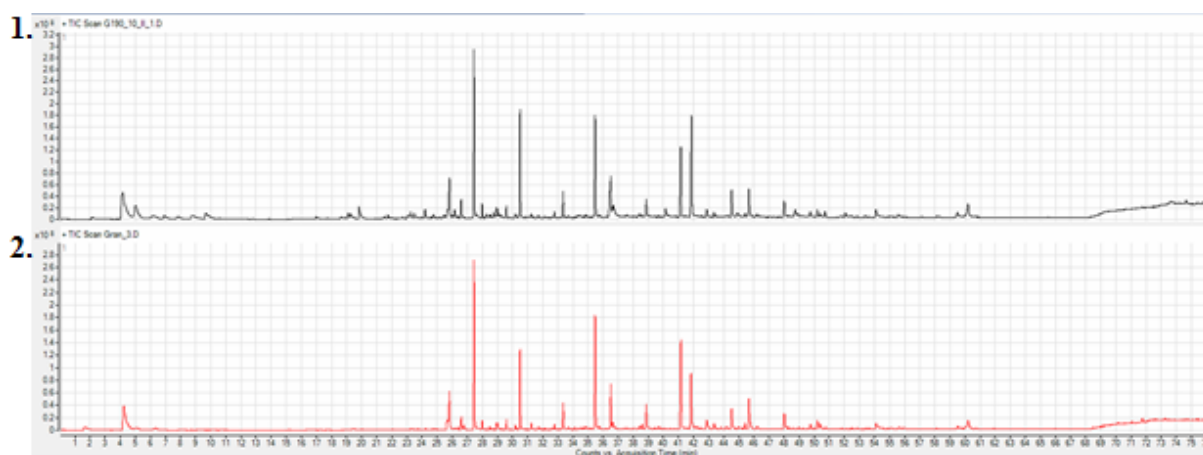


Figure 3.11: Pyrogram of MWL from steam exploded (1) and untreated spruce (2).

It was possible to identify 32 of 34 peak-separated compounds. Spectra of the two unknown compounds are shown in Figure 3.12. The molecular ion of compound **6** is the base peak at  $m/z$  102 and other abundant peaks are at  $m/z$  73,58,44, indicating that it contains one or more alkyl chains and thus not an aromatic derived from lignin. Compound **31** has the molecular ion at  $m/z$  178 and the base peak at  $m/z$  151. Other abundant peaks are at  $m/z$  135, 123, 108, 91, 77, 65, and 55, indicating the presence of a methyl- and hydroxyl-substituted benzene ring. Therefore, **31** must be an aromatic compound derived from lignin.

Compounds with match factor lower than 800 or not available in NIST MS library, or compounds not verified by standards, were considered not undisputedly identified (marked with \* in Table 3.8). However, these pyrolyzates had match factor over 750 and/or structural features indicating that they were derived from spruce lignin. Compounds **1** and **2** had match factor over 775 and probability over 80%, while compound **5** had a match factor 770 and 56% probability. Two isomers of methyl-1,2-benzenediol were suggested by NIST, with the methyl substituent at position 3 (match factor 757, probability 39%) and 4 (match factor 750, probability 30%). Compound **21** was considered more likely because of more resemblance to



## Results and Discussion

G-lignin substructures. The benzofurans **24** and **25** were not available in NIST and were considered more likely than the isomer (6-methoxy-3-methyl-benzofuran) suggested by NIST, due to structural features of phenylcoumarans. The benzaldehyde **29** had a match factor 723, 23% probability and G-lignin structure. The methoxyphenol **30** was not available in NIST, but suggested as the *Z* isomer (**33**) with match factor 765 and 38% probability. Finally, **32** had a match factor 752 and 54% probability.

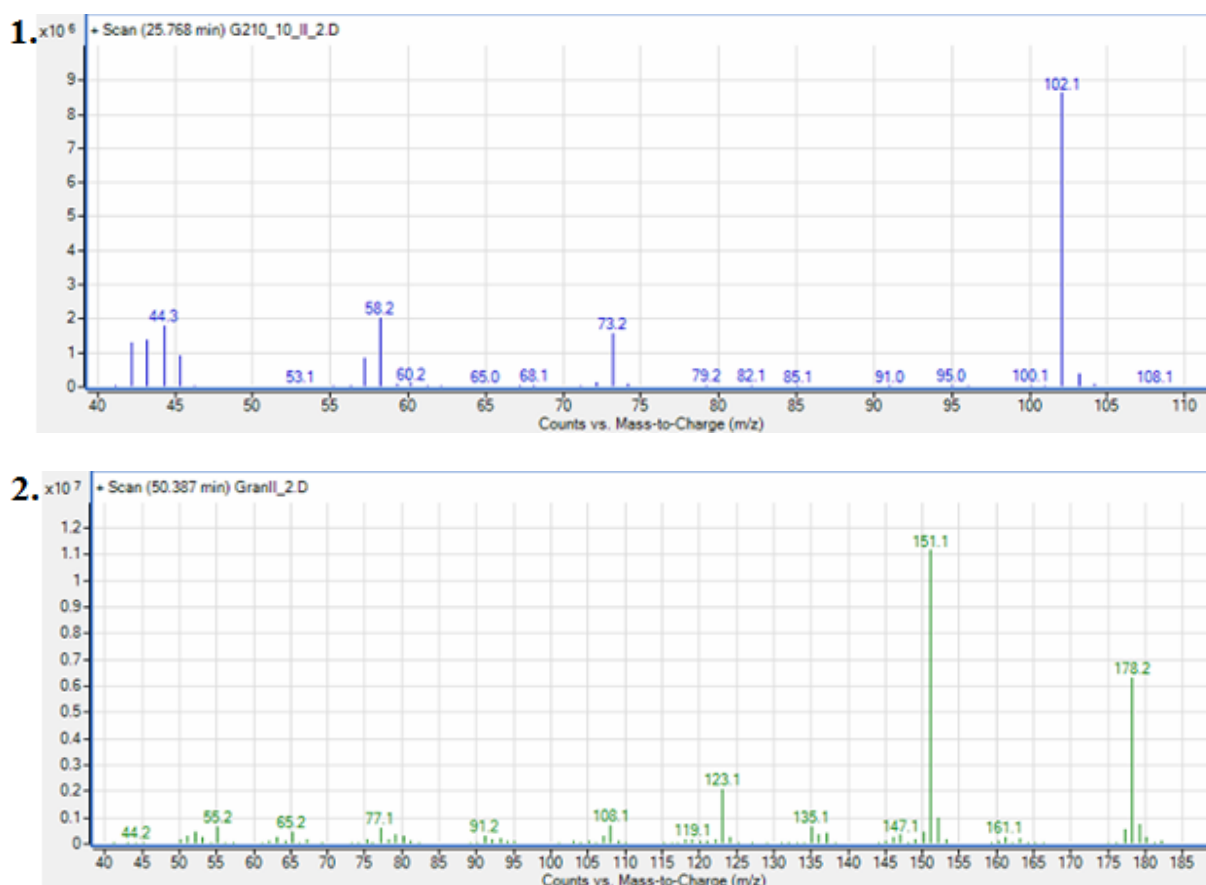


Figure 3.12: Mass spectra of compound no. 6 (1) and compound no. 31 (2).

All 34 peaks were detected in MWL from steam exploded spruce, but only 26 peaks in untreated spruce MWL. Pyrograms of MWL from spruce treated at 180 °C for 10 min and untreated spruce MWL are shown in Figure 3.13 to demonstrate the difference between volatile pyrolyzates formed by untreated spruce MWL and MWL from steam exploded spruce. Most of the compounds (**1**, **3**, **4**, **5**, and **7**) that are only formed in MWL from steam exploded spruce are originate from carbohydrates, but **19** and **21** are lignin derived pyrolyzates. Some carbohydrate derived pyrolyzates were expected due to the dilute acid pretreatment (DAP) of the spruce prior to the steam explosion. DAP is known to facilitate the repolymerization of polysaccharides degradation products such as **3** and polymerization with lignin to form a lignin-like material, termed pseudo-lignin<sup>33, 109</sup>. These compounds are

## Results and Discussion

therefore isolated with the lignin and present in MWL from steam exploded spruce. The aromatic compounds **19** and **21** are however derived from lignin, but nevertheless not detected in untreated spruce MWL. This can be explained by the degree of degradation lignin needs to undergo to form these compounds. Catechols such as **19** and **21** are formed via secondary pyrolysis reactions of guaiacols that require H-acceptors (radicals) and H-donors<sup>69</sup>. Since untreated spruce MWL is not depolymerized and secondary reactions minimal in fast pyrolysis, the route to catechols requires more energy than provided. Steam exploded MWL is however partially depolymerized and needs therefore less energy to form catechols.

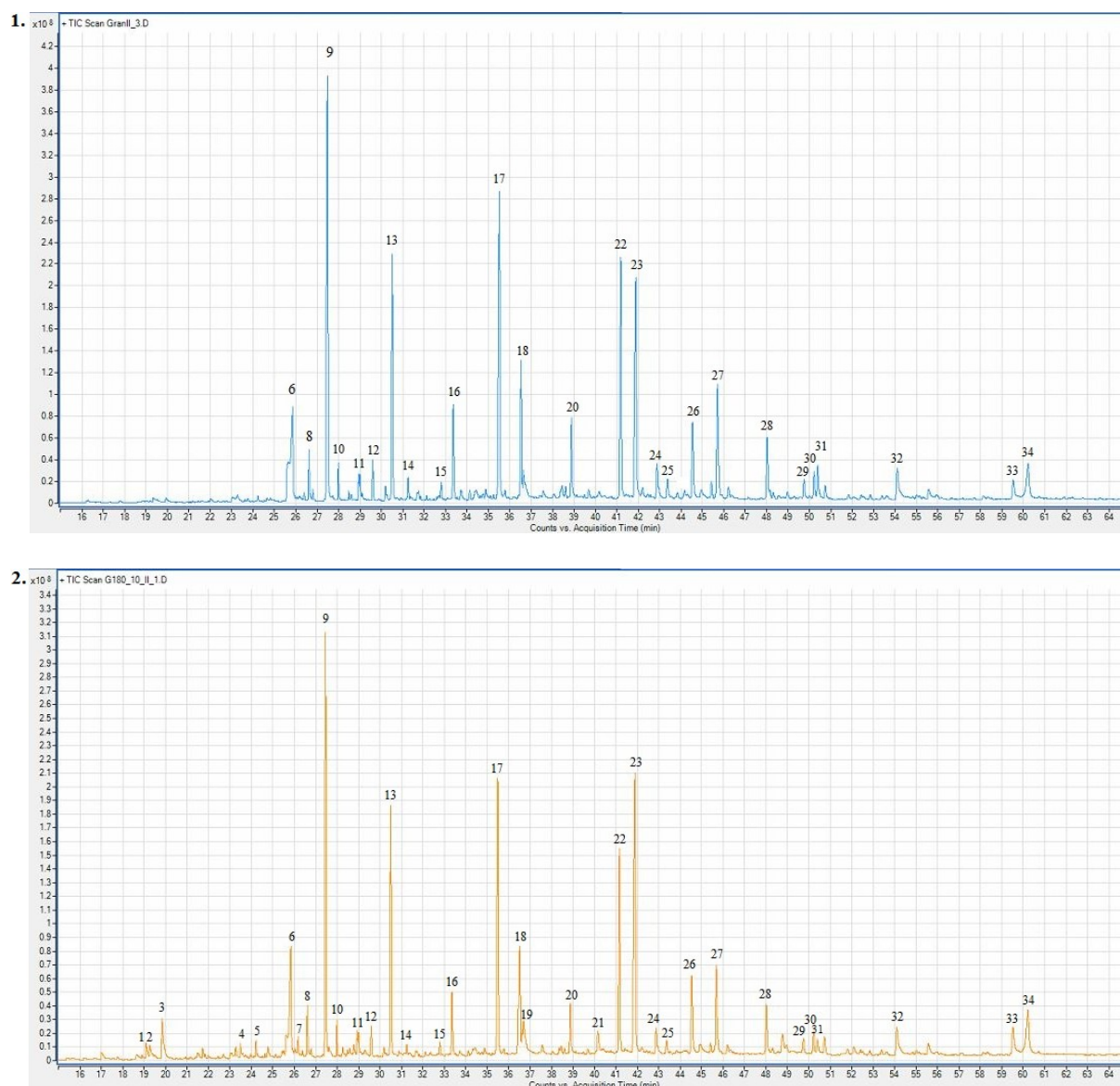


Figure 3.13: Pyrograms of untreated spruce MWL (1) and MWL from SE treated (180 °C for 10 min) spruce (2). The chromatographic window between 15 and 65 min is displayed.

Almost all the volatile pyrolyzates identified in the MWL samples were also identified in the corresponding THF dissolvable MWL samples (see appendix). All major products were

clearly detected, but some less abundant compounds were difficult to detect and their presence confirmed by extracting the molecular ion from the total ion chromatogram (TIC), thereby creating an extracted ion chromatogram (EIC). Only compound **21** that was identified in MWL from steam exploded spruce was not detected in the corresponding THF dissolved MWL samples. All integrated compounds from untreated spruce MWL were also identified and integrated in the corresponding THF dissolved MWL sample. These minor differences confirm that by dissolving MWL in THF, a useful sample is obtained for identification of volatile pyrolyzates from lignin isolated both from steam exploded and untreated spruce.

### 3.3.2 Relative Quantification of Volatile Pyrolyzates

The peaks from the compounds in Table 3.8 were integrated and the total sum of the areas used to calculate the relative amount for each compound for the MWL and the THF dissolvable MWL samples. In addition, the molecular ion of all integrated compounds was extracted from the TIC to obtain EIC due to low signal-to-noise values for most of the low abundant compounds. The relative amount for each compound was calculated from the average of the peak areas from the pyrograms of three replicates using a new portion of sample each time. The experimental error for each value was calculated using standard deviation. Tables for the relative amount and standard deviation for each value from all MWL and THF dissolvable MWL samples are in the appendix.

#### 3.3.2.1 Untreated Spruce MWL

Figure 3.14 shows the relative amount of each integrated compound in untreated spruce MWL. The TIC values are used for comparing different compounds, but the EIC values are included to demonstrate the difference between the values from TIC and EIC. Since EIC is a single chromatogram for each selected  $m/z$  value, the use is limited to comparing the same compounds from different samples, but not for comparing different compounds. However, Figure 3.14 shows that TIC and EIC give approximately the same relative amount for most compounds.

## Results and Discussion

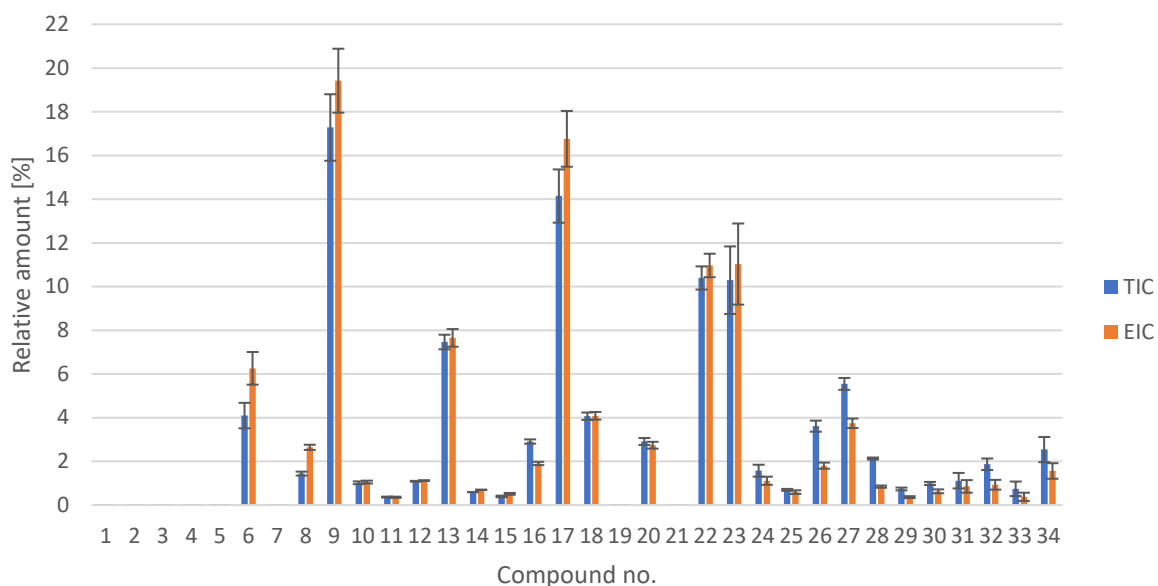


Figure 3.14: Relative amount of the integrated compounds calculated from pyrograms ( $n = 3$ ) of untreated spruce MWL.

Even though there are twenty-six compounds originating from the fast pyrolysis of untreated spruce MWL, only six have relative peak area percentiles exceeding 5% that make up over 65% of the total area. The relative amounts of those six compounds are: **9**: 17.3%, **17**: 14.1%, **22**: 10.4%, **23**: 10.3%, **13**: 7.5%, and **27**: 5.5%. These pyrolyzates were expected to be major products in the pyrolysis of spruce MWL. Du *et al.*<sup>100</sup> performed isothermal temperature pyrolysis on spruce MWL at 500 °C for 1 min. Of nineteen integrated products, these six had combined over 59% of the total area. The relative amounts for each of those compounds were comparable to this study: **9**: 14.1%, **17**: 11.3%, **22**: 8.1%, **23**: 11.0%, **13**: 9.8%, and **27**: 4.8%. However, two other major products were reported that had only low abundance in this study. The alcohol **33** was reported 13.3% and the aldehyde **34** was reported 8.8%, compared to 0.9% and 2.7% respectively in this study. Higher pyrolysis temperature in this study can explain the lower amounts of these pyrolyzates. Compounds **33** and **34** are the alcohol and aldehyde of the same structure that includes propenyl chain that can be degraded in side-chain conversions as shown in Figure 3.15. The relative oxidation/reduction efficiency of **34** side-chains varies with the pyrolysis temperature. At relatively low temperatures, radical conditions are expected, enhancing hydrogen abstraction reactions causing the oxidation product **33** to be the major monomer from lignin pyrolysis.<sup>110</sup> However, by increasing pyrolysis temperature to over 350 °C, the pyrolysis environment becomes richer in H-donor species, resulting in increased monomer yields and the formation of side-chain reduction products such as **22**.<sup>110</sup> With further increased temperature, **33** and **34** continue to

## Results and Discussion

relatively decrease and lower molecular weight guaiacol derivatives become more abundant, while repolymerization and char formation decreases. Another factor causing differences in pyrolysis products and mechanisms is considerably higher heating rate in this study compared to the studies by Du *et al.*<sup>100</sup> and Kotaka *et al.*<sup>110</sup>, neither being fast pyrolysis studies.

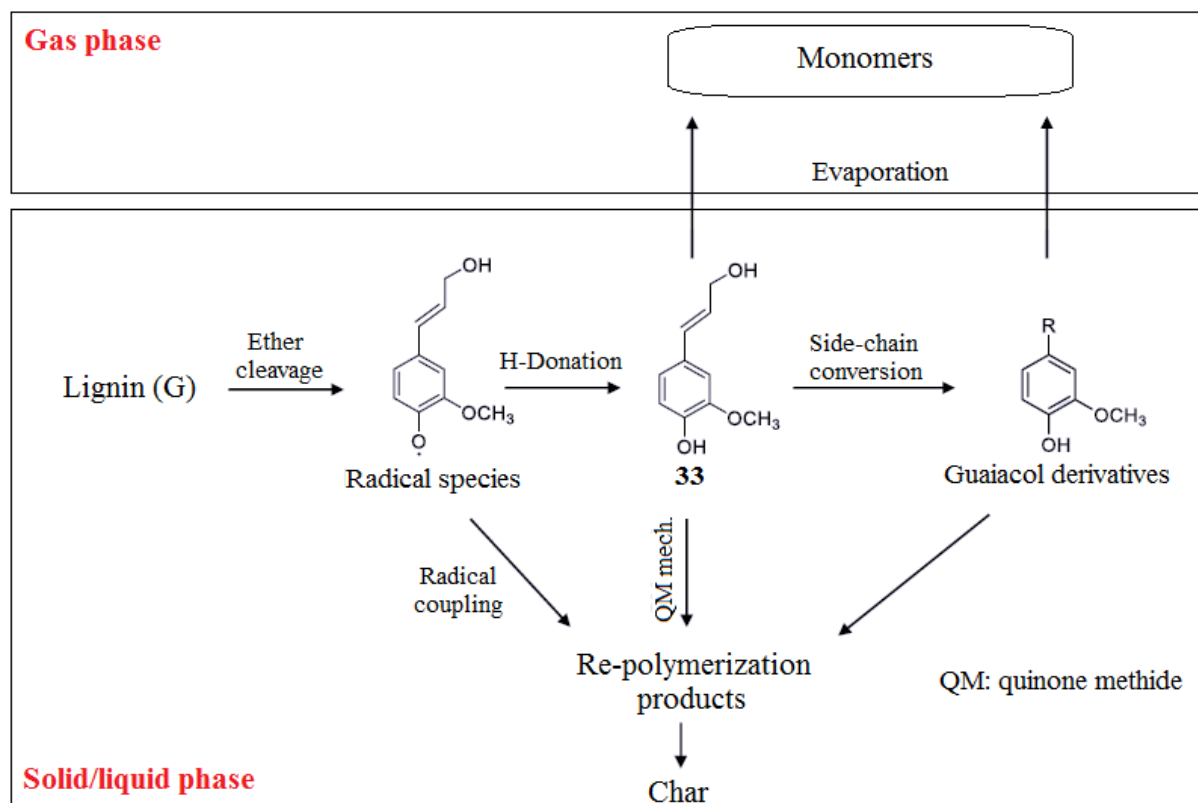


Figure 3.15: Competitive pathways from coniferyl alcohol radical, a primary pyrolysis product, as proposed for the production of monomers and char during pyrolysis of G-type lignin. Adapted from Kawamoto *et al.*<sup>111</sup>

The seven compounds that have 2.1–4.1% abundance are responsible for over 22% of the total amount. The relative amounts of those seven compounds are: **6**: 4.1%, **18**: 4.1%, **26**: 3.6%, **16**: 2.9%, **20**: 2.9%, **34**: 2.5 and **28**: 2.1%. All those products are guaiacol derivatives formed in side-chain conversion reactions except **6**, which is an unknown compound that is not lignin derived according to previous assumption (Figure 3.12.1 and section 3.3.1). The other six compounds are reported by Du *et al.*<sup>100</sup>, consisting of 21% of total amount: **18**: 2.2%, **26**: 2.3%, **16**: 2.2%, **20**: 1.4%, **34**: 8.8 and **28**: 1.5%. All values except for **34** (previously discussed) were a bit lower than in this study, supporting the previous claim that the relative amount of side-chain converted guaiacol derivatives increase with higher pyrolysis temperature. Finally, the cis isomer of **33**, compound **30**, was reported 2.5% of total amount by Du *et al.*<sup>100</sup>, while expectedly only 0.9% in this study according to the previous argument.

### 3.3.2.2 Steam Exploded Spruce MWL

Figure 3.16 shows the relative amount of each integrated compound in MWL from stream exploded spruce treated at 200 °C for 10 min. The TIC values are used for comparing different compounds, but the EIC values are included to demonstrate the difference between the values from TIC and EIC. Compared to untreated spruce MWL in Figure 3.14, the differences between TIC and EIC values are similar for each compound that is identified in both MWL from untreated and steam exploded spruce.

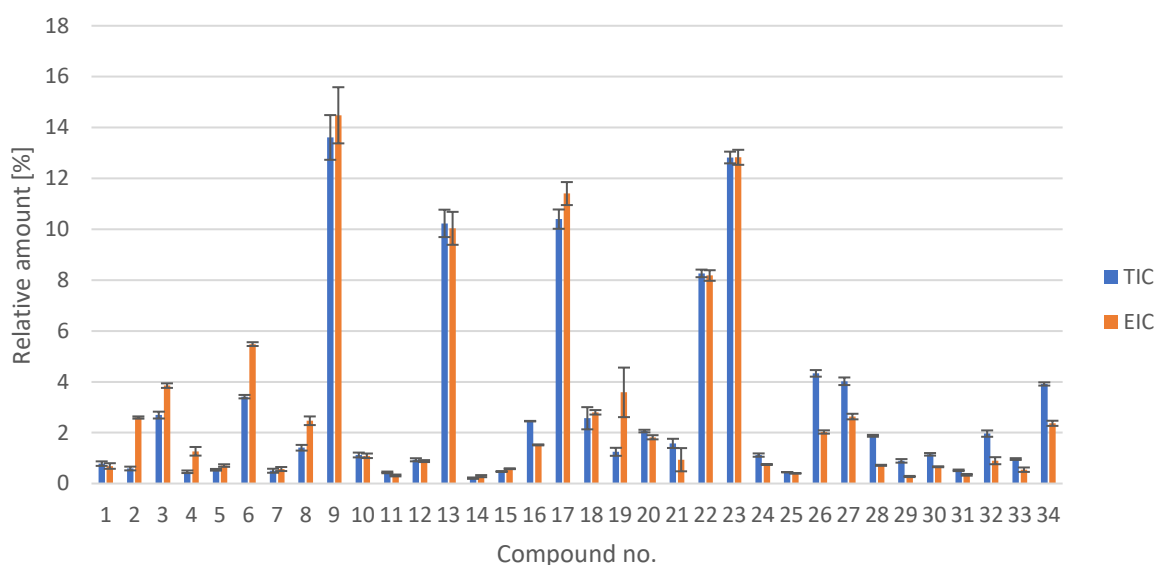


Figure 3.16: Relative amount of the integrated compounds calculated from pyrograms ( $n = 3$ ) of MWL from steam exploded spruce treated at 200 °C for 10 min.

The amount of each volatile pyrolyzate was generally similar in the steam exploded spruce MWL samples, analyzed in this study. Figure 3.17 shows the relative amount of the integrated compounds calculated from pyrograms (TIC) of MWL from steam exploded spruce treated at different temperatures for 5 min (1) and 10 min (2). The six most abundant pyrolyzates from untreated spruce were also major products for all the steam exploded spruce samples. However, the variations were considerable for some of those pyrolyzates and their relative amounts: **9**: 11-16%, **13**: 7-14%, **17**: 9-11%, **22**: 7.5-8.5%, **23**: 9-17%, and **27**: 4-5%. When combining the amount of each of those compounds, the variation was interestingly small, or 58-62%, which is comparable to the 65.2% of total area for untreated spruce MWL. The 5-11% lower values can be explained by the combined relative amount of the compounds that were only identified in MWL from steam exploded spruce. Compounds **1-5**, **7**, **19**, and **21**

## Results and Discussion

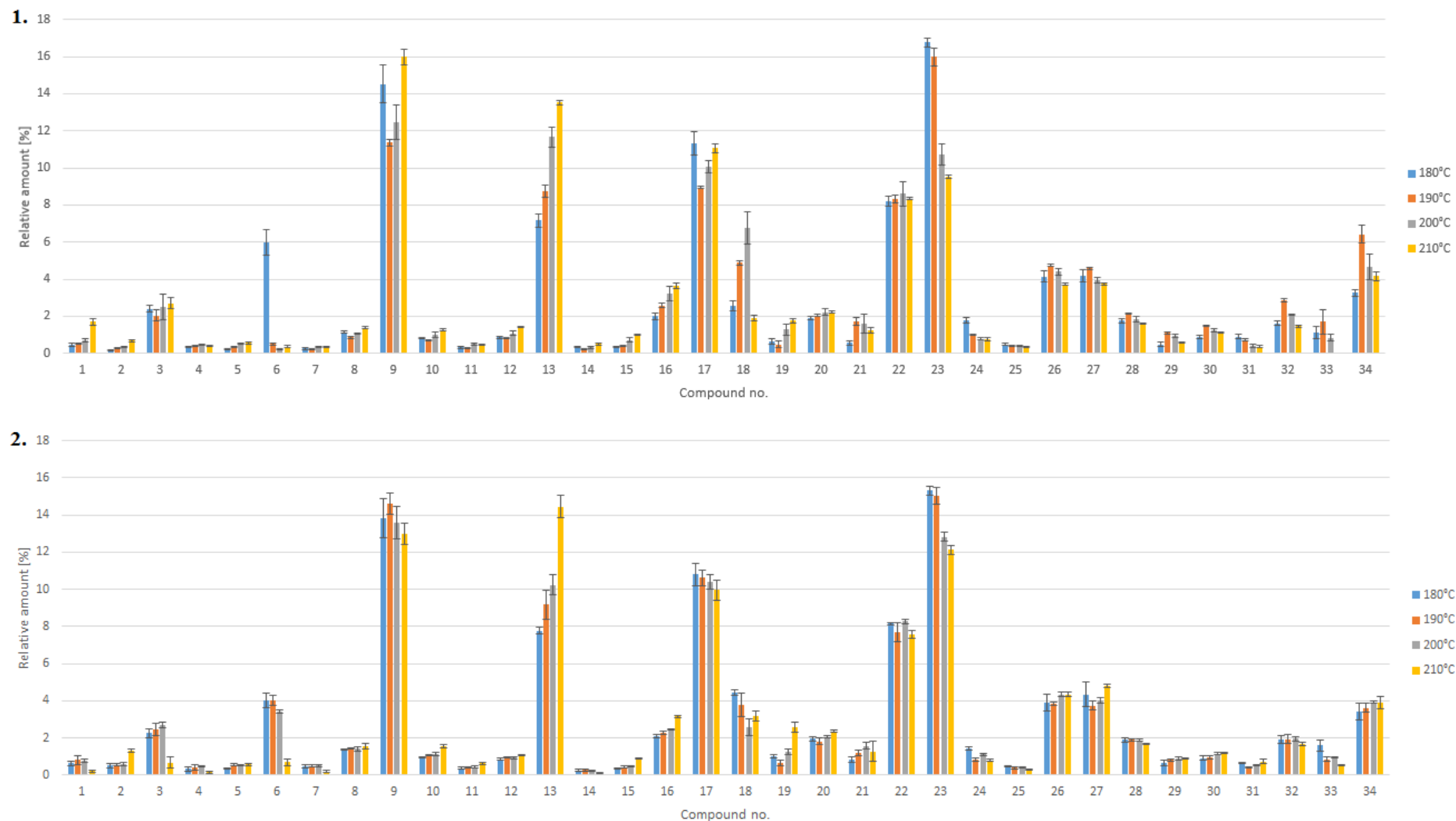


Figure 3.17: Relative amount of the integrated compounds calculated from pyrograms ( $n = 3$ ) of MWL from steam exploded spruce treated at different temperatures for 5 min (1) and for 10 min (2).

are responsible for 3-7% of the total peak area for the MWL samples from steam exploded spruce.

The seven products next in abundance that contain over 22% of the total area in the untreated spruce MWL pyrograms show also considerable variations in relative amount for some of those compounds. The relative amounts of those seven compounds are: **6**: 0.1-6.0%, **16**: 2-4%, **18**: 2-7%, **20**: 1.9-2.1%, **26**: 4-5%, **28**: 1.6-2.0% and **34**: 3-6%. The combined amounts are 18-23%, which the total area for those seven compounds in untreated spruce MWL is within. Even though variations for some of those compounds are considerable, no relationship is between the variation magnitude and behavior of the compound with increased severity of SE conditions. Furthermore, whether the SE residence time is five or ten minutes does not seem to impact the relative amount of pyrolyzates formed. However, the amount formed of some major and minor compounds is affected by what SE temperature was used in the sample pretreatment.

Figure 3.18 demonstrates how relative amount of selected pyrolyzates changes with increased temperature of steam explosion, both for the 5 min (1) and 10 min (2) residence time samples. The relative amount of untreated spruce MWL is included on both graphs for comparison. Since these graphs are shown to demonstrate the changes within each compound, EIC values are used. Although using the TIC values is sufficient to evaluate the changes for **13**, **16**, and **23**, these values do not reveal the increase with higher temperature for compounds **15**, **19**, and **21**. For **15** and **21**, TIC did not show the increase because of low abundance, resulting in low signal-to-noise values and therefore unreliable integration values. The diol **19** peak was broad and partly overlapped in most of the pyrograms, resulting in difficulties in integration, but by extracting  $m/z$  110 from the TIC and integrating the EIC peaks, an obvious increase with SE temperature was observed.

The guaiacol derivatives **13** and **16** contain side-chains  $R = CH_3$  and  $R = CH_2CH_3$ , respectively, and show similar patterns when comparing untreated spruce MWL and different SE temperatures (Figure 3.18). Differences in the relative amount is minimal for untreated spruce and 180 °C SE treated spruce MWL, but the increase substantial with higher SE temperature. This pattern can be explained by increased depolymerization of lignin with higher SE temperature. The alkyl chain is thereby partially reduced in the SE treated samples and side-chain conversion during pyrolysis (Figure 3.15) are further towards shorter and more reduced alkyl chains because the same energy is applied in the pyrolysis of all samples. Furthermore, guaiacol derivatives containing longer and less reduced side-chains such as **17**



## Results and Discussion

and **22** are considerably more abundant in untreated spruce MWL than in SE spruce MWL (Figure 3.14 and Figure 3.16), supporting the previous claim.

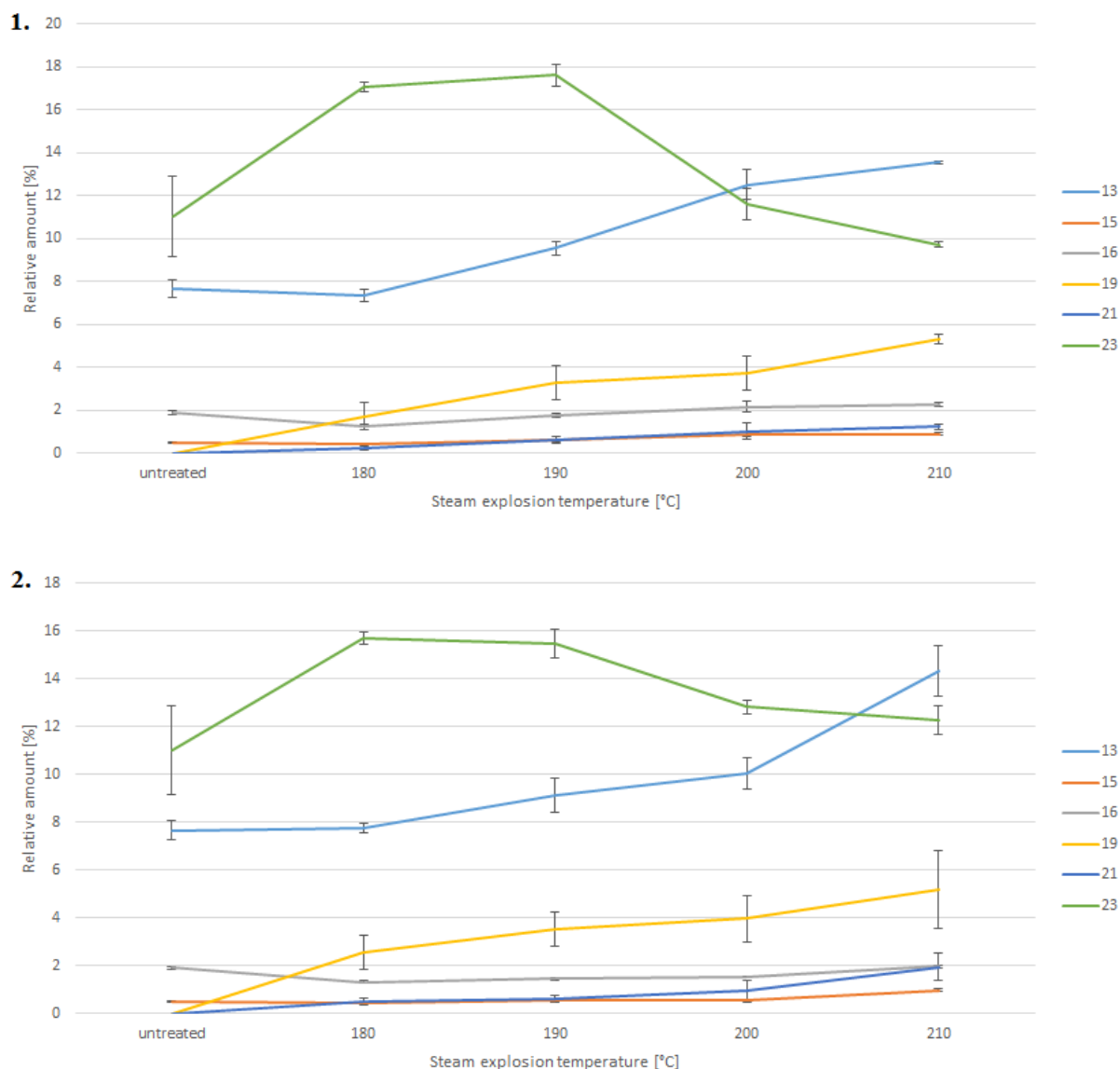


Figure 3.18: Relative amount ( $n = 3$ ) of selected compounds as a function of steam explosion temperature, 5 min (1) and for 10 min (2). Untreated spruce MWL is included in both graphs.

The catechols **19** and **21** are also derived from guaiacol, and show similar patterns when comparing untreated spruce MWL and different SE temperatures (Figure 3.18). The absence of **19** and **21** was explained in section 3.3.1 and similar reasons apply for their increasing amount with higher SE temperatures. Since the most severely treated sample has undergone highest level of degradation, more amount of highly degraded compounds such as **19** and **21** are formed. The degree of degradation lignin needs to undergo to form these compounds during pyrolysis becomes less with more partially degraded lignin samples.

The aromatic diol **15** has a condensed, rearranged lignin structure and the amount increases slightly with higher SE temperatures. Since condensation of lignin increases with more severe steam explosion conditions, the formation of methyl substituted aromatic pyrolyzates is expected to increase. However, the abundance of **15** is very low and it is difficult to draw conclusions.

The aldehyde **23** has a completely different pattern than the other compounds in Figure 3.18. Relative amount of **23** increases considerably from untreated spruce MWL to the least severely treated sample, but decreases with increased SE temperature. After the dilute acid and steam explosion pretreatment, the aryl ether ( $\beta$ -O-4) linkages are partially hydrolyzed, leading to the formation of compounds **36**, **37**, and **38** (). He *et al.*<sup>112</sup> suggested those three routes in a study of a lignin model compound (**35**) pyrolysis pathways. Route 2 leads to the formation of **23**. Phenylallyl alcohol **37** can be formed in a concerted reaction, but the enol structure is unstable and would tautomerize to phenyl acetone alcohol **40**. Compound **40** may decarbonylate to form compound **41** and carbon monoxide, then decomposing to **23**. Pretreatment of spruce seems to facilitate the formation of **37** and thereby **23**, but since aldehydes become less stable and can decarbonylate with increased temperature, the formation of **23** decreases with increased SE temperature.

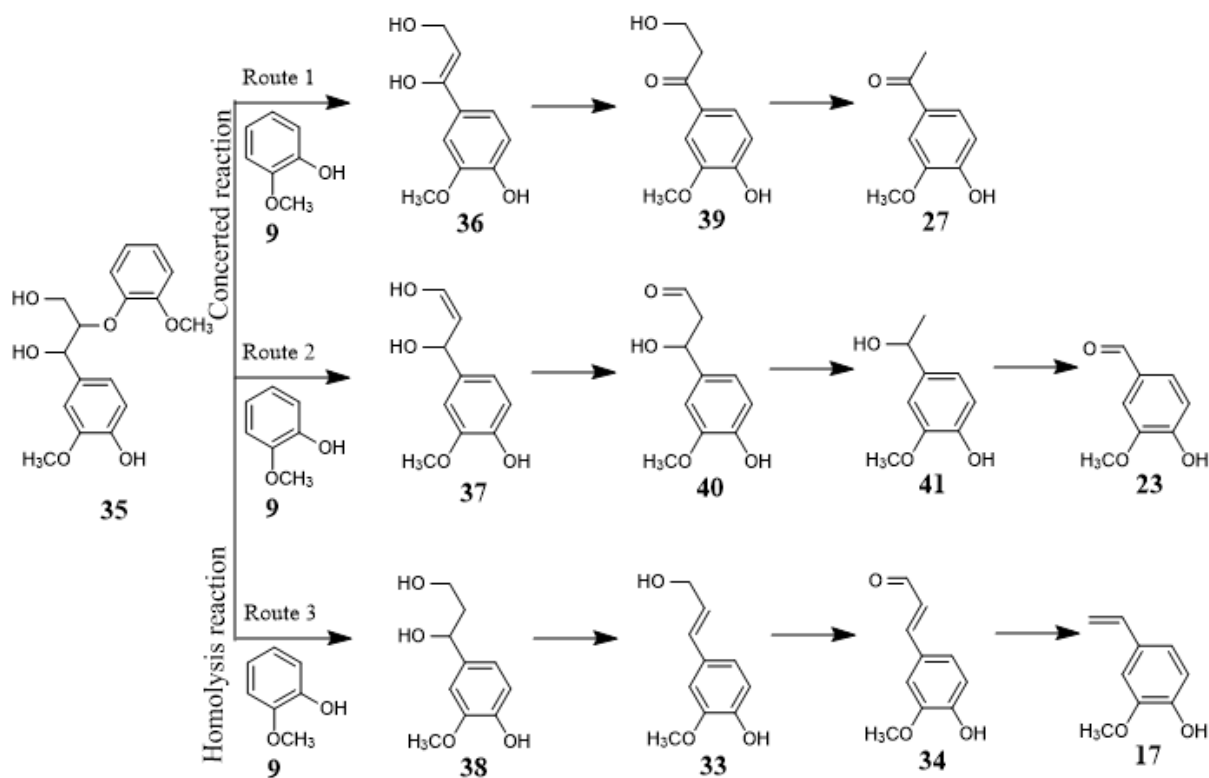


Figure 3.19: Pyrolysis pathways of a lignin model compound. Adapted from He *et al.*<sup>112</sup>

### 3.3.2.3 THF dissolvable MWL: Comparison to MWL

Figure 3. shows the relative amount of each integrated compound in THF dissolvable MWL from untreated spruce and MWL from untreated spruce. Even though all identified pyrolyzates from untreated spruce MWL are detected in the corresponding THF dissolvable MWL, considerable differences are between the relative amount for most compounds. The abundance is higher in spruce MWL for compounds **6-22**, but lower for **23-34**. The structural similarities are clear for these groups of compounds. The pyrolyzates from **23** and up all contain one or more oxygen atoms on the side-chain, while compounds **6-22** either do not contain a side-chain or the side-chain is an alkene or an alkane. A good example of these differences are compounds **17** and **23**. The only difference between the structures is that the alkene **17** has a CH<sub>2</sub> group connected to the double bond at the end of the side-chain, while the aldehyde **23** has an oxygen atom instead. For the THF dissolvable MWL, **17** has a relative amount of 10% and **23** has 18%, but **17** has 14% and **23** has 10% for MWL. Total relative amount of compounds that contain ketone-, aldehyde-, or alcohol side-chain is 42% for THF dissolvable MWL, but only 26% for MWL. These differences in relative amount of pyrolyzates demonstrate the heterogeneity of the lignin polymer and how lignin analysis is dependent of purification methods. Furthermore, the pyrolysis results from those two samples indicate that the lignin obtained after dissolving MWL in THF is probably less representative of native spruce lignin.

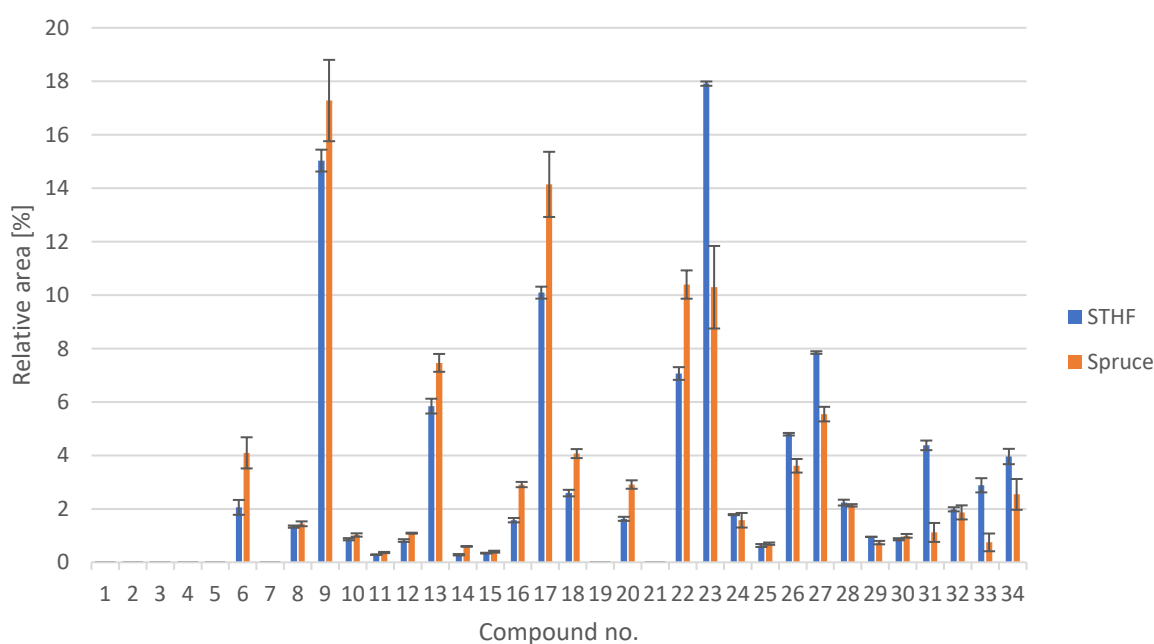


Figure 3.20: Relative amount of the integrated compounds calculated from pyrograms ( $n = 3$ ) of THF dissolvable MWL from untreated spruce and MWL from untreated spruce.

Figure 3. shows the relative amount of the integrated compounds calculated from pyrograms (TIC) of MWL from steam exploded spruce treated at different temperatures for 10 min (1) and the corresponding THF dissolvable MWL samples (2). In contrast to the large differences between most compounds for the untreated spruce (Figure 3.), only few compounds show considerable differences in relative amount when comparing MWL and THF dissolvable MWL steam exploded spruce samples. The seven most abundant pyrolyzates from MWL were also the most abundant from THF dissolvable MWL for the steam exploded spruce samples. However, the variations in pyrolyzate relative amounts between different SE temperatures were generally more for the THF dissolvable MWL samples: **9**: 12-19%, **13**: 7-15%, **17**: 8-11%, **22**: 7-8%, **23**: 11-21%, **26**: 3.9-4.2% and **27**: 4.0-4.2%, compared to MWL amounts: **9**: 14-15%, **13**: 8-14%, **17**: 10-11%, **22**: 7.5-8.0%, **23**: 12-14%, **26**: 3.9-4.1% and **27**: 4-5%. When combining the amount of each of those compounds, the variation was interestingly small, or 67-72% for the THF dissolvable MWL pyrolyzates and 63-66% for the MWL pyrolyzates. For each SE temperature, the MWL values were 3-8% lower.

Only two of the six compounds that showed either increase or decrease with higher SE temperature for MWL from steam exploded spruce, did also show the same behavior for the THF dissolvable MWL samples. The diol **21** was not detected in the THF dissolvable MWL samples. Figure 3. demonstrates how relative amount of those five pyrolyzates changes with increased temperature of steam explosion, for the 10 min MWL samples (1) and the corresponding THF dissolvable MWL (2). Both graphs include the relative amount of untreated spruce MWL for comparison. Since these graphs are shown to demonstrate the changes within each compound, EIC values are used. Compounds **13** and **23** show similar behavior in MWL and THF dissolvable MWL, comparing the two graphs. However, considerably higher relative amount of **23** was observed for THF dissolvable MWL, especially for the untreated sample and the two lowest temperatures. The curve then becomes steeper and for the sample treated with most severe SE conditions, the amount is measured higher for the MWL sample. The relative amount of compound **13** increases with SE temperature in both graphs with minor differences in the curve. The considerable increase with SE temperature for **19** observed in MWL, is not observed for the corresponding THF dissolvable MWL, only irregular variations. Pyrolyzates **15** and **16** that showed minor increase with temperature in MWL, did not show clear increase in THF dissolvable MWL.

## Results and Discussion

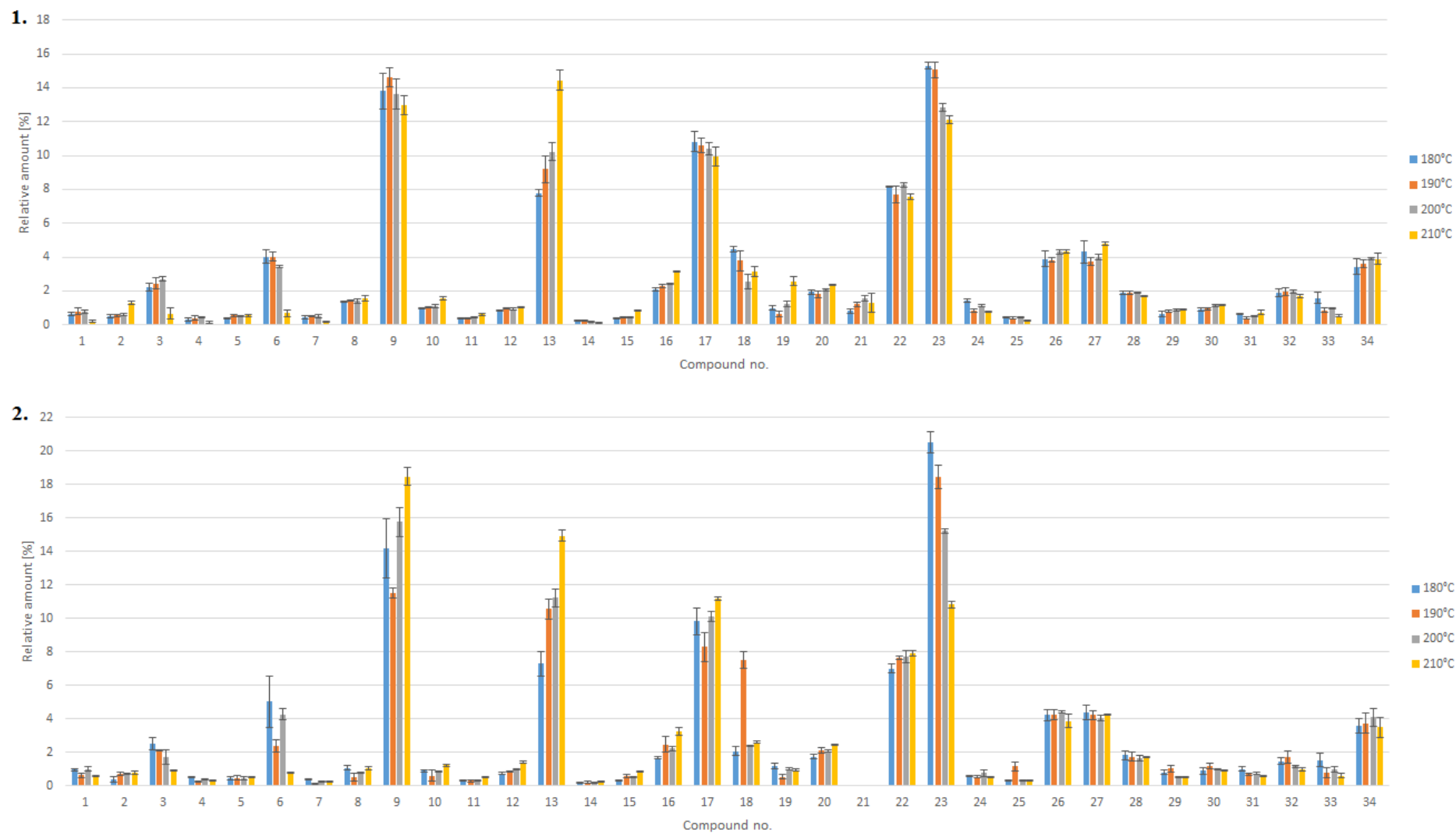


Figure 3.21: Relative amount of the integrated compounds calculated from pyrograms ( $n = 3$ ) of MWL from steam exploded spruce treated at different temperatures for 10 min (1) and the corresponding THF dissolvable MWL samples (2).

## Results and Discussion

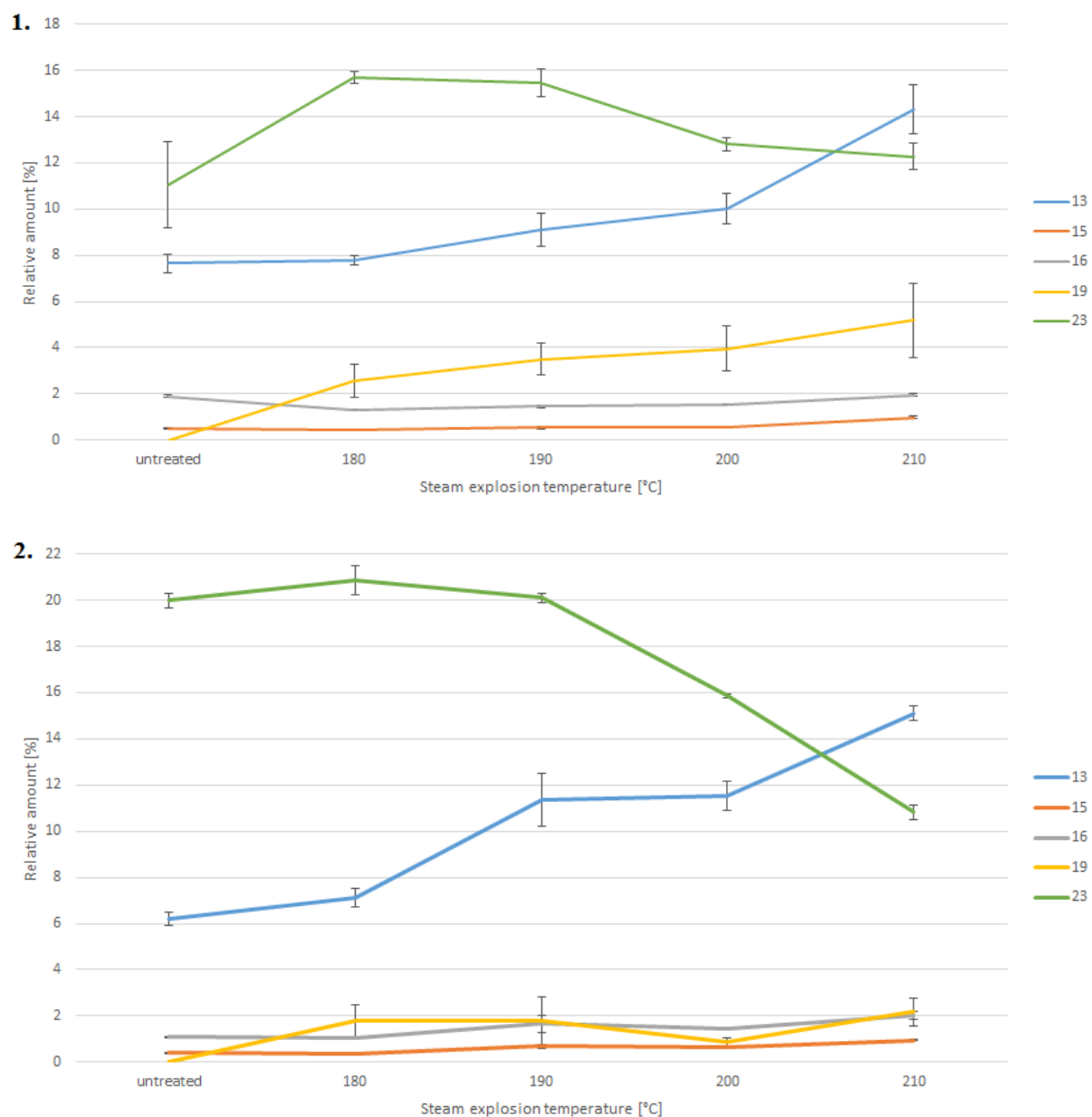


Figure 3.22: Relative amount ( $n = 3$ ) of selected compounds as a function of steam explosion temperature, MWL 10 min (1) and the corresponding THF dissolvable MWL samples (2). Untreated spruce MWL is included in both graphs.

Relative quantification of pyrolyzates from the THF dissolvable MWL samples showed generally considerable differences compared to the corresponding MWL samples, especially for untreated spruce. The steam exploded samples showed more similarities, indicating less heterogeneity of lignin from SE treated than untreated spruce. However, the trends for increased SE temperatures were only observed for two of six pyrolyzates in THF dissolvable MWL compared to MWL. These differences in relative amount of pyrolyzates demonstrate the heterogeneity of the lignin polymer and that lignin analysis depends on purification methods. Furthermore, the pyrolysis results from those samples indicate that the lignin

## Results and Discussion

obtained after dissolving MWL in THF is probably less representative of lignin isolated from steam exploded spruce and native spruce lignin.

## 4. Conclusion

The steam explosion pretreatment altered the structure of lignin considerably. The HSQC experiments revealed how increasing SE temperature facilitated the degradation of  $\beta$ -O-4' linkages, partially resulting in condensation reactions to form  $\beta$ -5' linkages among other C-C bonds. Furthermore, the similar amount of  $\beta$ - $\beta'$  linkages for all samples indicated degradation and formation of those linkages during SE treatment at a similar rate. The lowest abundant linkages (5-5'-O-4,  $\beta$ -1', and  $\alpha$ -O- $\alpha'$ ) were only detected in untreated spruce and therefore completely degraded by the SE treatment.

Formation of carbohydrate derived pyrolyzates in the py-GC-MS experiments indicated condensation reactions between lignin and carbohydrates or during the pretreatment, forming pseudo-lignin that was isolated as MWL. Increased amount of G-lignin derivatives with shorter and more reduced side-chains confirmed increased depolymerization with higher SE temperature. The higher relative amount of 4-hydroxy-3-methoxybenzaldehyde after the mildest SE treatment indicated the partial hydrolysis of  $\beta$ -O-4' linkages during the pretreatment, but decreased amount with higher SE temperature confirmed thermal degradation of the aldehyde. Furthermore, comparison between pyrolyzates from MWL and THF dissolvable MWL indicated less heterogeneity in the lignin polymer after SE treatment.

Since less heterogeneous lignin provides generally more possibilities for valuable end products<sup>13</sup>, steam explosion pretreatment of spruce can facilitate valorization of lignin. Structural changes in spruce lignin during SE treatment were found almost entirely dependent on steam temperature, and only minimally residence time, indicating that optimal steam treatment conditions for spruce are rather towards lower temperature and longer residence time, since less condensation is favorable for sugar recovery.<sup>29</sup>



## Conclusion

## 5. References

1. Ragauskas, A. J., Williams, C. K., Davison, B. H., Britovsek, G., Cairney, J., Eckert, C. A., Frederick, W. J., Hallett, J. P., Leak, D. J., Liotta, C. L., et al. (2006). The path forward for biofuels and biomaterials. *Science*, 311 (5760): 484-489.
2. Sun, Y. & Cheng, J. Y. (2002). Hydrolysis of lignocellulosic materials for ethanol production: a review. *Bioresource Technology*, 83 (1): 1-11.
3. Simionescu, C. I., Macoveanu, M. M., Vasile, C., Ciobanu, F., Esanu, M., Ioanid, A., Vidrascu, P. & GeorgescuBuruntea, N. (1996). Polyolefins/lignosulfonates blends. *Cellulose Chemistry and Technology*, 30 (5-6): 411-429.
4. Wang, Q., Aitkadi, A. & Kaliaguine, S. (1992). Catalytic Grafting - a New Technique for Polymer Fiber Composites .2. Plasma Treated Uhmpe Fibers Polyethylene Composites. *Journal of Applied Polymer Science*, 45 (6): 1023-1033.
5. Felby, C., Hassingboe, J. & Lund, M. (2002). Pilot-scale production of fiberboards made by laccase oxidized wood fibers: board properties and evidence for cross-linking of lignin. *Enzyme and Microbial Technology*, 31 (6): 736-741.
6. Felby, C., Thygesen, L. G., Sanadi, A. & Barsberg, S. (2004). Native lignin for bonding of fiber boards - evaluation of bonding mechanisms in boards made from laccase-treated fibers of beech (*Fagus sylvatica*). *Industrial Crops and Products*, 20 (2): 181-189.
7. Kleinert, M. & Barth, T. (2008). Towards a lignin-cellulosic biorefinery: Direct one-step conversion of lignin to hydrogen-enriched biofuel. *Energy & Fuels*, 22 (2): 1371-1379.
8. Vinardell, M. P., Ugartondo, V. & Mitjans, M. (2008). Potential applications of antioxidant lignins from different sources. *Industrial Crops and Products*, 27 (2): 220-223.
9. Baker, D. A., Gallego, N. C. & Baker, F. S. (2012). On the characterization and spinning of an organic-purified lignin toward the manufacture of low-cost carbon fiber. *Journal of Applied Polymer Science*, 124 (1): 227-234.
10. Norberg, I., Nordstrom, Y., Drougge, R., Gellerstedt, G. & Sjöholm, E. (2013). A new method for stabilizing softwood kraft lignin fibers for carbon fiber production. *Journal of Applied Polymer Science*, 128 (6): 3824-3830.

## References

11. Dizhbite, T., Telysheva, G., Jurkjaņe, V. & Viesturs, U. (2004). Characterization of the radical scavenging activity of lignins - natural antioxidants. *Bioresource Technology*, 95 (3): 309-317.
12. Sakagami, H., Kohno, S., Takeda, M., Nakamura, K., Nomoto, K., Ueno, I., Kanegasaki, S., Naoe, T. & Kawazoe, Y. (1992). O-2 Scavenging Activity of Lignins, Tannins and Psk. *Anticancer Research*, 12 (6b): 1995-2000.
13. Stewart, D. (2008). Lignin as a base material for materials applications: Chemistry, application and economics. *Industrial Crops and Products*, 27 (2): 202-207.
14. Akin, D. E., Rigsby, L. L., Sethuraman, A., Morrison, W. H., Gamble, G. R. & Eriksson, K. E. L. (1995). Alterations in Structure, Chemistry, and Biodegradability of Grass Lignocellulose Treated with the White-Rot Fungi *Ceriporiopsis-Subvermispora* and *Cyathus-Stercoreus*. *Applied and Environmental Microbiology*, 61 (4): 1591-1598.
15. Excoffier, G., Toussaint, B. & Vignon, M. R. (1991). Saccharification of Steam-Exploded Poplar Wood. *Biotechnology and Bioengineering*, 38 (11): 1308-1317.
16. Ghosh, P. & Singh, A. (1993). Physicochemical and Biological Treatments for Enzymatic/Microbial Conversion of Lignocellulosic Biomass. *Advances in Applied Microbiology*, Vol 39, 39: 295-333.
17. Khanal, S. K., Montalbo, M., van Leeuwen, J., Srinivasan, G. & Grewell, D. (2007). Ultrasound enhanced glucose release from corn in ethanol plants. *Biotechnology and Bioengineering*, 98 (5): 978-985.
18. Lynd, L. R., Cushman, J. H., Nichols, R. J. & Wyman, C. E. (1991). Fuel Ethanol from Cellulosic Biomass. *Science*, 251 (4999): 1318-1323.
19. Schwald, W., Breuil, C., Brownell, H. H., Chan, M. & Saddler, J. N. (1989). Assessment of Pretreatment Conditions to Obtain Fast Complete Hydrolysis on High Substrate Concentrations. *Applied Biochemistry and Biotechnology*, 20-1: 29-44.
20. Toussaint, B., Excoffier, G. & Vignon, M. R. (1991). Effect of Steam Explosion Treatment on the Physicochemical Characteristics and Enzymatic-Hydrolysis of Poplar Cell-Wall Components. *Animal Feed Science and Technology*, 32 (1-3): 235-242.
21. Eriksson, K. E., Gruenewald, A. & Vallander, L. (1980). Studies of growth conditions in wood for three white-rot fungi and their cellulaseless mutants. *Biotechnol. Bioeng.*, 22 (2): 363-76.

## References

22. Tsukihara, T., Honda, Y., Sakai, R., Watanabe, T. & Watanabe, T. (2006). Exclusive overproduction of recombinant versatile peroxidase MnP2 by genetically modified white rot fungus, *Pleurotus ostreatus*. *Journal of Biotechnology*, 126 (4): 431-439.
23. Yang, B. & Wyman, C. E. (2008). Pretreatment: the key to unlocking low-cost cellulosic ethanol. *Biofuels Bioproducts & Biorefining-Biofpr*, 2 (1): 26-40.
24. Mosier, N., Wyman, C., Dale, B., Elander, R., Lee, Y. Y., Holtzapple, M. & Ladisch, M. (2005). Features of promising technologies for pretreatment of lignocellulosic biomass. *Bioresource Technology*, 96 (6): 673-686.
25. von Sivers, M. & Zacchi, G. (1995). A techno-economical comparison of three processes for the production of ethanol from pine. *Bioresour. Technol.*, 51 (1): 43-52.
26. Millett, M. A., Baker, A. J. & Satter, L. D. (1976). Physical and Chemical Pretreatments for Enhancing Cellulose Saccharification. *Biotechnology and Bioengineering* (6): 125-153.
27. FitzPatrick, M., Champagne, P., Cunningham, M. F. & Whitney, R. A. (2010). A biorefinery processing perspective: Treatment of lignocellulosic materials for the production of value-added products. *Bioresource Technology*, 101 (23): 8915-8922.
28. Teramoto, Y., Tanaka, N., Lee, S. H. & Endo, T. (2008). Pretreatment of eucalyptus wood chips for enzymatic saccharification using combined sulfuric acid-free ethanol cooking and ball milling. *Biotechnology and Bioengineering*, 99 (1): 75-85.
29. Ramos, L. P. (2003). The chemistry involved in the steam treatment of lignocellulosic materials. *Quimica Nova*, 26 (6): 863-871.
30. Overend, R. P. & Chornet, E. (1987). Fractionation of Lignocellulosics by Steam-Aqueous Pretreatments. *Philosophical Transactions of the Royal Society a-Mathematical Physical and Engineering Sciences*, 321 (1561): 523-536.
31. Vivekanand, V., Olsen, E. F., Eijsink, V. G. H. & Horn, S. J. (2013). Effect of different steam explosion conditions on methane potential and enzymatic saccharification of birch. *Bioresource Technology*, 127: 343-349.
32. Fengel, D. & Wegener, G. (1983). *Wood: chemistry, ultrastructure, reactions*: De Gruyter.
33. Li, J. B., Henriksson, G. & Gellerstedt, G. (2007). Lignin depolymerization/repolymerization and its critical role for delignification of aspen wood by steam explosion. *Bioresource Technology*, 98 (16): 3061-3068.
34. Chabannes, M., Ruel, K., Yoshinaga, A., Chabbert, B., Jauneau, A., Joseleau, J. P. & Boudet, A. M. (2001). In situ analysis of lignins in transgenic tobacco reveals a

## References

- differential impact of individual transformations on the spatial patterns of lignin deposition at the cellular and subcellular levels. *Plant Journal*, 28 (3): 271-282.
35. Jones, L., Ennos, A. R. & Turner, S. R. (2001). Cloning and characterization of irregular xylem4 (irx4): a severely lignin-deficient mutant of Arabidopsis. *Plant Journal*, 26 (2): 205-216.
  36. Campbell, M. M. & Sederoff, R. R. (1996). Variation in lignin content and composition - Mechanism of control and implications for the genetic improvement of plants. *Plant Physiology*, 110 (1): 3-13.
  37. Dewick, P. M. (2009). The Shikimate Pathway: Aromatic Amino Acids and Phenylpropanoids. In *Medicinal Natural Products*, pp. 137-186: John Wiley & Sons, Ltd.
  38. Adler, E. (1977). Lignin Chemistry - Past, Present and Future. *Wood Science and Technology*, 11 (3): 169-218.
  39. Boerjan, W., Ralph, J. & Baucher, M. (2003). Lignin biosynthesis. *Annual Review of Plant Biology*, 54: 519-546.
  40. Sette, M., Wechselberger, R. & Crestini, C. (2011). Elucidation of Lignin Structure by Quantitative 2D NMR. *Chemistry-a European Journal*, 17 (34): 9529-9535.
  41. Yaku, F., Tanaka, R. & Koshijima, T. (1981). Lignin Carbohydrate Complex .4. Lignin as Side-Chain of the Carbohydrate in Bjorkman Lcc. *Holzforschung*, 35 (4): 177-181.
  42. Balakshin, M. Y., Capanema, E. A. & Chang, H. M. (2007). MWL fraction with a high concentration of lignin-carbohydrate linkages: Isolation and 2D NMR spectroscopic analysis. *Holzforschung*, 61 (1): 1-7.
  43. Lawoko, M., Henriksson, G. & Gellerstedt, G. (2005). Structural differences between the lignin-carbohydrate complexes present in wood and in chemical pulps. *Biomacromolecules*, 6 (6): 3467-3473.
  44. Balakshin, M., Capanema, E., Gracz, H., Chang, H. M. & Jameel, H. (2011). Quantification of lignin-carbohydrate linkages with high-resolution NMR spectroscopy. *Planta*, 233 (6): 1097-1110.
  45. Wen, J. L., Sun, S. L., Xue, B. L. & Sun, R. C. (2013). Quantitative Structures and Thermal Properties of Birch Lignins after Ionic Liquid Pretreatment. *Journal of Agricultural and Food Chemistry*, 61 (3): 635-645.

## References

46. Guerra, A., Filpponen, I., Lucia, L. A., Saquing, C., Baumberger, S. & Argyropoulos, D. S. (2006). Toward a better understanding of the lignin isolation process from wood. *Journal of Agricultural and Food Chemistry*, 54 (16): 5939-5947.
47. Obst, J. R. & Kirk, T. K. (1988). Isolation of Lignin. *Methods in Enzymology*, 161: 3-12.
48. Wu, S. & Argyropoulos, D. S. (2003). An improved method for isolating lignin in high yield and purity. *Journal of Pulp and Paper Science*, 29 (7): 235-240.
49. Gellerstedt, G. (1992). *Chemical degradation methods: permanganate oxidation [of lignin in solution]*: Springer. 322-33 pp.
50. Erickson, M., Larsson, S. & Miksche, G. E. (1973). Gas chromatographic analysis of lignin oxidation products. VII. Improved method for the characterization of lignins by methylation and oxidative degradation. *Acta Chem. Scand.*, 27 (1): 127-40.
51. Lapiere, C., Pollet, B., Monties, B. & Rolando, C. (1991). Thioacidolysis of Spruce Lignin - Gc-Ms Analysis of the Main Dimers Recovered after Raney-Nickel Desulfuration. *Holzforschung*, 45 (1): 61-68.
52. Lu, F. C. & Ralph, J. (1998). The DFRC method for lignin analysis. 2. Monomers from isolated lignins. *Journal of Agricultural and Food Chemistry*, 46 (2): 547-552.
53. Holtman, K. M., Chang, H. M., Jameel, H. & Kadla, J. F. (2003). Elucidation of lignin structure through degradative methods: Comparison of modified DFRC and thioacidolysis. *Journal of Agricultural and Food Chemistry*, 51 (12): 3535-3540.
54. Galletti, G. C. & Bocchini, P. (1995). Pyrolysis/Gas Chromatography/Mass Spectrometry of Lignocellulose. *Rapid Communications in Mass Spectrometry*, 9 (9): 815-826.
55. Amen-Chen, C., Pakdel, H. & Roy, C. (2001). Production of monomeric phenols by thermochemical conversion of biomass: a review. *Bioresource Technology*, 79 (3): 277-299.
56. Jarvis, M. W., Daily, J. W., Carstensen, H. H., Dean, A. M., Sharma, S., Dayton, D. C., Robichaud, D. J. & Nimlos, M. R. (2011). Direct Detection of Products from the Pyrolysis of 2-Phenethyl Phenyl Ether. *Journal of Physical Chemistry A*, 115 (4): 428-438.
57. Nowakowski, D. J., Bridgwater, A. V., Elliott, D. C., Meier, D. & de Wild, P. (2010). Lignin fast pyrolysis: Results from an international collaboration. *Journal of Analytical and Applied Pyrolysis*, 88 (1): 53-72.

## References

58. Watanabe, T., Kawamoto, H. & Saka, S. (2009). Radical chain reactions in pyrolytic cleavage of the ether linkages of lignin model dimers and a trimer. *Holzforschung*, 63 (4): 424-430.
59. Ledesma, E. B., Mullery, A. A., Vu, J. V. & Hoang, J. N. (2015). Lumped Kinetics for Biomass Tar Cracking Using 4-Propylguaiaicol as a Model Compound. *Industrial & Engineering Chemistry Research*, 54 (21): 5613-5623.
60. Zhou, H., Wu, C. F., Onwudili, J. A., Meng, A. H., Zhang, Y. G. & Williams, P. T. (2014). Polycyclic Aromatic Hydrocarbon Formation from the Pyrolysis/Gasification of Lignin at Different Reaction Conditions. *Energy & Fuels*, 28 (10): 6371-6379.
61. Elder, T. (2014). Bond Dissociation Enthalpies of a Pinoresinol Lignin Model Compound. *Energy & Fuels*, 28 (2): 1175-1182.
62. Kim, S., Chmely, S. C., Nimos, M. R., Bomble, Y. J., Foust, T. D., Paton, R. S. & Beckham, G. T. (2011). Computational Study of Bond Dissociation Enthalpies for a Large Range of Native and Modified Lignins. *Journal of Physical Chemistry Letters*, 2 (22): 2846-2852.
63. Parthasarathi, R., Romero, R. A., Redondo, A. & Gnanakaran, S. (2011). Theoretical Study of the Remarkably Diverse Linkages in Lignin. *Journal of Physical Chemistry Letters*, 2 (20): 2660-2666.
64. Younker, J. M., Beste, A. & Buchanan, A. C. (2012). Computational study of bond dissociation enthalpies for lignin model compounds: beta-5 Arylcoumaran. *Chemical Physics Letters*, 545: 100-106.
65. Evans, R. J. & Milne, T. A. (1987). Molecular Characterization of the Pyrolysis of Biomass .1. Fundamentals. *Energy & Fuels*, 1 (2): 123-137.
66. Haw, J. F. & Schultz, T. P. (1985). C-13 Cp Mas Nmr and Ft-Ir Study of Low-Temperature Lignin Pyrolysis. *Holzforschung*, 39 (5): 289-296.
67. Kawamoto, H., Horigoshi, S. & Saka, S. (2007). Pyrolysis reactions of various lignin model dimers. *Journal of Wood Science*, 53 (2): 168-174.
68. Nakamura, T., Kawamoto, H. & Saka, S. (2008). Pyrolysis behavior of Japanese cedar wood lignin studied with various model dimers. *Journal of Analytical and Applied Pyrolysis*, 81 (2): 173-182.
69. Dorrestijn, E. & Mulder, P. (1999). The radical-induced decomposition of 2-methoxyphenol. *Journal of the Chemical Society-Perkin Transactions 2* (4): 777-780.

## References

70. Asmadi, M., Kawamoto, H. & Saka, S. (2011). Thermal reactions of guaiacol and syringol as lignin model aromatic nuclei. *Journal of Analytical and Applied Pyrolysis*, 92 (1): 88-98.
71. Asmadi, M., Kawamoto, H. & Saka, S. (2012). The effects of combining guaiacol and syringol on their pyrolysis. *Holzforschung*, 66 (3): 323-330.
72. Vuori, A. (1986). Pyrolysis Studies of Some Simple Coal Related Aromatic Methyl Ethers. *Fuel*, 65 (11): 1575-1583.
73. Chiavari, G., Francioso, O., Galletti, G. C., Piccaglia, R. & Zadrazil, F. (1989). Characterization by Pyrolysis-Gas Chromatography of Wheat Straw Fermented with White Rot Fungus *Stropharia-Rugosoannulata*. *Journal of Analytical and Applied Pyrolysis*, 15: 129-136.
74. Reeves, J. B. & Galletti, G. C. (1993). Use of Pyrolysis-Gas Chromatography Mass-Spectrometry in the Study of Lignin Assays. *Journal of Analytical and Applied Pyrolysis*, 24 (3): 243-255.
75. Evans, R. J., Milne, T. A. & Soltys, M. N. (1986). Direct Mass-Spectrometric Studies of the Pyrolysis of Carbonaceous Fuels .3. Primary Pyrolysis of Lignin. *Journal of Analytical and Applied Pyrolysis*, 9 (3): 207-236.
76. del Rio, J. C., Rencoret, J., Prinsen, P., Martinez, A. T., Ralph, J. & Gutierrez, A. (2012). Structural Characterization of Wheat Straw Lignin as Revealed by Analytical Pyrolysis, 2D-NMR, and Reductive Cleavage Methods. *Journal of Agricultural and Food Chemistry*, 60 (23): 5922-5935.
77. Faix, O., Bremer, J., Meier, D., Fortmann, I., Scheijen, M. A. & Boon, J. J. (1992). Characterization of Tobacco Lignin by Analytical Pyrolysis and Fourier Transform-Infrared Spectroscopy. *Journal of Analytical and Applied Pyrolysis*, 22 (3): 239-259.
78. Rencoret, J., Ralph, J., Marques, G., Gutierrez, A., Martinez, A. T. & del Rio, J. C. (2013). Structural Characterization of Lignin Isolated from Coconut (*Cocos nucifera*) Coir Fibers. *Journal of Agricultural and Food Chemistry*, 61 (10): 2434-2445.
79. Saariaho, A. M., Jaaskelainen, A. S., Nuopponen, M. & Vuorinen, T. (2003). Ultra violet resonance Raman Spectroscopy in lignin analysis: Determination of characteristic vibrations of p-hydroxyphenyl, guaiacyl, and syringyl lignin structures. *Applied Spectroscopy*, 57 (1): 58-66.
80. Capanema, E. A., Balakshin, M. Y. & Kadla, J. F. (2004). A comprehensive approach for quantitative lignin characterization by NMR spectroscopy. *Journal of Agricultural and Food Chemistry*, 52 (7): 1850-1860.



## References

81. Lundquist, K. (1980). Nmr-Studies of Lignins .4. Investigation of Spruce Lignin by H-1-Nmr Spectroscopy. *Acta Chemica Scandinavica Series B-Organic Chemistry and Biochemistry*, 34 (1): 21-26.
82. Lundquist, K. (1981). Nmr-Studies of Lignins .5. Investigation of Non-Derivatized Spruce and Birch Lignin by H-1-Nmr Spectroscopy. *Acta Chemica Scandinavica Series B-Organic Chemistry and Biochemistry*, 35 (7): 497-501.
83. Gellerstedt, G. & Robert, D. (1987). Structural-Changes in Lignin during Kraft Cooking .7. Quantitative C-13 Nmr Analysis of Kraft Lignins. *Acta Chemica Scandinavica Series B-Organic Chemistry and Biochemistry*, 41 (7): 541-546.
84. Hawkes, G. E., Smith, C. Z., Utley, J. H. P., Vargas, R. R. & Viertler, H. (1993). A Comparison of Solution and Solid-State C-13 Nmr-Spectra of Lignins and Lignin Model Compounds. *Holzforschung*, 47 (4): 302-312.
85. Pan, D. R., Tai, D. S., Chen, C. L. & Robert, D. (1990). Comparative-Studies on Chemical-Composition of Wood Components in Recent and Ancient Woods of Bischofia-Polycarpa. *Holzforschung*, 44 (1): 7-16.
86. Xia, Z. C., Akim, L. G. & Argyropoulos, D. S. (2001). Quantitative C-13 NMR analysis of lignins with internal standards. *Journal of Agricultural and Food Chemistry*, 49 (8): 3573-3578.
87. Williams, D. H. & Fleming, I. (2008). *Spectroscopic Methods in Organic Chemistry*: McGraw-Hill.
88. Ralph, S. A. R., J.; Landucci, L.L. (2009). *NMR Database of Lignin and Cell Wall Model Compounds*. Available at: [https://www.glbrc.org/databases\\_and\\_software/nmrdatabase/NMR\\_DataBase\\_2009\\_Complete.pdf](https://www.glbrc.org/databases_and_software/nmrdatabase/NMR_DataBase_2009_Complete.pdf) (accessed: 05.05.2017).
89. Karhunen, P., Rummakko, P., Sipila, J., Brunow, G. & Kilpelainen, I. (1995). Dibenzodioxocins - a Novel Type of Linkage in Softwood Lignins. *Tetrahedron Letters*, 36 (1): 169-170.
90. Setälä, H., Pajunen, A., Rummakko, P., Sipila, J. & Brunow, G. (1999). A novel type of spiro compound formed by oxidative cross coupling of methyl sinapate with a syringyl lignin model compound. A model system for the beta-1 pathway in lignin biosynthesis. *Journal of the Chemical Society-Perkin Transactions 1* (4): 461-464.
91. Zhang, L. M. & Gellerstedt, G. (2001). NMR observation of a new lignin structure, a spiro-dienone. *Chemical Communications* (24): 2744-2745.

## References

92. Yuan, T. Q., Sun, S. N., Xu, F. & Sun, R. C. (2011). Characterization of Lignin Structures and Lignin-Carbohydrate Complex (LCC) Linkages by Quantitative C-13 and 2D HSQC NMR Spectroscopy. *Journal of Agricultural and Food Chemistry*, 59 (19): 10604-10614.
93. del Rio, J. C., Rencoret, J., Marques, G., Li, J. B., Gellerstedt, G., Jimenez-Barbero, J., Martinez, A. T. & Gutierrez, A. (2009). Structural Characterization of the Lignin from Jute (*Corchorus capsularis*) Fibers. *Journal of Agricultural and Food Chemistry*, 57 (21): 10271-10281.
94. Martinez, A. T., Rencoret, J., Marques, G., Gutierrez, A., Ibarra, D., Jimenez-Barbero, J. & del Rio, J. C. (2008). Monolignol acylation and lignin structure in some nonwoody plants: A 2D NMR study. *Phytochemistry*, 69 (16): 2831-2843.
95. Wen, J. L., Xue, B. L., Xu, F. & Sun, R. C. (2012). Unveiling the Structural Heterogeneity of Bamboo Lignin by In Situ HSQC NMR Technique. *Bioenergy Research*, 5 (4): 886-903.
96. Horn, S. J., Nguyen, Q. D., Westereng, B., Nilsen, P. J. & Eijsink, V. G. H. (2011). Screening of steam explosion conditions for glucose production from non-impregnated wheat straw. *Biomass & Bioenergy*, 35 (12): 4879-4886.
97. Bjorkman, A. (1956). Finely divided wood. I. Extraction of lignin with neutral solvents. *Sven. Papperstidn.*, 59: 477-85.
98. Shuai, L., Amiri, M. T., Questell-Santiago, Y. M., Heroguel, F., Li, Y. D., Kim, H., Meilan, R., Chapple, C., Ralph, J. & Luterbacher, J. S. (2016). Formaldehyde stabilization facilitates lignin monomer production during biomass depolymerization. *Science*, 354 (6310): 329-333.
99. Alves, A., Schwanninger, M., Pereira, H. & Rodrigues, J. (2006). Analytical pyrolysis as a direct method to determine the lignin content in wood - Part 1: Comparison of pyrolysis lignin with Klason lignin. *Journal of Analytical and Applied Pyrolysis*, 76 (1-2): 209-213.
100. Du, X. Y., Perez-Boada, M., Fernandez, C., Rencoret, J., del Rio, J. C., Jimenez-Barbero, J., Li, J. B., Gutierrez, A. & Martinez, A. T. (2014). Analysis of lignin-carbohydrate and lignin-lignin linkages after hydrolase treatment of xylan-lignin, glucomannan-lignin and glucan-lignin complexes from spruce wood. *Planta*, 239 (5): 1079-1090.
101. Heikkinen, H., Elder, T., Maaheimo, H., Rovio, S., Rahikainen, J., Kruus, K. & Tamminen, T. (2014). Impact of Steam Explosion on the Wheat Straw Lignin

## References

- Structure Studied by Solution-State Nuclear Magnetic Resonance and Density Functional Methods. *Journal of Agricultural and Food Chemistry*, 62 (43): 10437-10444.
102. Yuan, T. Q., Sun, S. N., Xu, F. & Sun, R. C. (2011). Isolation and Physico-Chemical Characterization of Lignins from Ultrasound Irradiated Fast-Growing Poplar Wood. *Bioresources*, 6 (1): 414-433.
103. Yuan, T. Q., Sun, S. N., Xu, F. & Sun, R. C. (2011). Structural Characterization of Lignin from Triploid of *Populus tomentosa* Carr. *Journal of Agricultural and Food Chemistry*, 59 (12): 6605-6615.
104. Zhang, L. M., Gellerstedt, G., Ralph, J. & Lu, F. C. (2006). NMR studies on the occurrence of spirodienone structures in lignins. *Journal of Wood Chemistry and Technology*, 26 (1): 65-79.
105. Robert, D. (1992). Carbon-13 Nuclear Magnetic Resonance Spectrometry. In Lin, S. Y. & Dence, C. W. (eds) *Methods in Lignin Chemistry*, pp. 250-273. Berlin, Heidelberg: Springer Berlin Heidelberg.
106. Li, S. M., Lundquist, K. & Westermark, U. (2000). Cleavage of arylglycerol beta-aryl ethers under neutral and acid conditions. *Nordic Pulp & Paper Research Journal*, 15 (4): 292-299.
107. Nimz, H. (1966). A New Type of Rearrangement in Lignin Field. *Angewandte Chemie-International Edition*, 5 (9): 843-&.
108. Rahikainen, J. L., Martin-Sampedro, R., Heikkinen, H., Rovio, S., Marjamaa, K., Tamminen, T., Rojas, O. J. & Kruus, K. (2013). Inhibitory effect of lignin during cellulose bioconversion: The effect of lignin chemistry on non-productive enzyme adsorption. *Bioresource Technology*, 133: 270-278.
109. Li, J. B., Henriksson, G. & Gellerstedt, G. (2005). Carbohydrate reactions during high-temperature steam treatment of aspen wood. *Applied Biochemistry and Biotechnology*, 125 (3): 175-188.
110. Kotake, T., Kawamoto, H. & Saka, S. (2014). Mechanisms for the formation of monomers and oligomers during the pyrolysis of a softwood lignin. *Journal of Analytical and Applied Pyrolysis*, 105: 309-316.
111. Kawamoto, H. (2017). Lignin pyrolysis reactions. *J. Wood Sci.*, 63 (2): 117-132.
112. He, T., Zhang, Y. M., Zhu, Y. A., Wen, W., Pan, Y., Wu, J. L. & Wu, J. H. (2016). Pyrolysis Mechanism Study of Lignin Model Compounds by Synchrotron Vacuum Ultraviolet Photoionization Mass Spectrometry. *Energy & Fuels*, 30 (3): 2204-2208.

## 6. Appendix

### 6.1 HSQC Spectra of MWL From All Steam Exploded Samples

Each of the figures in this section shows HSQC spectra of MWL from a steam exploded spruce sample, displaying the region  $\delta_C/\delta_H$  50-135/2.7-8.0. The lowest abundant signals are not shown.

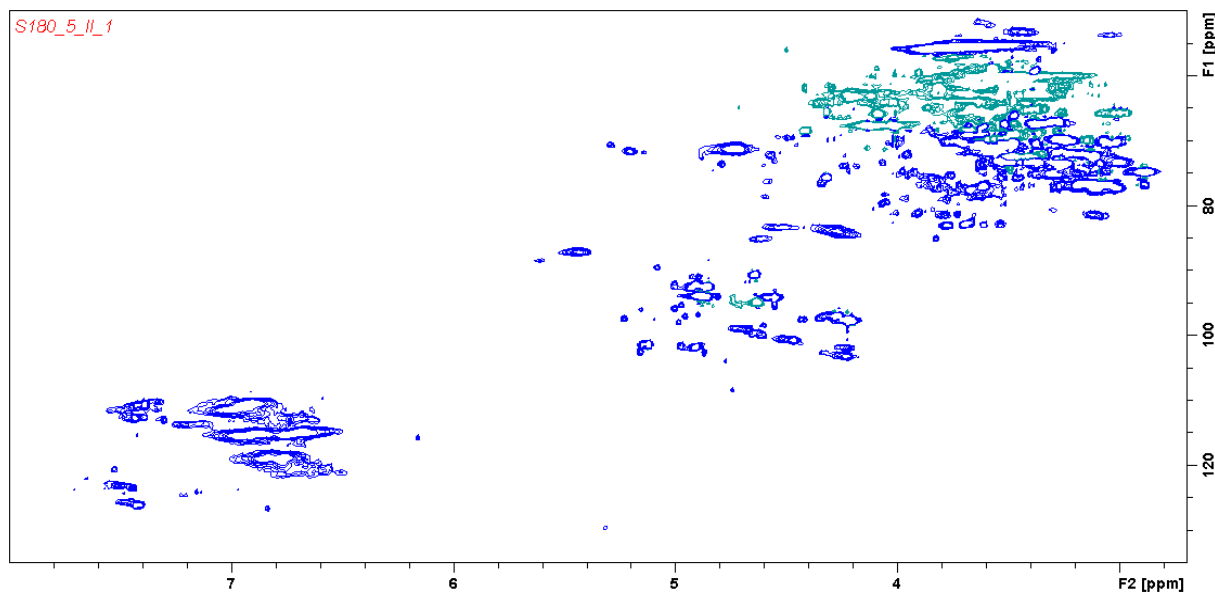


Figure 6.1: HSQC spectrum of MWL from steam exploded spruce; 180 °C for 5 min. The spectrum displays the region  $\delta_C/\delta_H$  50-135/2.7-8.0.

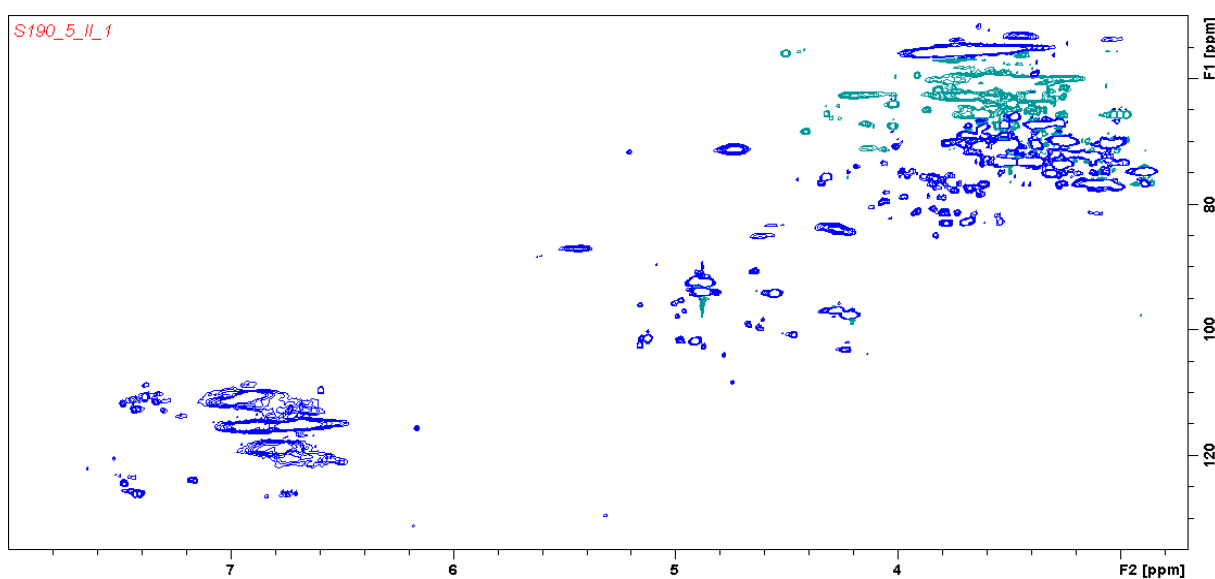


Figure 6.2: HSQC spectrum of MWL from steam exploded spruce; 190 °C for 5 min. The spectrum displays the region  $\delta_C/\delta_H$  50-135/2.7-8.0.

## Appendix

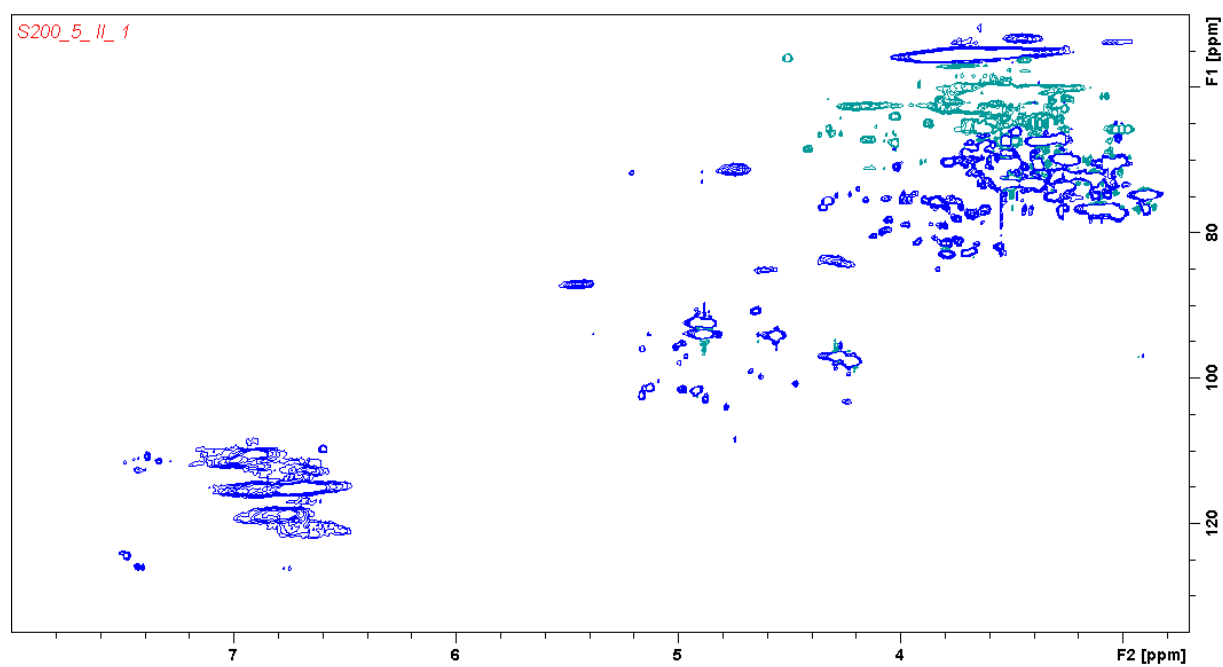


Figure 6.3: HSQC spectrum of MWL from steam exploded spruce; 200 °C for 5 min. The spectrum displays the region  $\delta_C/\delta_H$  50-135/2.7-8.0.

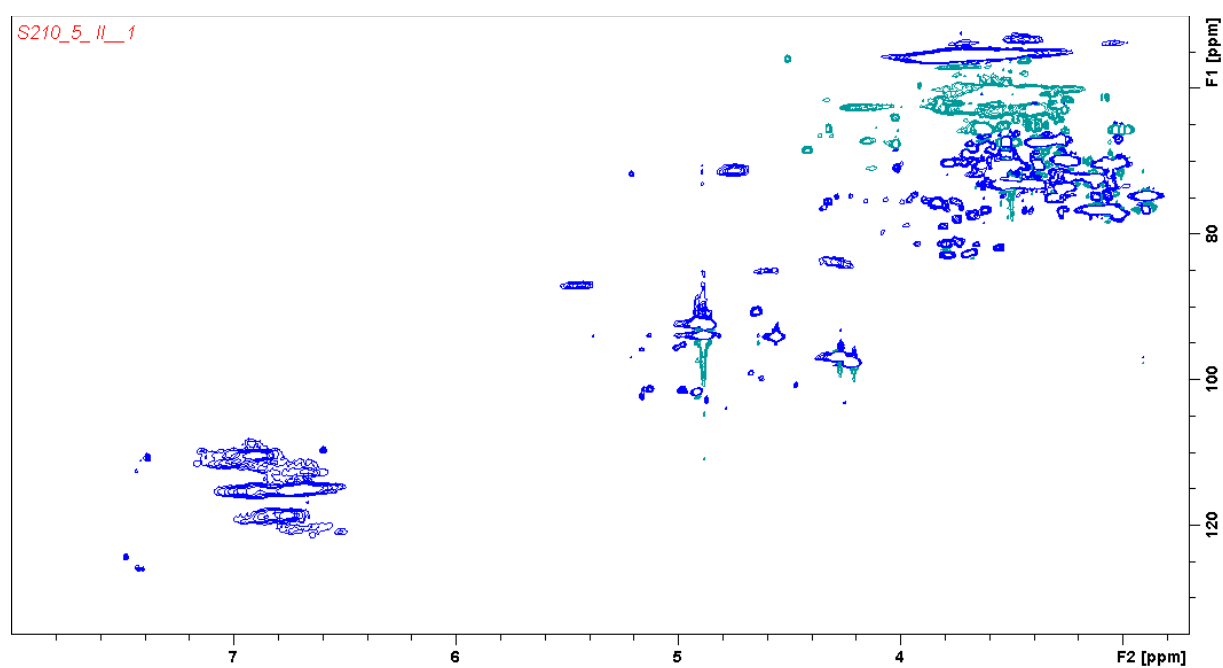


Figure 6.4: HSQC spectrum of MWL from steam exploded spruce; 210 °C for 5 min. The spectrum displays the region  $\delta_C/\delta_H$  50-135/2.7-8.0.

## Appendix

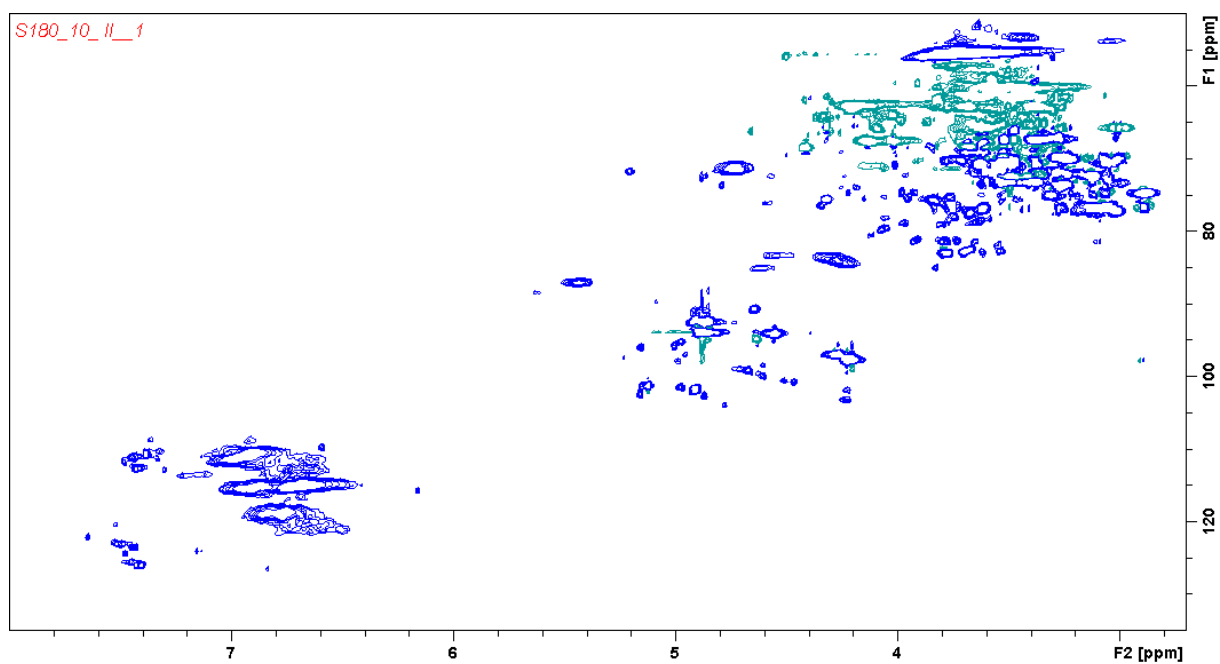


Figure 6.5: HSQC spectrum of MWL from steam exploded spruce; 180 °C for 10 min. The spectrum displays the region  $\delta_C/\delta_H$  50-135/2.7-8.0.

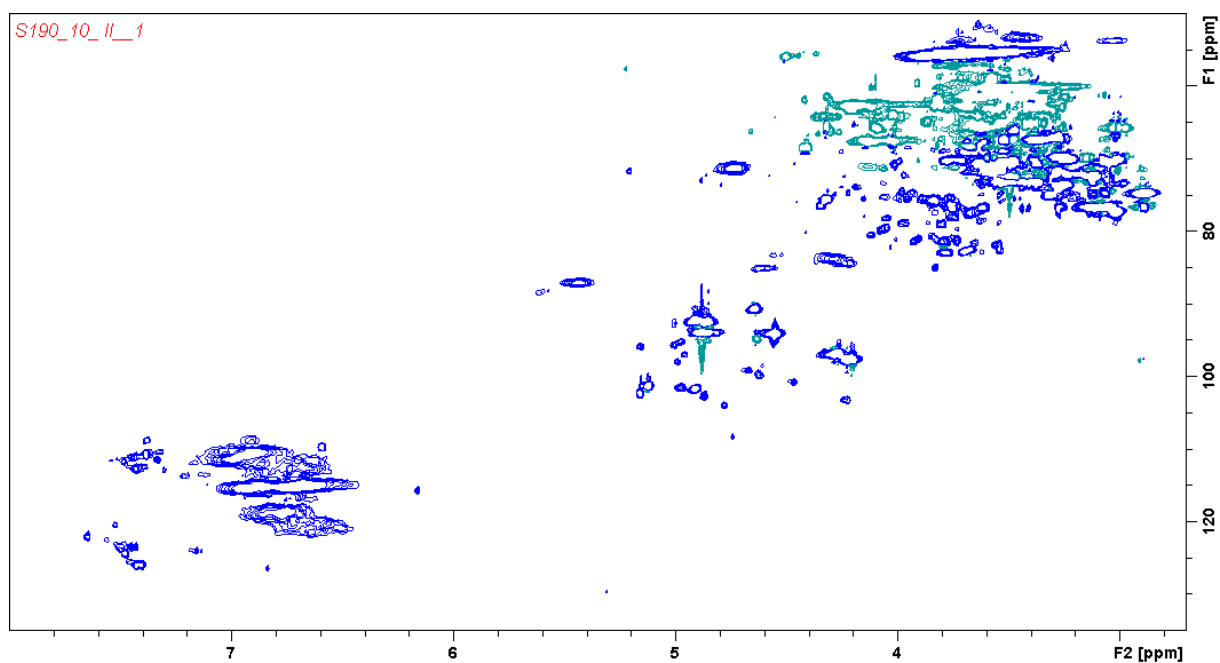


Figure 6.6: HSQC spectrum of MWL from steam exploded spruce; 190 °C for 10 min. The spectrum displays the region  $\delta_C/\delta_H$  50-135/2.7-8.0.

## Appendix

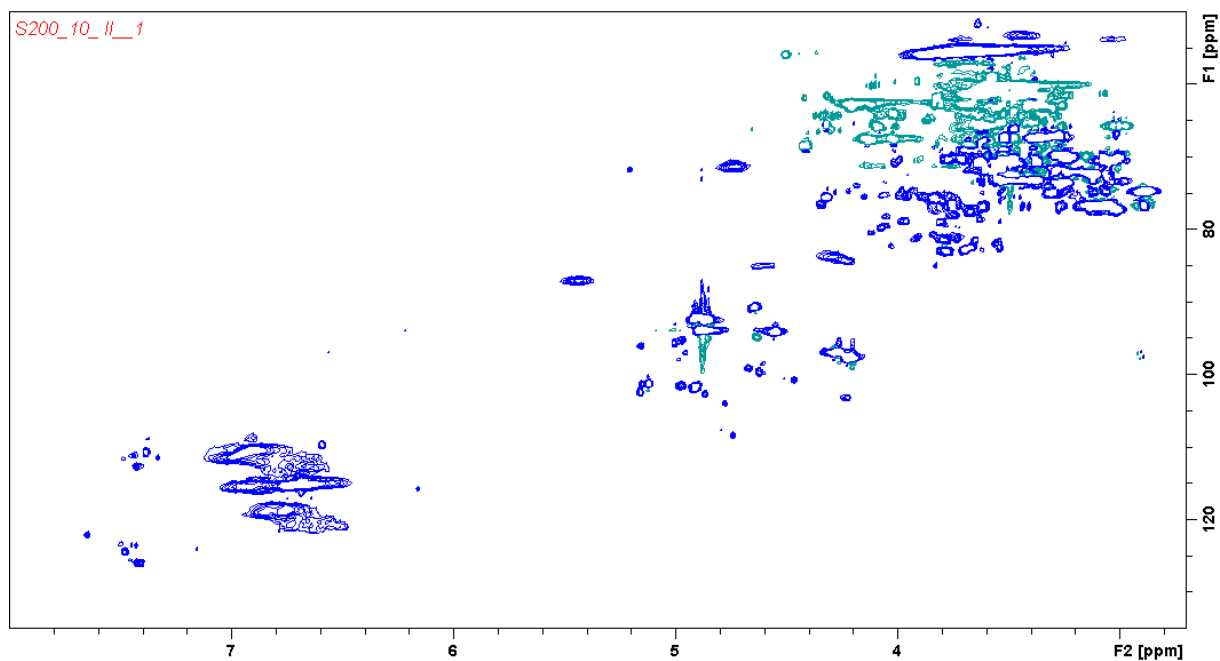


Figure 6.7: HSQC spectrum of MWL from steam exploded spruce; 200 °C for 10 min. The spectrum displays the region  $\delta_C/\delta_H$  50-135/2.7-8.0.

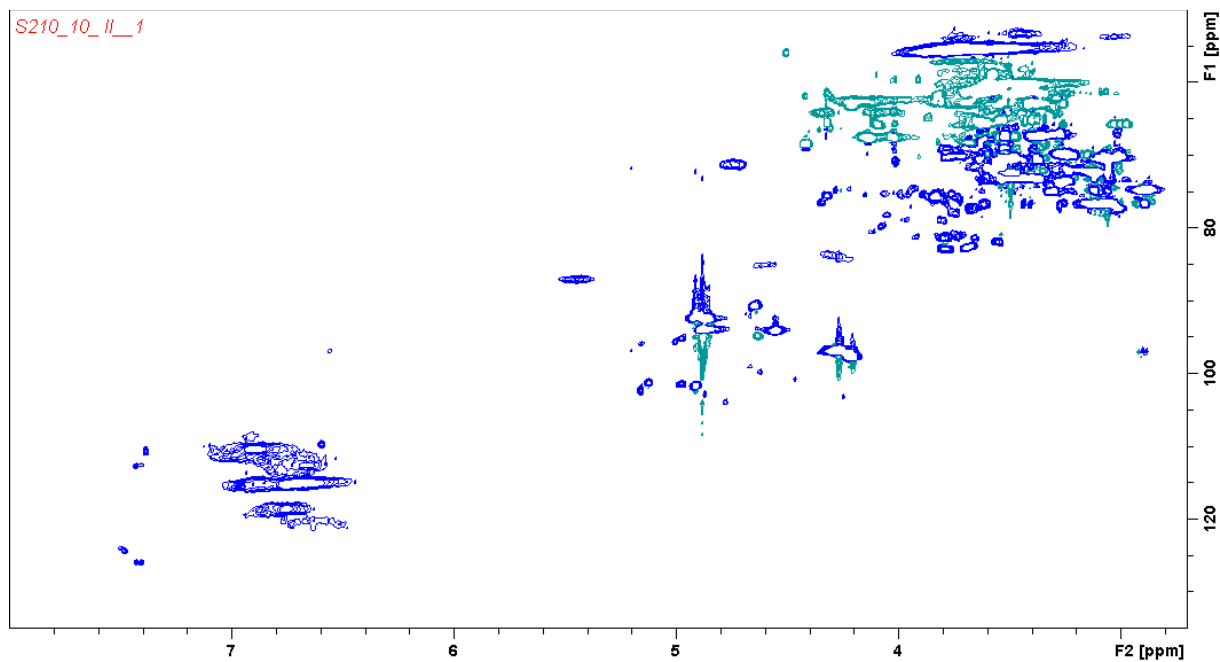


Figure 6.8: HSQC spectrum of MWL from steam exploded spruce; 210 °C for 10 min. The spectrum displays the region  $\delta_C/\delta_H$  50-135/2.7-8.0.

## 6.2 HSQC Spectra of THF Dissolvable MWL From Spruce Samples

Each of the figures in this section shows HSQC spectra of THF dissolvable MWL from a steam exploded spruce sample, displaying the region  $\delta_C/\delta_H$  50-135/2.7-8.0. The lowest abundant signals are not shown. HSQC experiments were not performed for THF dissolvable MWL from 5 min SE samples.

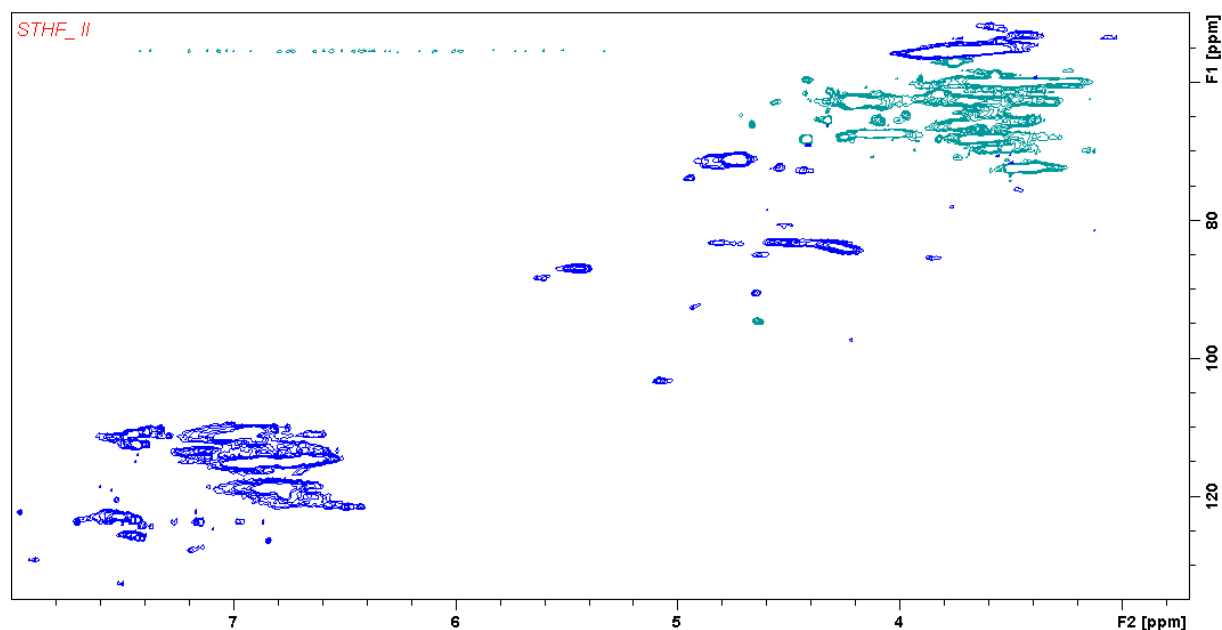


Figure 6.9: HSQC spectrum of THF dissolvable MWL from untreated spruce. The spectrum displays the region  $\delta_C/\delta_H$  50-135/2.7-8.0.

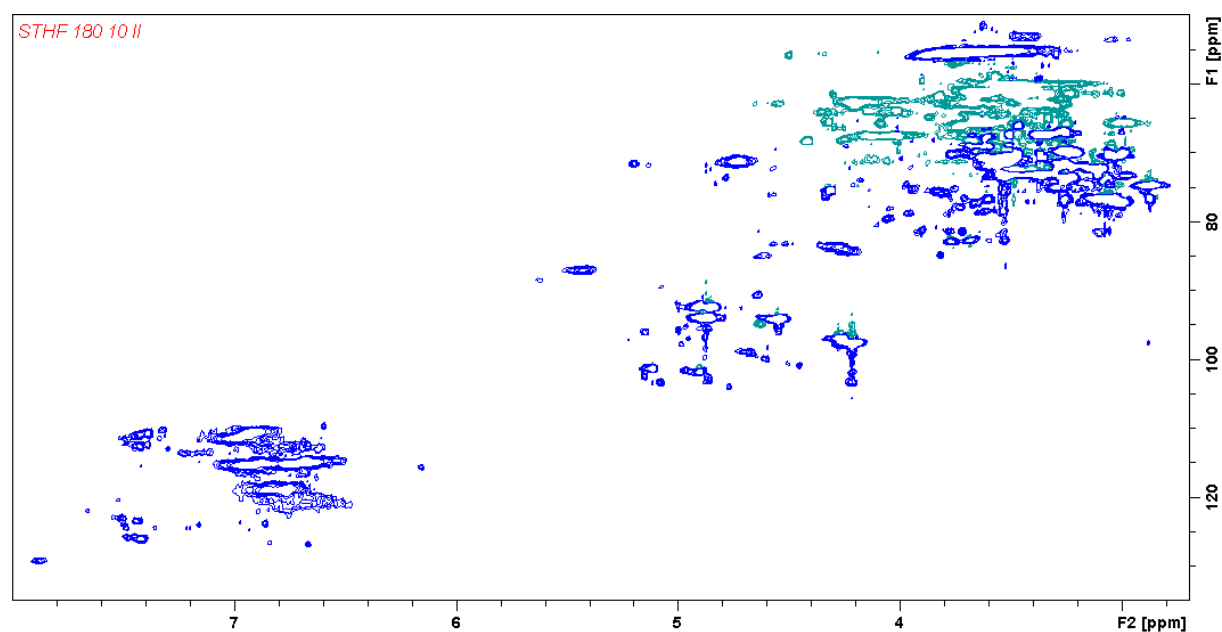


Figure 6.10: HSQC spectrum of THF dissolvable MWL from steam exploded spruce; 180 °C for 10 min. The spectrum displays the region  $\delta_C/\delta_H$  50-135/2.7-8.0.



## Appendix

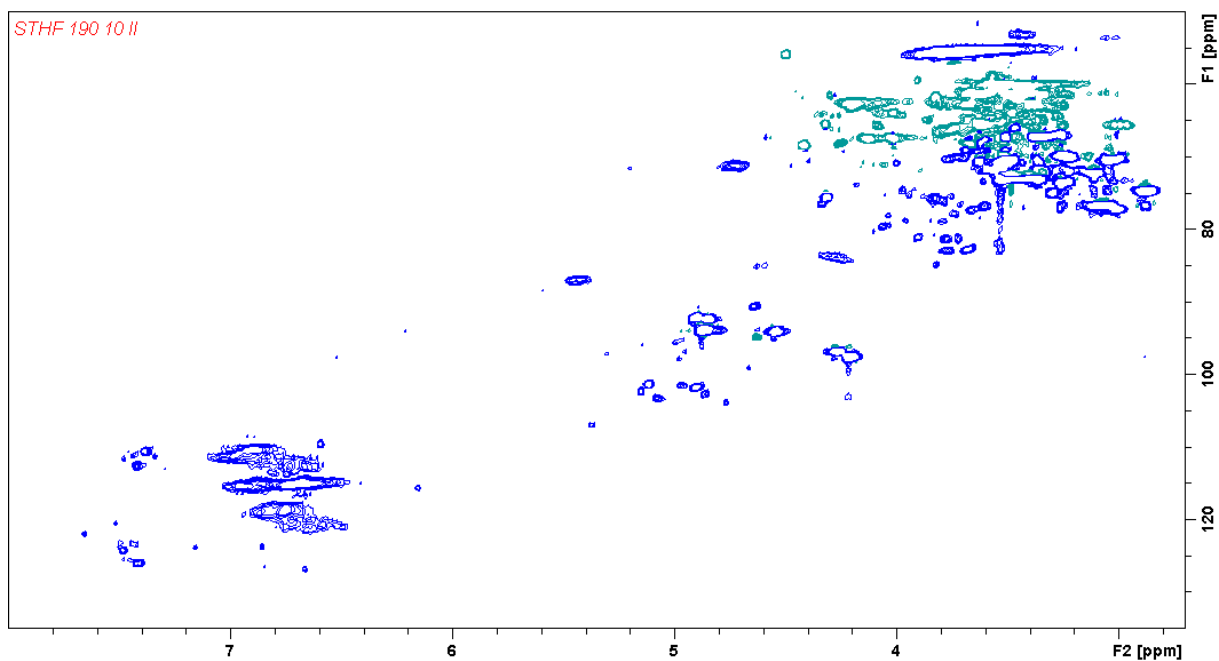


Figure 6.11: HSQC spectrum of THF dissolvable MWL from steam exploded spruce; 190 °C for 10 min. The spectrum displays the region  $\delta_C/\delta_H$  50-135/2.7-8.0.

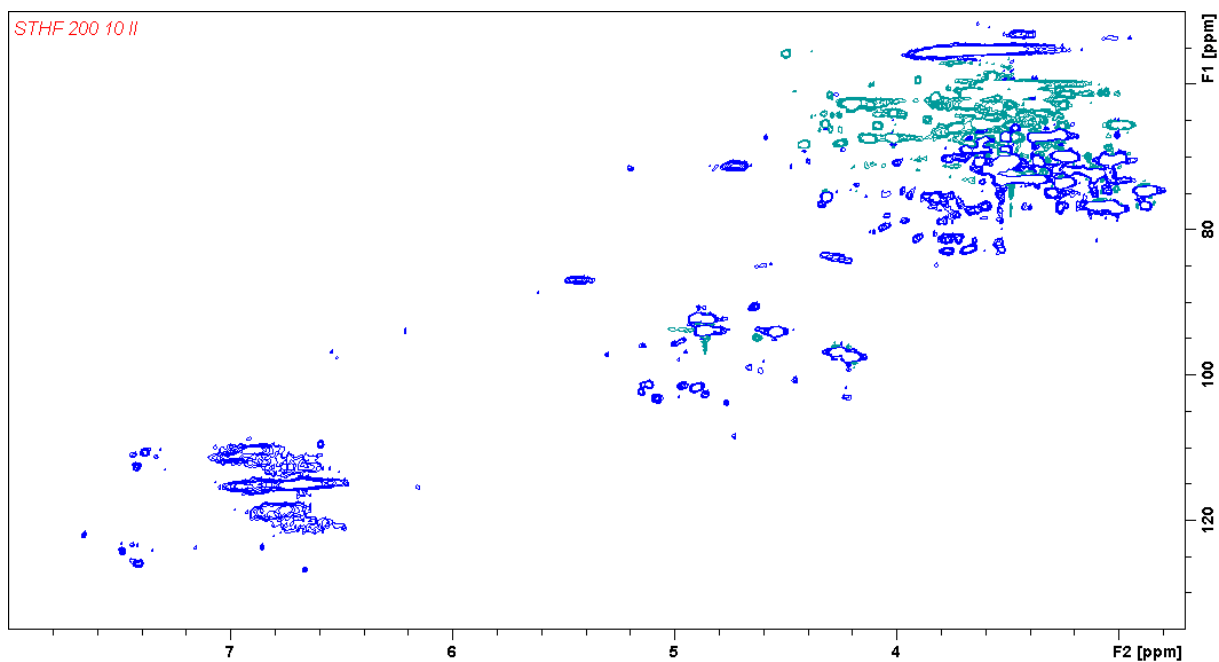


Figure 6.12: HSQC spectrum of THF dissolvable MWL from steam exploded spruce; 200 °C for 10 min. The spectrum displays the region  $\delta_C/\delta_H$  50-135/2.7-8.0.

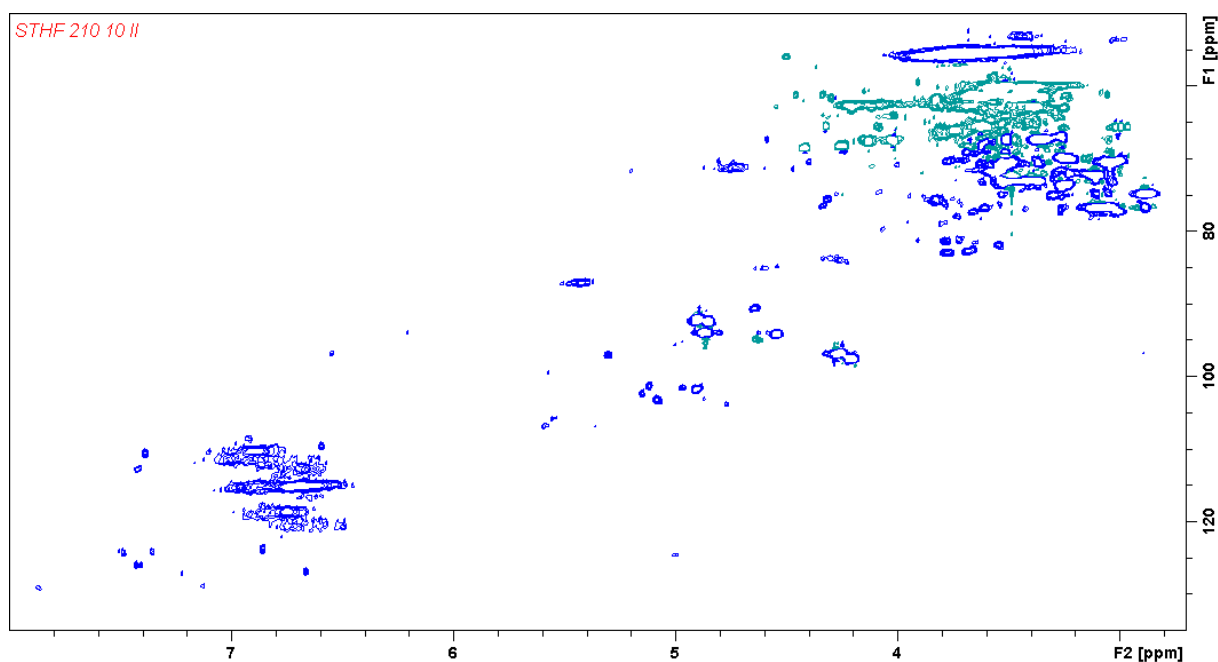


Figure 6.13: HSQC spectrum of THF dissolvable MWL from steam exploded spruce; 210 °C for 10 min. The spectrum displays the region  $\delta_C/\delta_H$  50-135/2.7-8.0.

### 6.3 Pyrograms of MWL and THF Dissolvable MWL from All Samples

Each of the figures in this section shows a pyrogram of MWL or THF dissolvable MWL from a spruce sample. Retention time from 15 to 65 minutes is displayed.

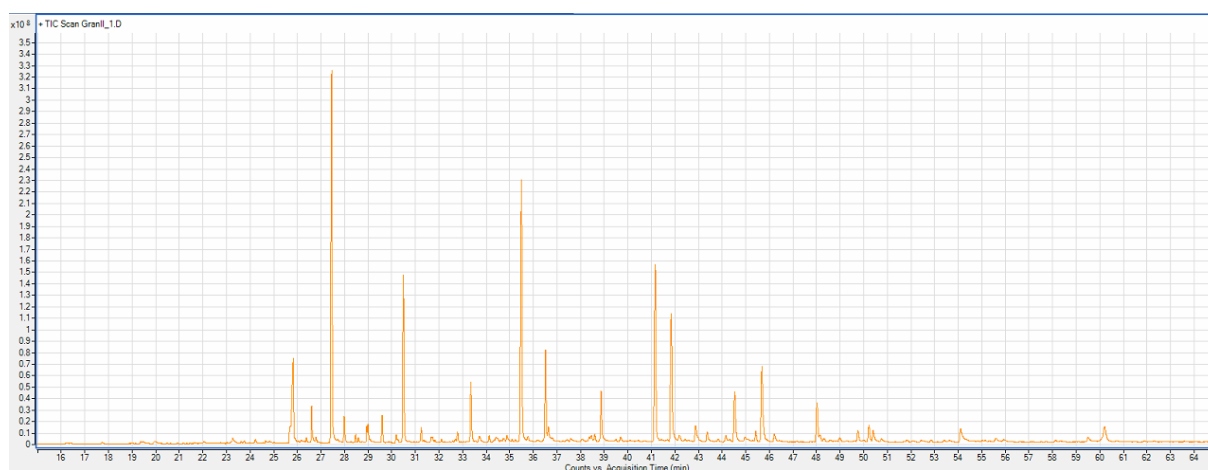


Figure 6.14: Pyrogram of MWL from untreated spruce.

## Appendix

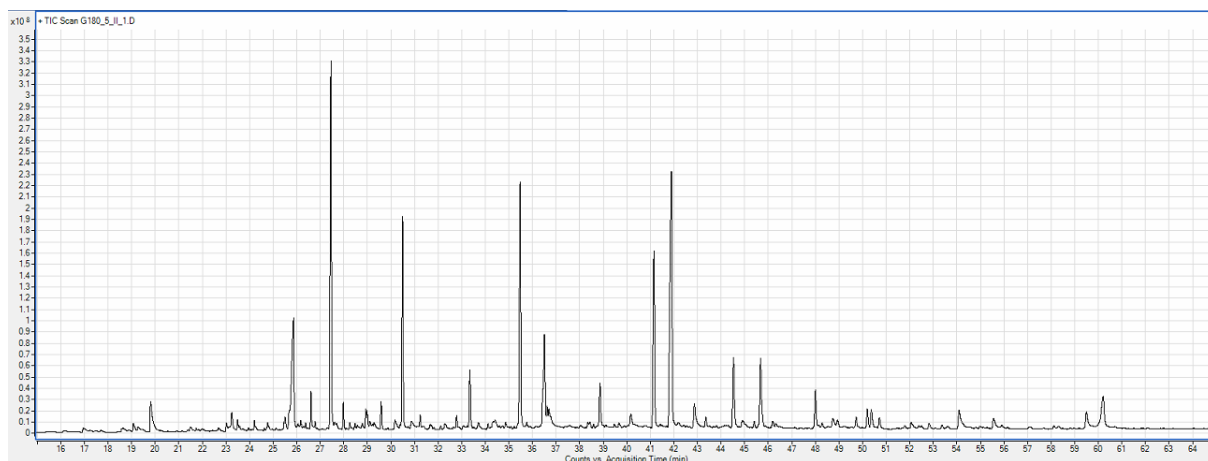


Figure 6.15: Pyrogram of MWL from SE treated (180 °C for 5 min) spruce.

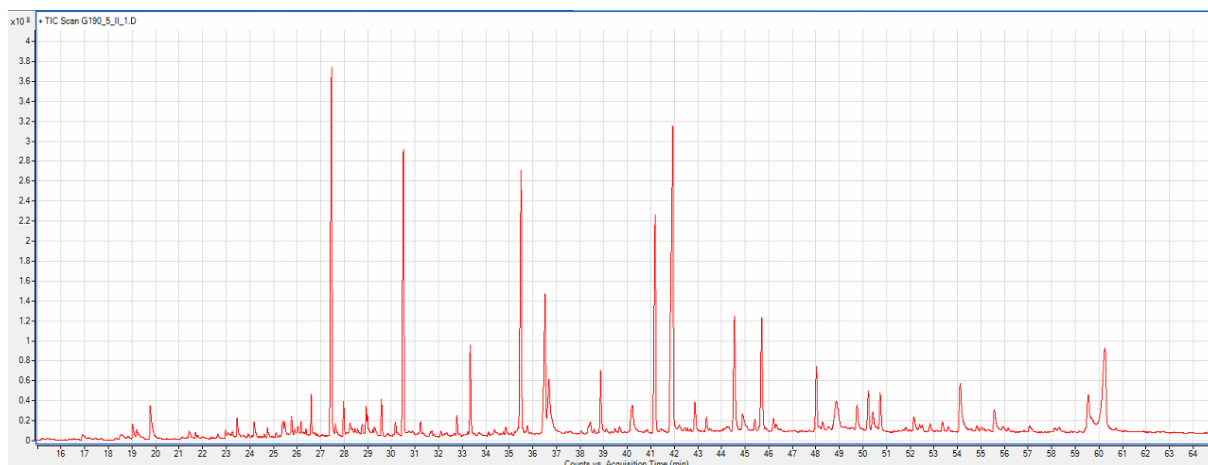


Figure 6.16: Pyrogram of MWL from SE treated (190 °C for 5 min) spruce.

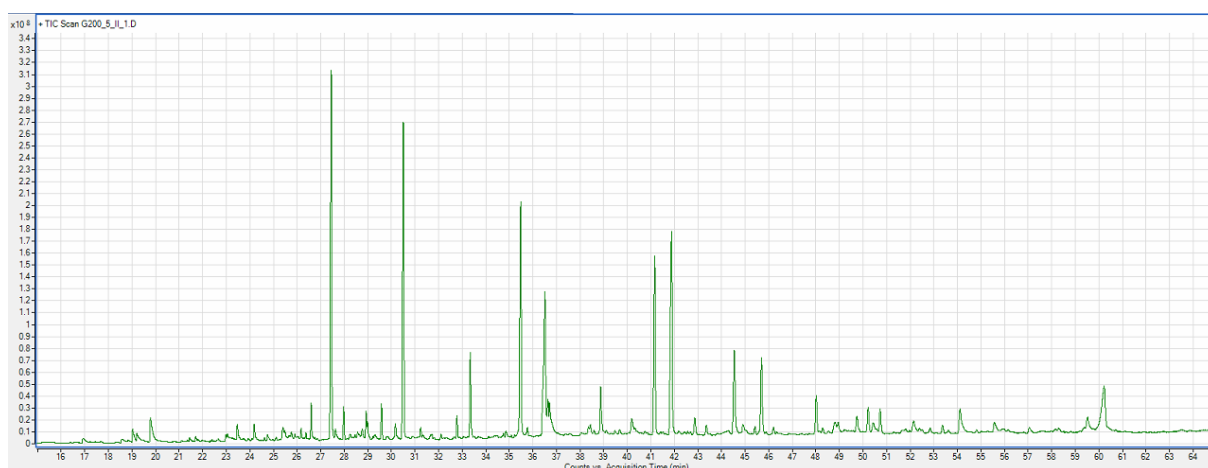


Figure 6.17: Pyrogram of MWL from SE treated (200 °C for 5 min) spruce.

## Appendix

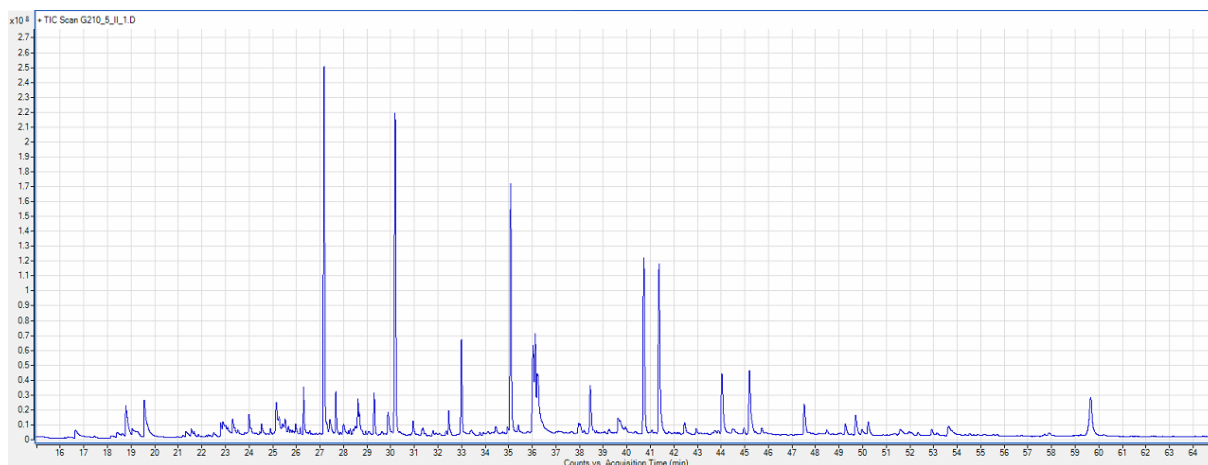


Figure 6.18: Pyrogram of MWL from SE treated (210 °C for 5 min) spruce.

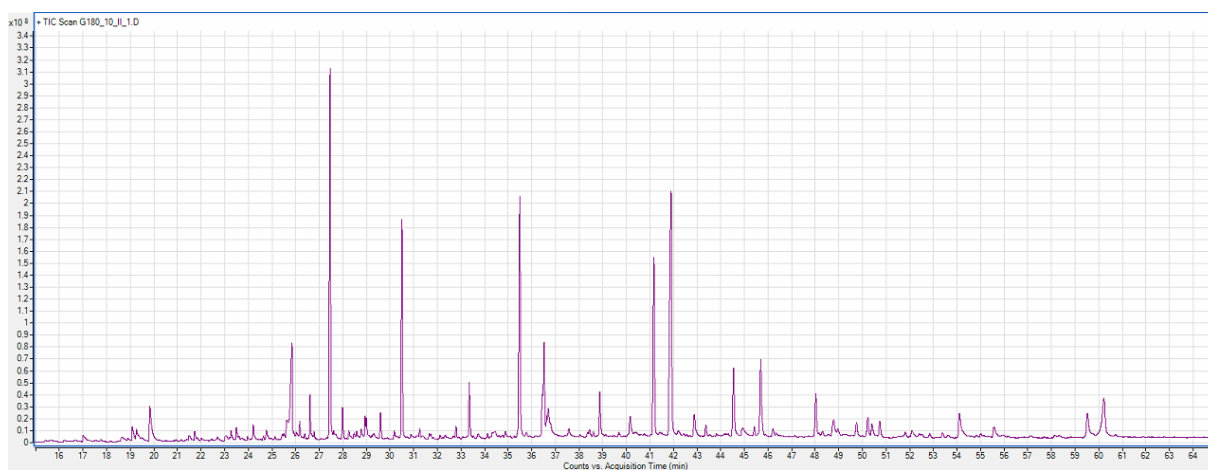


Figure 6.19: Pyrogram of MWL from SE treated (180 °C for 10 min) spruce.

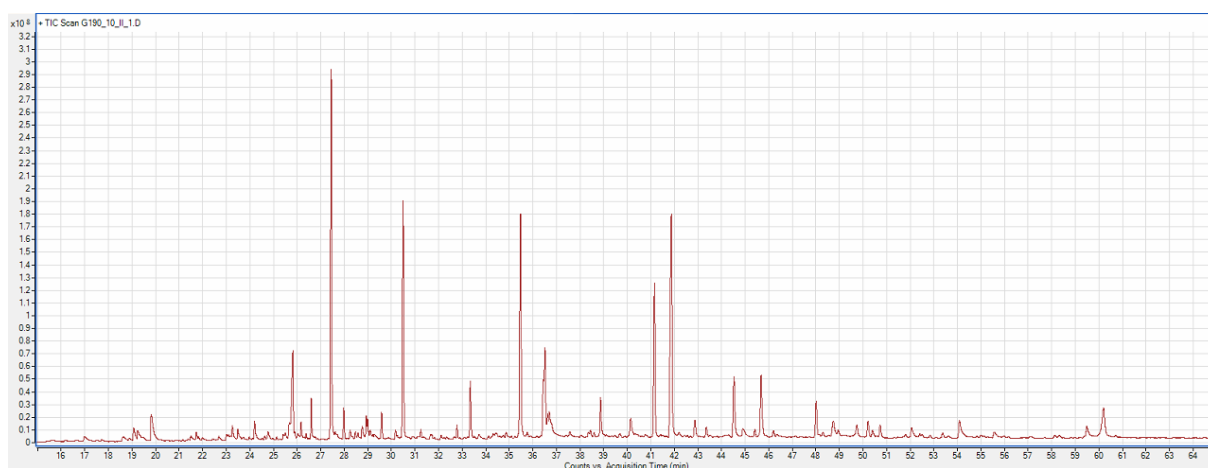


Figure 6.20: Pyrogram of MWL from SE treated (190 °C for 10 min) spruce.

## Appendix

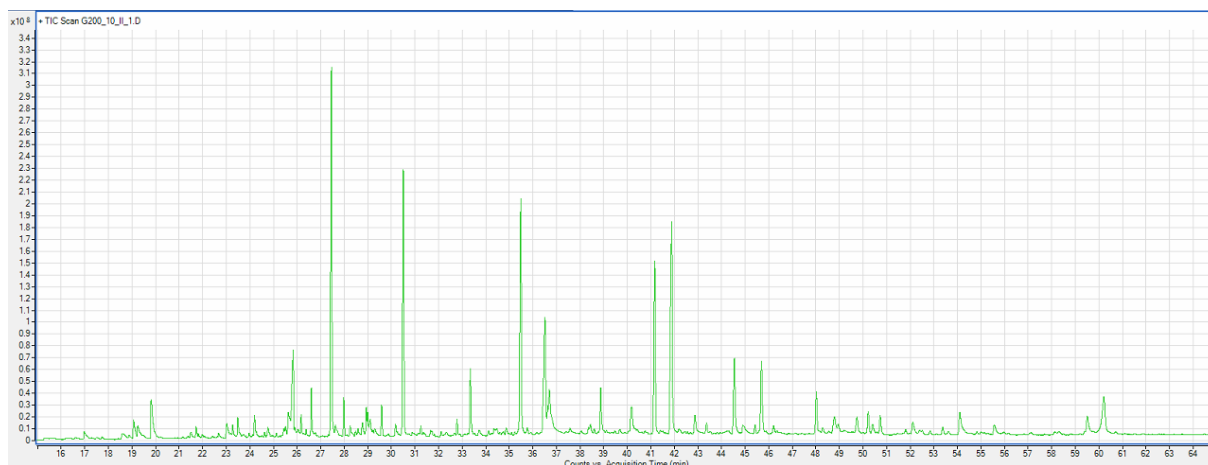


Figure 6.21: Pyrogram of MWL from SE treated (200 °C for 10 min) spruce.

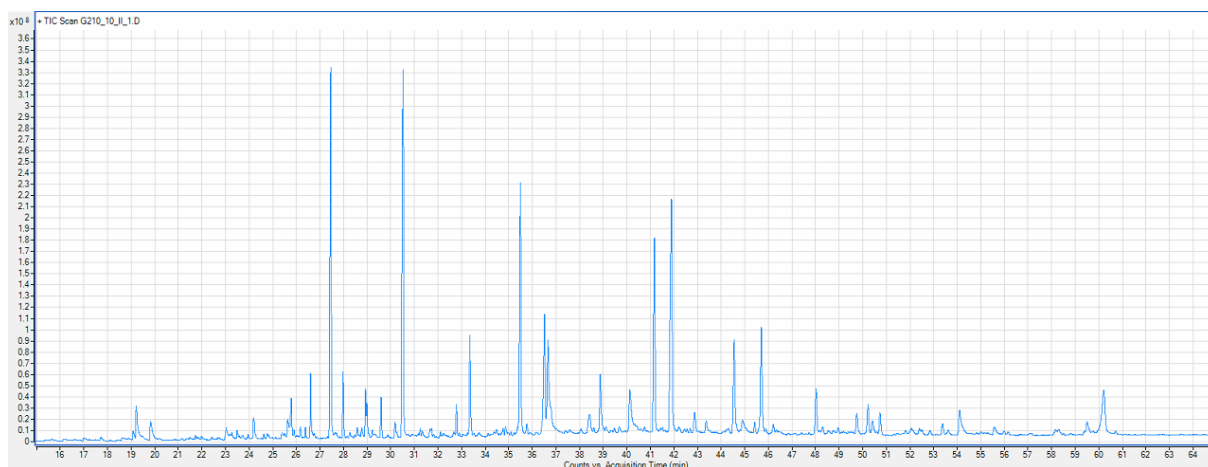


Figure 6.22: Pyrogram of MWL from SE treated (210 °C for 10 min) spruce.

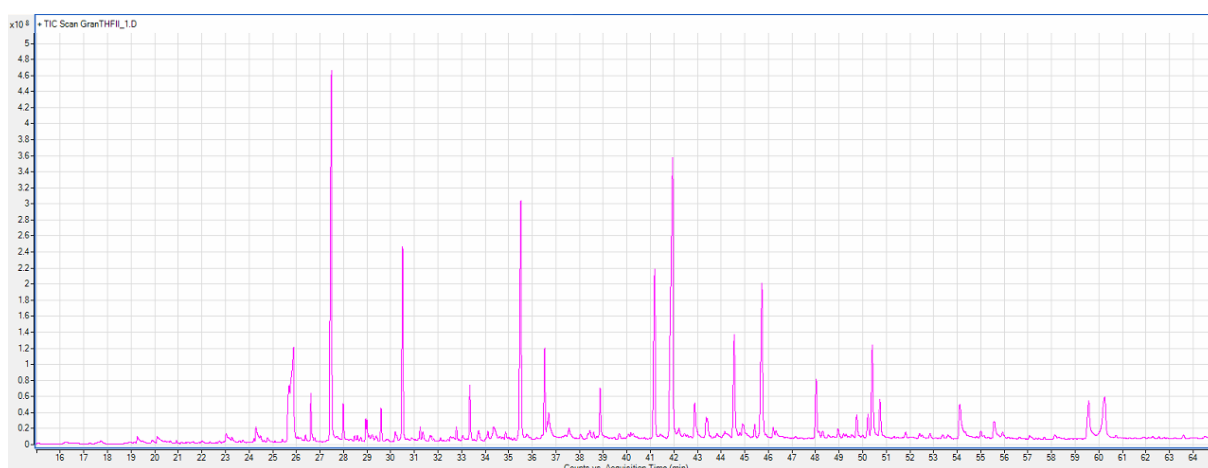


Figure 6.23: Pyrogram of THF dissolvable MWL from untreated spruce.

## Appendix

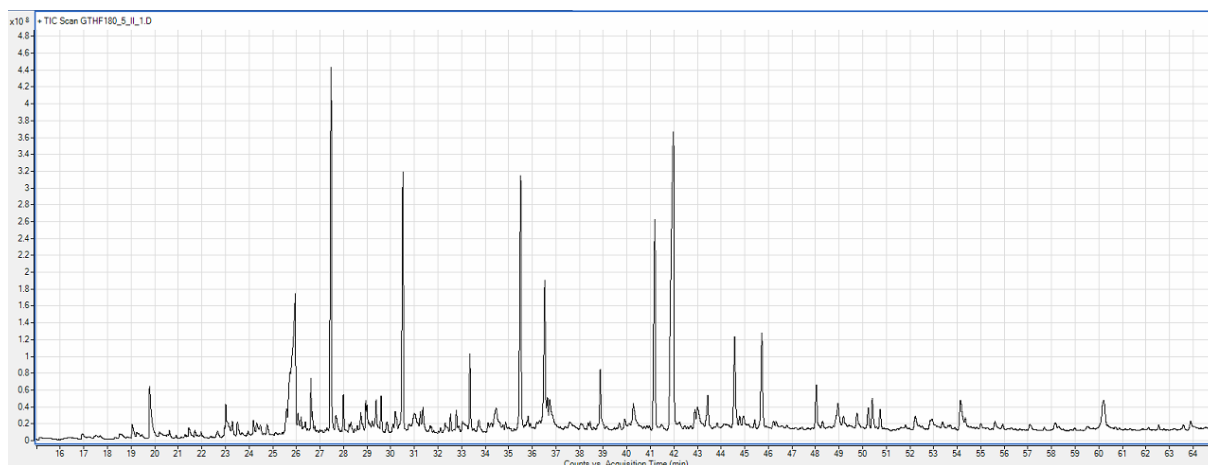


Figure 6.24: Pyrogram of THF dissolvable MWL from SE treated (180 °C for 5 min) spruce.

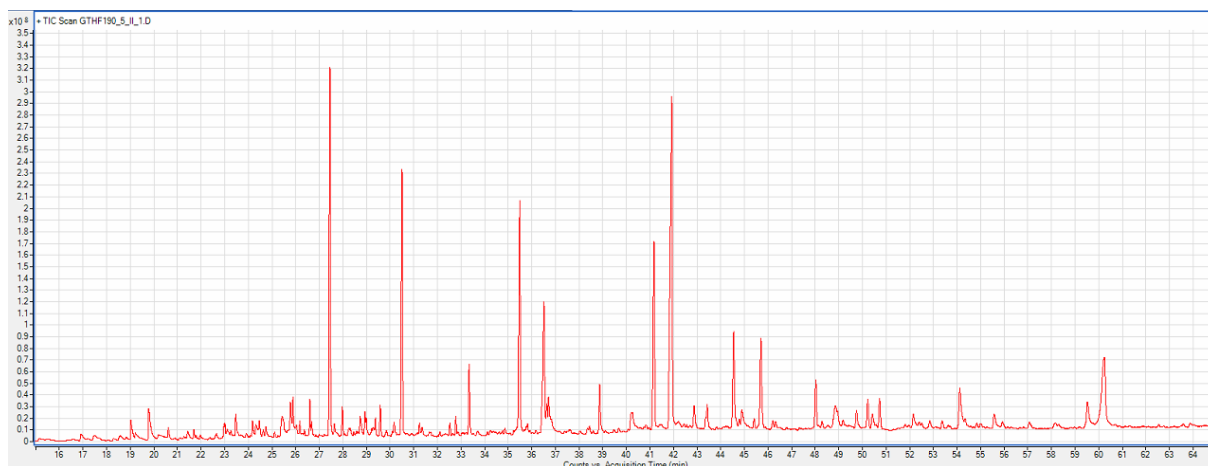


Figure 6.25: Pyrogram of THF dissolvable MWL from SE treated (190 °C for 5 min) spruce.

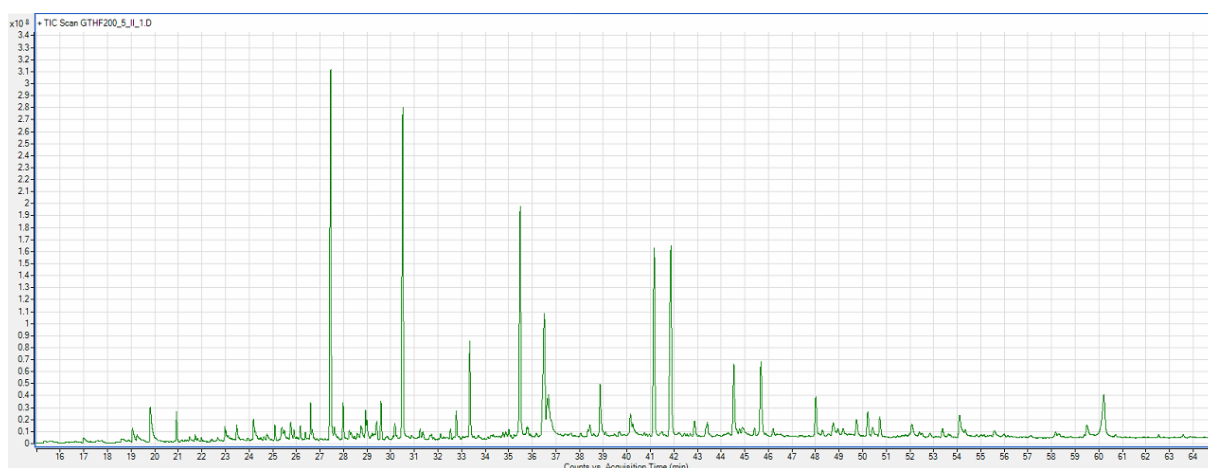


Figure 6.26: Pyrogram of THF dissolvable MWL from SE treated (200 °C for 5 min) spruce.

## Appendix

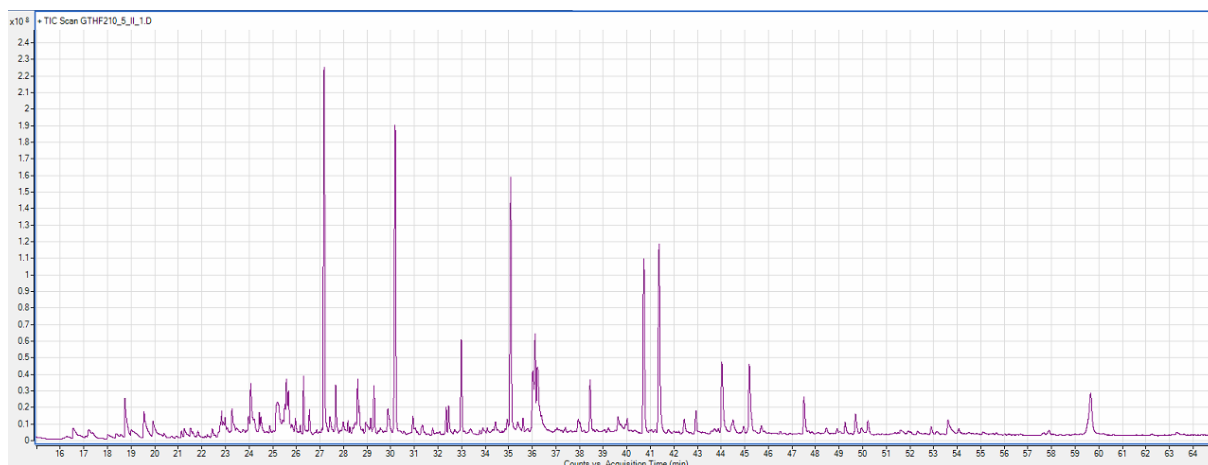


Figure 6.27: Pyrogram of THF dissolvable MWL from SE treated (210 °C for 5 min) spruce.

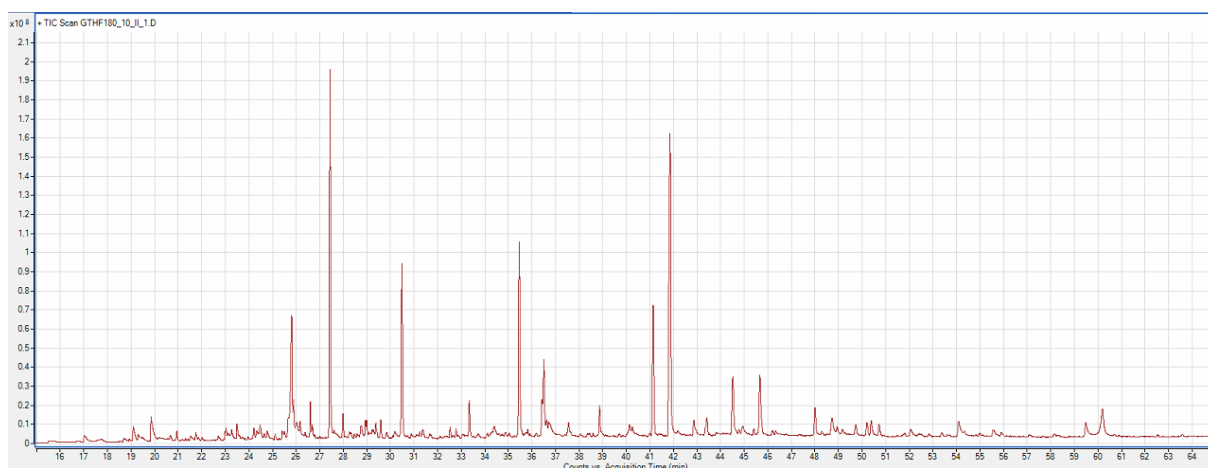


Figure 6.28: Pyrogram of THF dissolvable MWL from SE treated (180 °C for 10 min) spruce.

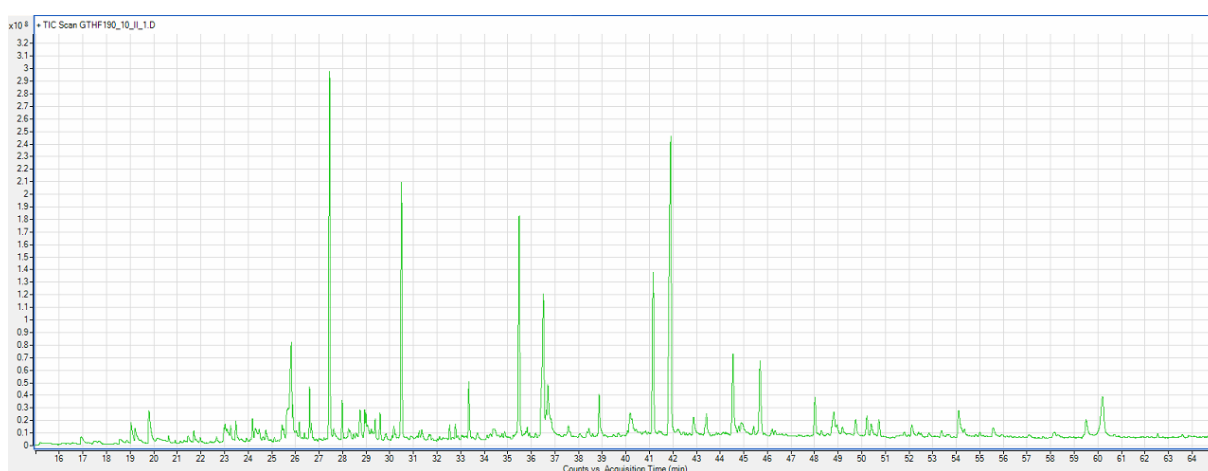


Figure 6.29: Pyrogram of THF dissolvable MWL from SE treated (190 °C for 10 min) spruce.

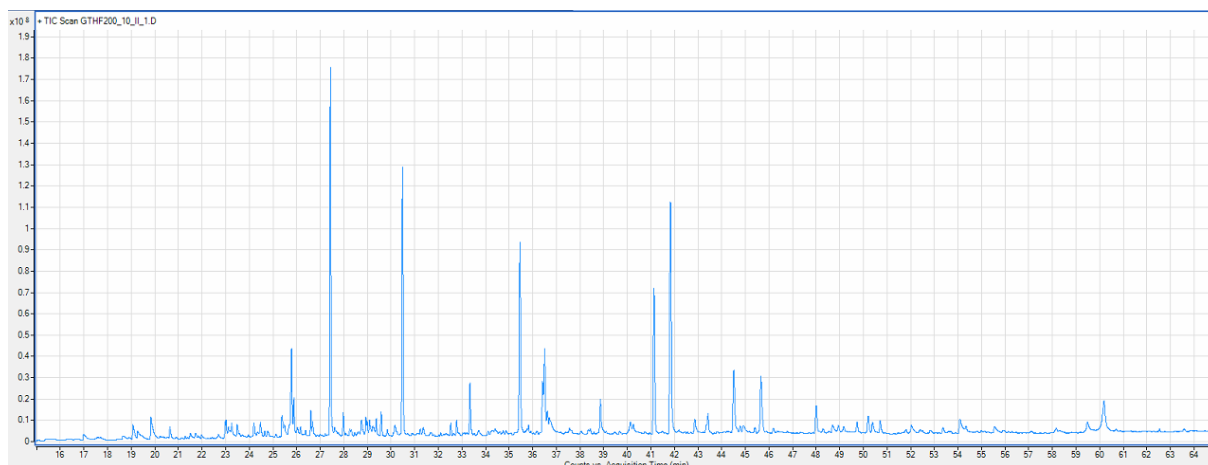


Figure 6.30: Pyrogram of THF dissolvable MWL from SE treated (200 °C for 10 min) spruce.

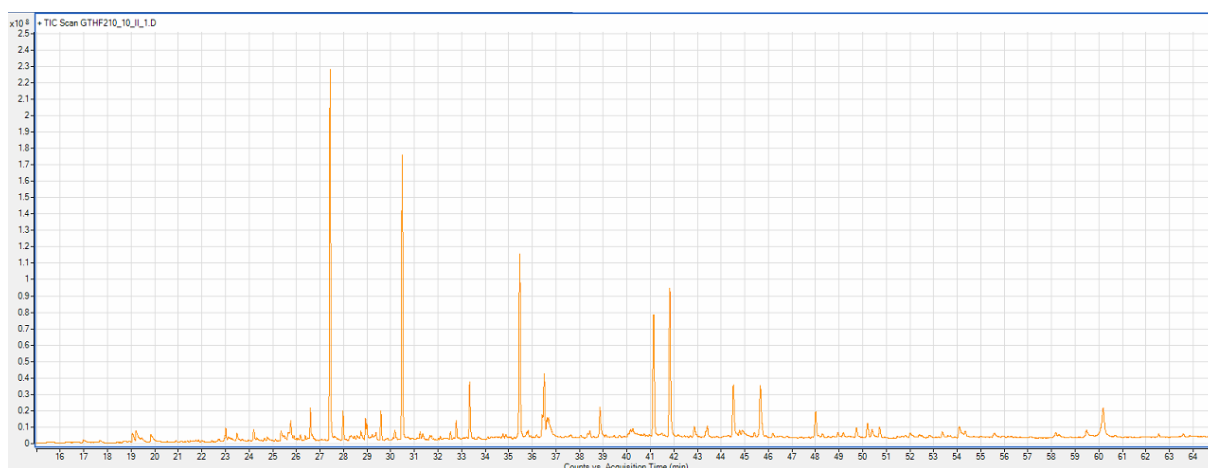


Figure 6.31: Pyrogram of THF dissolvable MWL from SE treated (210 °C for 10 min) spruce.

## 6.4 Relative Amount of Pyrolyzates Formed from All Lignin Samples

The relative amount and standard deviation for each compound formed from all MWL and THF dissolvable MWL samples are found in the tables in this section, both the TIC and EIC values.



Appendix

Table 6.1: TIC and EIC values for relative amount (R. am.) of the integrated compounds calculated from pyrograms (n = 3) of MWL and THF dissolvable MWL from untreated spruce and corresponding values for standard deviation (SD).

Compound no.	MWL Spruce-TIC		MWL Spruce-EIC		THF Spruce-TIC		THF Spruce-EIC	
	R. am. [%]	SD	R. am. [%]	SD	R. am. [%]	SD	R. am. [%]	SD
1	0.000	0.000	0.000	0.000	0.000	0.000	0.000	0.000
2	0.000	0.000	0.000	0.000	0.000	0.000	0.000	0.000
3	0.000	0.000	0.000	0.000	0.000	0.000	0.000	0.000
4	0.000	0.000	0.000	0.000	0.000	0.000	0.000	0.000
5	0.000	0.000	0.000	0.000	0.000	0.000	0.000	0.000
6	4.095	0.583	6.257	0.748	2.054	0,278	4.874	0.306
7	0.000	0.000	0.000	0.000	0.000	0.000	0.000	0.000
8	1.440	0.091	2.642	0.118	1.334	0,042	2.447	0.104
9	17.279	1.522	19.421	1.464	15.031	0,409	17.460	0.409
10	1.021	0.063	1.053	0.064	0.863	0,041	0.874	0.029
11	0.365	0.023	0.356	0.028	0.285	0,008	0.297	0.017
12	1.088	0.019	1.120	0.009	0.814	0,050	0.868	0.037
13	7.462	0.334	7.651	0.404	5.843	0,277	6.191	0.302
14	0.594	0.002	0.699	0.006	0.282	0,026	0.435	0.040
15	0.396	0.036	0.513	0.042	0.341	0,017	0.392	0.014
16	2.908	0.099	1.904	0.077	1.576	0,082	1.081	0.048
17	14.142	1.219	16.759	1.277	10.089	0,224	12.334	0.265
18	4.067	0.169	4.086	0.176	2.590	0,122	2.622	0.109
19	0.000	0.000	0.000	0.000	0.000	0,000	0.000	0.000
20	2.910	0.158	2.738	0.156	1.626	0,076	1.767	0.074
21	0.000	0.000	0.000	0.000	0.000	0,000	0.000	0.000
22	10.393	0.530	10.965	0.537	7.064	0,237	7.766	0.189
23	10.292	1.545	11.030	1.856	17.912	0,081	19.984	0.319
24	1.573	0.272	1.112	0.187	1.783	0,020	1.262	0.017
25	0.696	0.044	0.593	0.082	0.628	0,055	0.642	0.032
26	3.611	0.254	1.804	0.141	4.792	0,047	2.483	0.048
27	5.545	0.272	3.742	0.218	7.848	0,049	5.236	0.041
28	2.130	0.046	0.843	0.051	2.233	0,110	0.926	0.067
29	0.736	0.064	0.362	0.044	0.953	0,001	0.422	0.002
30	0.990	0.070	0.629	0.090	0.862	0,039	0.559	0.028
31	1.116	0.354	0.854	0.288	4.375	0,180	3.392	0.137
32	1.867	0.264	0.930	0.223	1.982	0,078	1.424	0.053
33	0.745	0.332	0.377	0.189	2.881	0,266	1.605	0.197
34	2.540	0.577	1.560	0.356	3.958	0,287	2.657	0.197

Table 6.2: TIC values for relative amount (R. am.) of the integrated compounds calculated from pyrograms ( $n = 3$ ) of MWL from steam exploded spruce treated at different temperatures for 5 min and corresponding values for standard deviation (SD).

MWL-TIC Compound no.	180 °C, 5 min		190 °C, 5 min		200 °C, 5 min		210 °C, 5 min	
	R. am. [%]	SD	R. am. [%]	SD	R. am. [%]	SD	R. am. [%]	SD
1	0.466	0.072	0.527	0.019	0.711	0.077	1.703	0.186
2	0.173	0.035	0.291	0.014	0.343	0.024	0.680	0.065
3	2.401	0.184	2.044	0.312	2.520	0.693	2.716	0.328
4	0.355	0.042	0.424	0.041	0.444	0.031	0.408	0.050
5	0.242	0.035	0.339	0.030	0.525	0.025	0.560	0.037
6	5.964	0.685	0.499	0.039	0.213	0.029	0.359	0.068
7	0.261	0.045	0.257	0.026	0.350	0.021	0.362	0.044
8	1.157	0.037	0.874	0.064	1.067	0.011	1.395	0.087
9	14.509	1.016	11.358	0.165	12.445	0.941	15.976	0.412
10	0.809	0.038	0.686	0.037	1.025	0.149	1.275	0.078
11	0.318	0.036	0.310	0.017	0.513	0.062	0.502	0.017
12	0.858	0.040	0.828	0.021	1.091	0.127	1.452	0.031
13	7.161	0.360	8.741	0.319	11.658	0.544	13.525	0.116
14	0.338	0.032	0.260	0.014	0.332	0.055	0.502	0.042
15	0.345	0.054	0.457	0.007	0.721	0.114	1.022	0.036
16	2.002	0.159	2.576	0.124	3.227	0.373	3.640	0.145
17	11.307	0.619	8.927	0.058	10.054	0.328	11.061	0.251
18	2.544	0.272	4.876	0.132	6.744	0.876	1.924	0.147
19	0.643	0.143	0.480	0.181	1.279	0.279	1.769	0.116
20	1.910	0.079	2.036	0.060	2.236	0.196	2.224	0.047
21	0.559	0.100	1.707	0.210	1.596	0.527	1.233	0.156
22	8.189	0.269	8.315	0.215	8.595	0.670	8.346	0.054
23	16.779	0.240	15.974	0.453	10.723	0.569	9.512	0.090
24	1.800	0.136	1.014	0.044	0.778	0.050	0.749	0.081
25	0.496	0.035	0.424	0.006	0.405	0.035	0.329	0.021
26	4.155	0.313	4.744	0.062	4.409	0.191	3.727	0.063
27	4.186	0.356	4.585	0.052	3.942	0.160	3.736	0.066
28	1.775	0.124	2.137	0.026	1.846	0.161	1.604	0.033
29	0.490	0.105	1.116	0.061	0.956	0.093	0.600	0.026
30	0.870	0.079	1.471	0.030	1.262	0.076	1.114	0.027
31	0.902	0.117	0.716	0.056	0.393	0.091	0.359	0.052
32	1.636	0.131	2.887	0.084	2.090	0.053	1.472	0.060
33	1.124	0.335	1.703	0.665	0.850	0.162	0.000	0.000
34	3.274	0.184	6.417	0.484	4.654	0.692	4.162	0.226

## Appendix

Table 6.3: TIC values for relative amount (R. am.) of the integrated compounds calculated from pyrograms ( $n = 3$ ) of MWL from steam exploded spruce treated at different temperatures for 10 min and corresponding values for standard deviation (SD).

MWL-TIC Compound no.	180 °C, 10 min		190 °C, 10 min		200 °C, 10 min		210 °C, 10 min	
	R. am. [%]	SD	R. am. [%]	SD	R. am. [%]	SD	R. am. [%]	SD
1	0.643	0.121	0.802	0.220	0.782	0.089	0.216	0.071
2	0.512	0.107	0.555	0.055	0.591	0.073	1.312	0.075
3	2.245	0.246	2.452	0.348	2.692	0.134	0.668	0.317
4	0.330	0.103	0.407	0.123	0.463	0.050	0.145	0.048
5	0.362	0.026	0.548	0.054	0.541	0.033	0.568	0.057
6	4.039	0.396	4.027	0.267	3.416	0.068	0.681	0.207
7	0.459	0.100	0.492	0.043	0.503	0.079	0.189	0.057
8	1.365	0.053	1.432	0.056	1.407	0.112	1.570	0.143
9	13.812	1.044	14.601	0.571	13.609	0.879	12.973	0.569
10	0.955	0.039	1.087	0.018	1.123	0.094	1.552	0.098
11	0.378	0.034	0.439	0.004	0.438	0.033	0.624	0.054
12	0.852	0.054	0.950	0.026	0.934	0.061	1.074	0.020
13	7.768	0.198	9.181	0.793	10.229	0.539	14.444	0.598
14	0.253	0.047	0.266	0.050	0.211	0.028	0.139	0.007
15	0.359	0.039	0.435	0.036	0.472	0.018	0.871	0.032
16	2.073	0.089	2.289	0.104	2.453	0.011	3.160	0.050
17	10.811	0.598	10.613	0.437	10.397	0.379	9.949	0.550
18	4.444	0.165	3.776	0.606	2.567	0.437	3.159	0.277
19	1.004	0.107	0.648	0.162	1.248	0.157	2.581	0.279
20	1.949	0.122	1.804	0.177	2.064	0.050	2.351	0.057
21	0.820	0.146	1.206	0.154	1.579	0.180	1.276	0.562
22	8.152	0.052	7.682	0.502	8.262	0.149	7.561	0.191
23	15.303	0.217	15.047	0.457	12.821	0.230	12.114	0.214
24	1.424	0.102	0.825	0.107	1.119	0.065	0.778	0.056
25	0.470	0.037	0.396	0.060	0.446	0.008	0.269	0.023
26	3.896	0.473	3.839	0.117	4.332	0.130	4.343	0.099
27	4.323	0.664	3.727	0.235	4.022	0.149	4.785	0.083
28	1.898	0.110	1.896	0.072	1.877	0.037	1.688	0.034
29	0.649	0.157	0.802	0.077	0.891	0.070	0.919	0.011
30	0.907	0.129	0.950	0.070	1.149	0.050	1.196	0.037
31	0.640	0.049	0.409	0.045	0.520	0.030	0.726	0.130
32	1.897	0.211	1.940	0.228	1.964	0.125	1.686	0.084
33	1.584	0.325	0.856	0.131	0.963	0.035	0.544	0.043
34	3.425	0.470	3.620	0.239	3.916	0.064	3.890	0.328

Table 6.4: EIC values for relative amount (R. am.) of the integrated compounds calculated from pyrograms ( $n = 3$ ) of MWL from steam exploded spruce treated at different temperatures for 5 min and corresponding values for standard deviation (SD).

MWL-EIC Compound no.	180 °C, 5 min		190 °C, 5 min		200 °C, 5 min		210 °C, 5 min	
	R. am. [%]	SD	R. am. [%]	SD	R. am. [%]	SD	R. am. [%]	SD
1	0.444	0.040	0.554	0.018	0.683	0.057	0.990	0.030
2	1.190	0.111	1.481	0.003	1.767	0.123	1.309	0.066
3	3.601	0.446	3.297	0.511	4.211	1.197	4.701	0.444
4	0.999	0.201	1.135	0.138	1.170	0.170	1.308	0.074
5	0.323	0.032	0.464	0.070	0.723	0.121	0.717	0.053
6	8.503	0.646	0.818	0.036	0.297	0.094	0.451	0.090
7	0.299	0.071	0.310	0.032	0.408	0.021	0.379	0.052
8	2.080	0.074	1.651	0.079	2.002	0.021	2.848	0.168
9	15.713	1.191	13.260	0.117	14.430	1.433	17.097	0.485
10	0.777	0.036	0.721	0.044	1.062	0.133	1.227	0.092
11	0.292	0.016	0.222	0.026	0.518	0.068	0.345	0.076
12	0.833	0.040	0.861	0.039	1.154	0.134	1.318	0.045
13	7.327	0.291	9.562	0.310	12.510	0.704	13.552	0.076
14	0.414	0.020	0.295	0.023	0.390	0.043	0.465	0.021
15	0.429	0.058	0.593	0.010	0.887	0.115	0.906	0.037
16	1.273	0.080	1.754	0.086	2.171	0.243	2.249	0.098
17	12.596	0.745	11.271	0.040	11.990	0.388	12.314	0.212
18	2.691	0.050	2.966	0.049	2.871	0.098	2.660	0.027
19	1.718	0.646	3.277	0.806	3.725	0.786	5.323	0.226
20	1.745	0.106	1.991	0.048	2.098	0.166	1.669	0.031
21	0.219	0.099	0.616	0.178	1.021	0.388	1.230	0.116
22	8.188	0.160	9.007	0.249	9.265	0.617	7.871	0.098
23	17.077	0.230	17.624	0.513	11.613	0.733	9.716	0.115
24	0.875	0.064	0.862	0.041	0.642	0.066	0.512	0.034
25	0.430	0.038	0.439	0.006	0.393	0.032	0.240	0.020
26	1.957	0.183	2.437	0.047	2.295	0.075	1.748	0.044
27	2.617	0.238	3.235	0.058	2.823	0.114	2.435	0.024
28	0.700	0.056	0.883	0.014	0.772	0.061	0.574	0.020
29	0.202	0.015	0.343	0.010	0.327	0.017	0.243	0.003
30	0.514	0.061	0.956	0.037	0.809	0.028	0.532	0.019
31	0.611	0.058	0.499	0.033	0.271	0.063	0.305	0.071
32	0.740	0.102	1.373	0.092	1.085	0.053	0.477	0.034
33	0.605	0.173	0.829	0.223	0.388	0.057	0.000	0.000
34	2.020	0.144	4.413	0.396	3.230	0.499	2.289	0.162

Appendix

Table 6.5: EIC values for relative amount (R. am.) of the integrated compounds calculated from pyrograms (n = 3) of MWL from steam exploded spruce treated at different temperatures for 10 min and corresponding values for standard deviation (SD).

MWL-EIC Compound no.	180 °C, 10 min		190 °C, 10 min		200 °C, 10 min		210 °C, 10 min	
	R. am. [%]	SD	R. am. [%]	SD	R. am. [%]	SD	R. am. [%]	SD
1	0.621	0.106	0.757	0.168	0.688	0.110	0.194	0.080
2	2.503	0.276	2.669	0.109	2.308	0.044	4.746	0.290
3	3.267	0.336	3.602	0.504	3.846	0.090	0.941	0.501
4	0.995	0.204	1.186	0.223	1.266	0.169	0.460	0.129
5	0.432	0.057	0.785	0.068	0.706	0.050	0.591	0.074
6	6.380	0.815	3.655	0.594	5.478	0.075	0.962	0.367
7	0.492	0.073	0.569	0.040	0.569	0.080	0.217	0.080
8	2.388	0.101	2.566	0.126	2.465	0.170	2.735	0.120
9	15.192	1.122	15.990	0.625	14.473	1.104	14.156	0.959
10	0.940	0.041	1.054	0.018	1.090	0.089	1.529	0.053
11	0.343	0.018	0.389	0.007	0.317	0.036	0.315	0.046
12	0.819	0.022	0.939	0.018	0.882	0.039	1.076	0.037
13	7.763	0.192	9.109	0.716	10.029	0.647	14.317	1.072
14	0.359	0.045	0.363	0.049	0.291	0.041	0.207	0.007
15	0.447	0.033	0.545	0.046	0.582	0.016	0.974	0.050
16	1.317	0.045	1.454	0.057	1.518	0.019	1.960	0.051
17	12.087	0.632	11.851	0.358	11.393	0.452	11.129	0.520
18	2.816	0.099	2.626	0.266	2.799	0.088	2.762	0.044
19	2.554	0.706	3.508	0.709	3.959	0.974	5.179	1.623
20	1.830	0.107	1.707	0.175	1.817	0.082	1.710	0.044
21	0.483	0.145	0.619	0.122	0.933	0.457	1.956	0.594
22	8.298	0.059	7.799	0.460	8.172	0.209	7.543	0.018
23	15.708	0.257	15.450	0.605	12.814	0.295	12.266	0.586
24	0.953	0.051	0.740	0.074	0.748	0.015	0.626	0.014
25	0.471	0.049	0.366	0.046	0.400	0.012	0.373	0.005
26	1.862	0.251	1.842	0.076	2.025	0.065	2.035	0.076
27	2.825	0.467	2.439	0.161	2.631	0.109	3.297	0.110
28	0.744	0.056	0.740	0.021	0.715	0.020	0.617	0.022
29	0.242	0.031	0.239	0.031	0.277	0.023	0.375	0.016
30	0.548	0.083	0.559	0.051	0.659	0.019	0.690	0.025
31	0.435	0.014	0.277	0.031	0.343	0.033	0.486	0.109
32	0.886	0.075	0.907	0.100	0.896	0.138	0.809	0.057
33	0.770	0.060	0.516	0.087	0.544	0.087	0.330	0.035
34	2.233	0.372	2.182	0.174	2.365	0.101	2.436	0.221

Table 6.6: TIC values for relative amount (R. am.) of the integrated compounds calculated from pyrograms ( $n = 3$ ) of THF dissolvable MWL from steam exploded spruce treated at different temperatures for 5 min and corresponding values for standard deviation (SD).

THF-TIC Compound no.	180 °C, 5 min		190 °C, 5 min		200 °C, 5 min		210 °C, 5 min	
	R. am. [%]	SD	R. am. [%]	SD	R. am. [%]	SD	R. am. [%]	SD
1	0.568	0.017	0.902	0.026	0.735	0.031	2.354	0.178
2	0.263	0.056	0.339	0.014	0.341	0.093	0.951	0.015
3	3.149	0.376	2.021	0.225	1.568	0.561	2.123	0.183
4	0.340	0.034	0.665	0.144	0.579	0.060	0.637	0.103
5	0.328	0.035	0.371	0.014	0.517	0.108	0.372	0.016
6	4.187	1.504	0.791	0.075	0.557	0.171	0.356	0.087
7	0.187	0.022	0.332	0.036	0.388	0.072	0.506	0.090
8	0.748	0.017	0.712	0.041	0.870	0.022	1.705	0.039
9	11.964	0.193	12.591	1.163	15.267	0.827	16.127	0.385
10	0.875	0.063	0.730	0.017	1.012	0.049	1.547	0.005
11	0.410	0.032	0.323	0.011	0.419	0.040	0.893	0.007
12	0.826	0.074	0.869	0.014	1.238	0.035	1.537	0.020
13	8.617	0.297	8.689	0.186	13.784	0.261	12.529	0.117
14	0.250	0.069	0.246	0.016	0.242	0.011	0.364	0.024
15	0.518	0.058	0.492	0.034	0.806	0.040	1.011	0.057
16	2.224	0.136	2.181	0.069	3.343	0.316	3.357	0.183
17	9.693	0.090	8.964	0.717	10.757	0.324	10.997	0.153
18	4.766	0.023	5.462	0.114	2.818	0.551	2.026	0.131
19	0.861	0.075	1.058	0.085	0.454	0.098	1.712	0.126
20	2.307	0.398	2.049	0.025	2.603	0.129	2.182	0.040
21	0.000	0.000	0.000	0.000	0.404	0.249	0.000	0.000
22	8.473	0.206	7.767	0.136	8.940	0.209	7.977	0.080
23	21.051	0.400	18.804	0.230	11.469	0.391	10.198	0.298
24	0.388	0.049	0.905	0.052	0.892	0.075	0.620	0.032
25	0.238	0.035	0.387	0.029	0.349	0.043	0.960	0.009
26	4.020	0.138	4.380	0.259	4.415	0.388	4.026	0.205
27	4.218	0.033	4.013	0.309	4.158	0.078	3.742	0.069
28	1.731	0.010	1.781	0.164	1.795	0.032	1.768	0.012
29	0.617	0.030	0.773	0.116	0.783	0.049	0.578	0.013
30	0.793	0.021	1.082	0.161	1.202	0.029	1.062	0.054
31	1.155	0.065	0.713	0.034	0.582	0.117	0.328	0.008
32	1.320	0.071	1.866	0.260	1.298	0.073	1.308	0.049
33	0.190	0.053	1.503	0.116	0.699	0.112	0.000	0.000
34	2.724	0.184	6.243	1.005	4.713	0.306	4.146	0.265

## Appendix

Table 6.7: TIC values for relative amount (R. am.) of the integrated compounds calculated from pyrograms ( $n = 3$ ) of THF dissolvable MWL from steam exploded spruce treated at different temperatures for 10 min and corresponding values for standard deviation (SD).

THF-TIC Compound no.	180 °C, 10 min		190 °C, 10 min		200 °C, 10 min		210 °C, 10 min	
	R. am. [%]	SD	R. am. [%]	SD	R. am. [%]	SD	R. am. [%]	SD
1	0.960	0.078	0.648	0.134	1.015	0,129	0.617	0.017
2	0.398	0.146	0.703	0.104	0.719	0,051	0.795	0.083
3	2.515	0.390	2.099	0.040	1.721	0,424	0.902	0.043
4	0.542	0.040	0.269	0.032	0.403	0,034	0.306	0.030
5	0.447	0.094	0.475	0.120	0.484	0,100	0.551	0.027
6	5.025	1.514	2.393	0.384	4.274	0,344	0.790	0.040
7	0.406	0.016	0.140	0.019	0.292	0,007	0.243	0.028
8	1.078	0.135	0.514	0.208	0.768	0,038	1.065	0.112
9	14.178	1.747	11.518	0.295	15.750	0,841	18.479	0.556
10	0.896	0.045	0.617	0.313	0.864	0,029	1.241	0.058
11	0.329	0.038	0.309	0.070	0.346	0,019	0.507	0.034
12	0.738	0.079	0.861	0.023	0.985	0,036	1.411	0.067
13	7.285	0.721	10.566	0.599	11.226	0,543	14.945	0.334
14	0.183	0.056	0.218	0.048	0.204	0,032	0.280	0.032
15	0.308	0.022	0.601	0.094	0.510	0,045	0.851	0.043
16	1.672	0.059	2.477	0.453	2.232	0,139	3.257	0.248
17	9.818	0.782	8.285	0.863	10.102	0,292	11.213	0.101
18	2.065	0.266	7.509	0.522	2.361	0,039	2.601	0.068
19	1.203	0.160	0.532	0.137	1.007	0,060	0.927	0.071
20	1.741	0.149	2.098	0.173	2.075	0,075	2.425	0.035
21	0.000	0.000	0.000	0.000	0.000	0,000	0.000	0.000
22	7.011	0.266	7.664	0.095	7.704	0,369	7.914	0.182
23	20.515	0.624	18.427	0.713	15.218	0,113	10.820	0.193
24	0.593	0.015	0.533	0.073	0.754	0,195	0.541	0.016
25	0.321	0.004	1.155	0.246	0.342	0,033	0.297	0.038
26	4.225	0.307	4.274	0.294	4.410	0,072	3.882	0.396
27	4.384	0.415	4.230	0.287	4.040	0,183	4.251	0.017
28	1.820	0.281	1.733	0.258	1.683	0,169	1.707	0.017
29	0.818	0.148	1.023	0.202	0.535	0,043	0.548	0.020
30	0.897	0.183	1.179	0.166	0.969	0,045	0.944	0.022
31	1.007	0.114	0.708	0.062	0.750	0,071	0.581	0.036
32	1.482	0.185	1.715	0.393	1.168	0,061	0.997	0.102
33	1.538	0.408	0.780	0.327	0.998	0,148	0.616	0.104
34	3.604	0.440	3.747	0.582	4.089	0,553	3.497	0.600

Table 6.8: EIC values for relative amount (R. am.) of the integrated compounds calculated from pyrograms ( $n = 3$ ) of THF dissolvable MWL from steam exploded spruce treated at different temperatures for 5 min and corresponding values for standard deviation (SD).

THF-EIC Compound no.	180 °C, 5 min		190 °C, 5 min		200 °C, 5 min		210 °C, 5 min	
	R. am. [%]	SD	R. am. [%]	SD	R. am. [%]	SD	R. am. [%]	SD
1	0.537	0.036	0.868	0.034	0.675	0.017	1.434	0.101
2	1.155	0.051	1.142	0.300	1.543	0.158	1.307	0.120
3	5.125	0.691	3.241	0.521	2.733	0.973	3.449	0.145
4	0.861	0.014	1.366	0.211	1.192	0.114	1.800	0.207
5	0.418	0.061	0.401	0.037	0.585	0.105	0.625	0.044
6	6.424	1.088	1.508	0.446	0.396	0.202	1.044	0.192
7	0.260	0.006	0.409	0.044	0.423	0.096	0.562	0.102
8	2.069	0.006	1.782	0.085	1.972	0.024	3.414	0.072
9	12.828	0.398	14.661	1.361	17.054	1.094	17.533	0.349
10	0.809	0.032	0.747	0.010	1.020	0.024	1.383	0.035
11	0.366	0.038	0.343	0.026	0.259	0.077	0.517	0.013
12	0.819	0.028	0.856	0.017	1.192	0.021	1.400	0.028
13	8.025	0.170	9.335	0.063	14.280	0.337	12.192	0.075
14	0.337	0.032	0.301	0.017	0.343	0.012	0.554	0.035
15	0.526	0.035	0.552	0.030	0.938	0.036	0.861	0.019
16	1.430	0.062	1.480	0.036	2.119	0.185	2.039	0.084
17	10.731	0.094	10.878	0.668	12.252	0.602	12.432	0.118
18	2.717	0.050	2.661	0.059	2.992	0.023	2.632	0.043
19	2.241	0.351	2.137	0.756	2.495	0.920	5.580	0.428
20	1.919	0.008	1.774	0.014	1.946	0.096	1.662	0.023
21	0.000	0.000	0.000	0.000	0.641	0.430	0.000	0.000
22	8.682	0.074	8.368	0.048	9.102	0.166	7.552	0.058
23	21.892	0.403	20.585	0.095	11.573	0.539	10.429	0.301
24	0.571	0.072	0.788	0.059	0.708	0.089	0.543	0.031
25	0.330	0.041	0.384	0.018	0.368	0.021	0.276	0.013
26	1.924	0.047	2.226	0.137	2.141	0.216	1.898	0.050
27	2.596	0.042	2.735	0.234	2.797	0.085	2.384	0.037
28	0.588	0.026	0.750	0.087	0.669	0.023	0.642	0.007
29	0.247	0.010	0.258	0.034	0.306	0.021	0.235	0.010
30	0.478	0.004	0.704	0.091	0.698	0.008	0.517	0.036
31	0.732	0.062	0.415	0.006	0.367	0.083	0.243	0.096
32	0.916	0.016	1.283	0.241	0.699	0.024	0.537	0.007
33	0.056	0.031	0.821	0.069	0.444	0.066	0.000	0.000
34	1.393	0.131	4.243	0.559	3.077	0.261	2.326	0.091



## Appendix

Table 6.9: EIC values for relative amount (R. am.) of the integrated compounds calculated from pyrograms ( $n = 3$ ) of THF dissolvable MWL from steam exploded spruce treated at different temperatures for 10 min and corresponding values for standard deviation (SD).

THF-EIC Compound no.	180 °C, 10 min		190 °C, 10 min		200 °C, 10 min		210 °C, 10 min	
	R. am. [%]	SD	R. am. [%]	SD	R. am. [%]	SD	R. am. [%]	SD
1	0.907	0.031	0.680	0.144	0.946	0.104	0.574	0.007
2	2.189	0.416	3.082	0.133	2.525	0.143	3.658	0.178
3	3.488	0.364	3.763	0.550	2.768	0.612	1.293	0.083
4	1.450	0.051	0.811	0.160	1.285	0.048	0.902	0.048
5	0.413	0.049	0.559	0.011	0.464	0.041	0.565	0.011
6	5.786	0.789	4.119	1.007	3.770	0.590	0.943	0.163
7	0.482	0.024	0.162	0.014	0.352	0.010	0.274	0.031
8	2.532	0.153	1.307	0.558	1.973	0.134	2.352	0.110
9	15.582	1.828	13.371	0.406	17.699	0.945	20.039	0.616
10	0.874	0.047	0.631	0.349	0.876	0.035	1.185	0.053
11	0.222	0.048	0.331	0.080	0.270	0.016	0.487	0.028
12	0.681	0.057	0.888	0.065	0.944	0.005	1.353	0.081
13	7.109	0.405	11.350	1.124	11.506	0.624	15.102	0.327
14	0.286	0.092	0.241	0.062	0.264	0.017	0.395	0.035
15	0.364	0.006	0.687	0.096	0.619	0.044	0.957	0.025
16	1.052	0.043	1.668	0.376	1.477	0.053	2.010	0.172
17	11.003	0.926	9.801	0.292	11.583	0.313	12.334	0.088
18	2.357	0.183	2.679	0.145	2.763	0.108	2.694	0.013
19	1.770	0.707	1.800	1.020	0.856	0.209	2.170	0.615
20	1.510	0.103	1.738	0.101	1.666	0.089	1.695	0.010
21	0.000	0.000	0.000	0.000	0.000	0.000	0.000	0.000
22	7.167	0.374	8.290	0.237	8.011	0.352	7.907	0.148
23	20.869	0.616	20.092	0.209	15.877	0.085	10.814	0.310
24	0.833	0.015	0.691	0.033	0.820	0.045	0.647	0.006
25	0.371	0.016	0.235	0.031	0.271	0.007	0.213	0.070
26	1.972	0.172	2.129	0.110	2.164	0.029	1.857	0.044
27	2.831	0.287	2.819	0.163	2.642	0.143	2.709	0.017
28	0.676	0.080	0.717	0.126	0.630	0.009	0.639	0.014
29	0.254	0.054	0.316	0.043	0.240	0.015	0.275	0.022
30	0.505	0.104	0.775	0.113	0.577	0.026	0.556	0.007
31	0.687	0.047	0.458	0.039	0.504	0.047	0.368	0.031
32	0.935	0.106	1.224	0.354	0.719	0.111	0.588	0.112
33	0.695	0.141	0.345	0.174	0.463	0.099	0.288	0.027
34	2.148	0.241	2.238	0.474	2.477	0.428	2.155	0.360



Norges miljø- og biovitenskapelig universitet  
Noregs miljø- og biovitenskapelige universitet  
Norwegian University of Life Sciences

Postboks 5003  
NO-1432 Ås  
Norway